

Convective Heat Transfer Model for Determining Quench Recovery of High Temperature Superconducting YBCO in Liquid Nitrogen

by

Joseph Edward Jankowski

B.S. in Mechanical Engineering
Loyola Marymount University, 2002

Submitted to the Department of Mechanical Engineering in partial fulfillment of the requirements for the degree of

Master of Science in Mechanical Engineering

at the

MASSACHUSETTS INSTITUTE OF TECHNOLOGY

September 2004

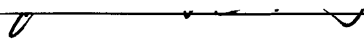
© Massachusetts Institute of Technology 2004. All Rights Reserved.

Author



Department of Mechanical Engineering
August 23, 2004

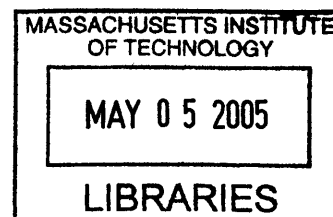
Certified by



Dr. Yukikazu Iwasa
Thesis Supervisor

Accepted by

Ain A. Sonin
Chairman, Departmental Graduate Committee



BARKER

Convective Heat Transfer Model for Determining Quench Recovery of High Temperature Superconducting YBCO in Liquid Nitrogen

By Joseph Edward Jankowski

Submitted to the Department of Mechanical Engineering
on August 23, 2004, in partial fulfillment of the requirements for the degree of
Master of Science in Mechanical Engineering

Abstract

Stability of a superconducting magnet is critical for reliable operation of a device in which the magnet plays a role. With the advent of high temperature superconductors (HTS), liquid nitrogen may be used to cool HTS devices. Yttrium barium copper oxide (YBCO), an HTS with critical temperature of 93 K, is a promising HTS for transmission cables and electric power devices. However, before the coated YBCO conductor can be used, stability of the superconductor must well understood. One important component for the superconductor to be used in these power devices is highly conductive normal metal such as copper that electrically shunts the superconductor when it is driven to the normal state, intentionally or during a fault mode.

In this thesis work, stability of coated YBCO conductor samples were studied both experimentally and analytically. Each test sample, 10-cm or 15-cm long and cooled directly by boiling liquid nitrogen, was investigated for its stability by means of an over-current pulse that exceeded the sample's nominal critical current at 77.3 K. Variables of the investigation include: 1) presence or absence of copper layer incorporated into the sample; 2) thickness of copper layer; 3) nominal operating current before and after the application of a current pulse; 4) pulse current amplitude, and 5) pulse current duration. Recorded signals were sample voltages, measured by two sets of voltage taps, and sample temperatures, measured by three thermocouples placed at the center and two ends.

The experimental and analytical results both demonstrated that for coated YBCO conductor to operate stably under operating conditions expected in the real device, it requires copper lamination whose thickness nearly doubles the original conductor thickness.

Thesis Supervisor: Dr. Yukikazu Iwasa
Title: Research Professor, Francis Bitter Magnet Laboratory, and Senior Lecturer,
Department of Mechanical Engineering, MIT

Acknowledgements

I would like to thank my thesis advisor, Dr. Yukikazu Iwasa for his countless help in supporting my research goals, both financially and intellectually. Over the last two years, he has guided me towards a path with the correct solution, and although magnet technology has often proven difficult, he has gone out of his way to help me understand several advanced topics in conductor and magnet design. Without his commitment, this would not have been possible.

I would like to thank Dr. Juan Bascuñán, whose insight into cryogenic heat transfer provided significant literature and understanding of the behavior and properties of liquid nitrogen, not to mention he was always available to help double check many calculations. I would also like to thank the other members of our research group, both past and present that have generously supported me and were always willing to contribute possible solutions to my questions. Those people include Dr. Haigun Lee, Dr. Ho Min Kim, Dr. Seung Yong Hahn, and Alexander Krull.

In addition, none of this would have been possible without the support of my parents who have guided and nurtured me in an academic friendly environment. Without question they stood behind me, providing a firm foundation in life, and I am lucky to have them. Lastly, I would like to thank Melinda, who has always been there for the emotional support needed to succeed in this tough environment. Without her understanding, patience, dedication, and continual proofreading I may not have made it this far.

This work was supported by the Department of Energy, while American Superconductor Inc. and IGC Inc. provided the YBCO samples.

This paper is dedicated to these people, as I am indebt to all of you, and without your help and support, none of this would have been possible.

Table of Contents

Chapter 1 – Introduction

1.1 History of Superconductivity.....	11
1.1.1 Discovery.....	11
1.1.2 Definition of Superconductivity.....	11
1.1.3 Type I Superconductors.....	12
1.1.4 Type II Superconductors.....	12
1.2 High Temperature Superconductors.....	12
1.2.1 Types of High Temperature Superconductors.....	12
1.2.2 Liquid Nitrogen Cooling.....	13
1.3 Thermal Stability.....	13
1.4 Overview.....	14
1.4.1 YBCO.....	14
1.4.2 Limits to Technology.....	14
1.4.3 Experimental Focus.....	15

Chapter 2 – Model for Liquid Nitrogen Cooling

2.1 Model for Quench and Recovery in YBCO Superconductor.....	16
2.1.1 Power Equation.....	16
2.1.2 Parallel Resistance Model.....	18
2.1.3 Numerical Solution.....	20
2.2 Heat Transfer.....	20
2.2.1 Overview.....	20
2.2.2 Simulation Model for Liquid Nitrogen Heat Transfer.....	21
2.3 Copper Properties.....	23
2.3.1 Specific Heat of Copper.....	23
2.3.2 Resistivity of Copper.....	24
2.4 Silver Properties.....	24
2.4.1 Specific Heat of Silver.....	24
2.4.2 Resistivity of Silver.....	24
2.5 Material Properties of Substrate.....	25
2.5.1 AMSC Substrate Resistivity.....	25
2.5.2 SPI Substrate Resistivity.....	25
2.6 Material Properties of YBCO.....	25
2.6.1 Specific Heat of YBCO.....	25

Chapter 3 – Experimental Verification of Model

3.1 Experimental Setup.....	27
3.1.1 Sample and Fixture.....	27
3.1.2 Experimental Procedure.....	30
3.2 Data Acquisition System.....	32

3.2.1 Equipment and Setup.....	32
3.2.2 Software Analysis.....	33
3.3 Block Diagram.....	34

Chapter 4 –Experimental Results

4.1 Silver only Stabilized Conductor: AMSC 10-mm Width.....	35
4.1.1 Sample Specifications.....	35
4.1.2 Experimental and Simulated Results.....	36
4.2 Silver Only Stabilized Conductor: SPI 4-mm Width.....	40
4.2.1 Sample Specifications.....	40
4.2.2 Experimental and Simulated Results.....	40
4.3 Ag-Cu Stabilized Conductor: AMSC 10-mm Width.....	45
4.3.1 Sample Specifications.....	45
4.3.2 Experimental and Simulated Results: 50- μ m Thick Copper Lamina.....	45
4.3.3 Experimental and Simulated Results: 76- μ m Thick Copper Lamina.....	52
4.4 Ag-Cu Stabilized Conductor: AMSC 4-mm Width.....	57
4.4.1 Sample Specifications.....	57
4.4.2 Experimental and Simulated Results.....	57
4.5 Ag-Cu Stabilized Conductor: SPI 4-mm Width.....	64
4.5.1 Sample Specifications.....	64
4.5.2 Experimental and Simulated Results: 46- μ m Thick Copper Lamina.....	64
4.5.3 Experimental and Simulated Results: 75- μ m Thick Copper Lamina.....	71
4.6 Summary of Results and Comparison of Data.....	77

Chapter 5 – Conclusions and Recommendations

5.1 Conclusions.....	79
5.2 Recommendations.....	80

References.....

81

Appendix A – Program Code.....

83

Appendix A1: Main.m.....	83
Appendix A2: Supplied_Current.m.....	86
Appendix A3: Cooling.m.....	88
Appendix A4: Embedded Functions.....	90
Appendix A4-1 - N_Value.m.....	90
Appendix A4-2 - Cu_Cp.m.....	90
Appendix A4-3 - Cu_Res.m.....	90
Appendix A4-4 - Ag_Cp.m.....	91

Appendix A4-5 - Ag_Res.m.....	91
Appendix A4-6 - Sub_Cp.m.....	91
Appendix A4-7 - Sub_Res.m.....	91
Appendix A4-8 - YBCO_Cp.m.....	92
Appendix A4-9 - YBCO_Ic.m.....	93
Appendix B – Material Properties.....	94
Appendix C – LabVIEW Code.....	98
Appendix D - Sample to DAQ Connection.....	101

List of Figures

Figure 1-1. Typical critical surface for a superconductor.....	11
Figure 1-2. Evolution of T_c since the discovery of superconductivity.....	13
Figure 2-1. Coordinate axis orientation in sample with origin at midpoint of conductor.....	16
Figure 2-2. Circuit model for a composite superconductor. Above: Model for $I_t \leq I_c$. Below: All three temperature ranges.....	18
Figure 2-3. Standard liquid nitrogen heat flux adapted from the data of Merte and Clark with a typical curve from the simulation superimposed.....	21
Figure 3-1. Copper leads to connect power supply lugs to YBCO sample.....	27
Figure 3-2. Complete sample holder and test assembly for liquid nitrogen cooling, shown in approximate scale except sample thickness, which has been exaggerated to show detail.....	28
Figure 3-3. Detailed sectional side view of thermocouple clamp system and the absorption of the pressure from the thermocouple into copper stabilizer and Styrofoam.....	29
Figure 3-4. Location of voltage taps and thermocouples on 15-cm long YBCO sample.....	30
Figure 3-5. Typical current pulse generated by HP6260B power supplies for experiment.....	31
Figure 3-6. Experimental setup with power supplies, DAQ, and test setup.....	31
Figure 3-7. Overall block diagram for experimental setup.....	34
Figure 4-1. Layer arrangements in sample for silver-only laminated superconductor.....	36
Figure 4-2. Virgin run for sample BDOE-L590. Measured using 5-cm voltage taps; $I_c = 140$ A with a $1 \mu\text{V}/\text{cm}$ criterion.....	37
Figure 4-3. Sample BDOE-L590: Run 4, $\tau = 150$ ms, $t_{hold} = 7.0$ s, $I_{op} = 109$ A, $I_p = 198$ A, $I_p/I_c = 1.41$	38
Figure 4-4. Sample BDOE-L590: Simulated results showing non-recovery. $\tau = 150$ ms, $t_{hold} = 7.0$ s, $I_{op} = 109$ A, $I_p = 221$ A, $I_p/I_c = 1.58$	39
Figure 4-5. Virgin run for sample SPCC-Ag-B-2. Measured using both 5-cm and 10-cm voltage taps; $I_{c\ 5\text{-cm}} = 58.5$ A and $I_{c\ 10\text{-cm}} = 58.5$ A with a $1 \mu\text{V}/\text{cm}$ criterion.....	41
Figure 4-6. Sample SPCC-Ag-B-2: Run 4, $\tau = 100$ ms, $t_{hold} = 7.0$ s, $I_{op} = 52$ A, $I_p = 73$ A, $I_p/I_c = 1.24$	42
Figure 4-7. Critical current for sample SPCC-Ag-B-2 after 6 th pulse. Measured using both 5-cm and 10-cm voltage taps; $I_{c\ 5\text{-cm}} = 58.5$ A and $I_{c\ 10\text{-cm}} = 58.5$ A with a $1 \mu\text{V}/\text{cm}$ criterion.....	43
Figure 4-8. Sample SPCC-Ag-B-2: Run 7, $\tau = 100$ ms, $t_{hold} = 7.0$ s, $I_{op} = 52$ A, $I_p = 78$ A, $I_p/I_c = 1.33$	44
Figure 4-9. Layer arrangements in sample for AMSC Ag-Cu laminated superconductor.....	47

Figure 4-10. Virgin run for sample CC52-335-LAM. Measured using 5-cm voltage taps; $I_{c\ 5\text{-cm}} = 129\text{ A}$ with a $1\ \mu\text{V/cm}$ criterion.....	47
Figure 4-11. Sample CC52-335-LAM: Run 15, $\tau = 150\text{ ms}$, $t_{\text{hold}} = 7.0\text{ s}$, $I_{\text{op}} = 117\text{ A}$, $I_p = 245\text{ A}$, $I_p/I_c = 1.90$	48
Figure 4-12. Sample CC52-335-LAM: Run 35, $\tau = 150\text{ ms}$, $t_{\text{hold}} = 7.0\text{ s}$, $I_{\text{op}} = 117\text{ A}$, $I_p = 552\text{ A}$, $I_p/I_c = 4.30$	49
Figure 4-13. Critical current for sample CC52-335-LAM after 35 th pulse. Measured using only 5-cm voltage taps; $I_{c\ 5\text{-cm}} = 129\text{ A}$ with a $1\ \mu\text{V/cm}$ criterion.....	50
Figure 4-14. Sample CC52-335-LAM: Predicted YBCO burnout, $\tau = 150\text{ ms}$, $t_{\text{hold}} = 7.0\text{ s}$, $I_{\text{op}} = 117\text{ A}$, $I_p = 80\text{ A}$, $I_p/I_c = 6.27$	51
Figure 4-15. Virgin run for sample CC51-R540-0-10. Measured using only 5-cm voltage taps; $I_{c\ 5\text{-cm}} = 110\text{ A}$ with a $1\ \mu\text{V/cm}$ criterion.....	53
Figure 4-16. Sample CC51-R540-0-10: Run 21, $\tau = 300\text{ ms}$, $t_{\text{hold}} = 7.0\text{ s}$, $I_{\text{op}} = 104\text{ A}$, $I_p = 500\text{ A}$, $I_p/I_c = 4.55$	54
Figure 4-17. Critical current for sample CC51-R540-0-10 after 21 st pulse. Measured using only 5-cm voltage taps; $I_{c\ 5\text{-cm}} = 110\text{ A}$ with a $1\ \mu\text{V/cm}$ criterion.....	55
Figure 4-18. Sample CC51-R540-0-10: Predicted YBCO burnout, $\tau = 300\text{ ms}$, $t_{\text{hold}} = 7.0\text{ s}$, $I_{\text{op}} = 104\text{ A}$, $I_p = 665\text{ A}$, $I_p/I_c = 6.04$	56
Figure 4-19. Virgin run for sample CC84-755-8. Measured using both 5-cm and 10-cm voltage taps; $I_{c\ 5\text{-cm}} = 94\text{ A}$ and $I_{c\ 10\text{-cm}} = 95\text{ A}$ with a $1\ \mu\text{V/cm}$ criterion.....	59
Figure 4-20. Critical current for sample CC84-755-8 after 31 st pulse. Measured using both 5-cm and 10-cm voltage taps; $I_{c\ 5\text{-cm}} = 91\text{ A}$ and $I_{c\ 10\text{-cm}} = 91\text{ A}$ with a $1\ \mu\text{V/cm}$ criterion.....	60
Figure 4-21. Sample CC84-755-8: Run 32, $\tau = 100\text{ ms}$, $t_{\text{hold}} = 7.0\text{ s}$, $I_{\text{op}} = 80\text{ A}$, $I_p = 360\text{ A}$, $I_p/I_c = 3.96$	61
Figure 4-22. Critical current for sample CC84-755-8 after 37 th pulse. Measured using both 5-cm and 10-cm voltage taps; $I_{c\ 5\text{-cm}} = 91\text{ A}$ and $I_{c\ 10\text{-cm}} = 91\text{ A}$ with a $1\ \mu\text{V/cm}$ criterion.....	62
Figure 4-23. Sample CC84-755-8: Run 38, $\tau = 100\text{ ms}$, $t_{\text{hold}} = 7.0\text{ s}$, $I_{\text{op}} = 80\text{ A}$, $I_p = 433\text{ A}$, $I_p/I_c = 4.76$	63
Figure 4-24. Layer arrangements in sample for SPI Ag-Cu laminated superconductor. Side copper layers electrically short upper and lower layers. The thickness of each side copper layer is not known exactly, though it is on the order of $\sim 10\text{-}\mu\text{m}$	65
Figure 4-25. Virgin run for sample SPCC-Cu-A-1. Measured using both 5-cm and 10-cm voltage taps; $I_{c\ 5\text{-cm}} = 59.5\text{ A}$ and $I_{c\ 10\text{-cm}} = 56.0\text{ A}$ with a $1\ \mu\text{V/cm}$ criterion.....	66
Figure 4-26. Sample SPCC-Cu-A-1: Run 2, $\tau = 100\text{ ms}$, $t_{\text{hold}} = 7.0\text{ s}$, $I_{\text{op}} = 51\text{ A}$, $I_p = 100\text{ A}$, $I_p/I_c = 1.68$	67
Figure 4-27. Sample SPCC-Cu-A-1: Run 12, $\tau = 100\text{ ms}$, $t_{\text{hold}} = 7.0\text{ s}$, $I_{\text{op}} = 51\text{ A}$, $I_p = 355\text{ A}$, $I_p/I_c = 5.92$	68

Figure 4-28. Critical current for sample SPCC-Cu-A-1 after 12 th pulse. Measured using both 5-cm and 10-cm voltage taps; $I_{c\ 5\text{-cm}} = 60.0\text{A}$ and $I_{c\ 10\text{-cm}} = 57.0\text{A}$ with a $1\ \mu\text{V/cm}$ criterion.....	69
Figure 4-29. Sample SPCC-Cu-A-1: Run 13, $\tau = 100\text{ms}$, $t_{\text{hold}} = 7.0\text{s}$, $I_{op} = 51\text{A}$, $I_p = 404\text{A}$, $I_p/I_c = 6.85$	70
Figure 4-30. Critical current for sample SPCC-Cu-A-1 after 13 th pulse. Measured using both 5-cm and 10-cm voltage taps; $I_{c\ 5\text{-cm}} = 58.5\text{A}$ and $I_{c\ 10\text{-cm}} = 57.0\text{A}$ with a $1\ \mu\text{V/cm}$ criterion.....	71
Figure 4-31. Virgin run for sample SPCC-Cu-G. Measured using both 5-cm and 10-cm voltage taps; $I_{c\ 5\text{-cm}} = 40.8\text{A}$ and $I_{c\ 10\text{-cm}} = 40.5\text{A}$ with a $1\ \mu\text{V/cm}$ criterion.....	72
Figure 4-32. Sample SPCC-Cu-G: Run 4, $\tau = 300\text{ms}$, $t_{\text{hold}} = 7.0\text{s}$, $I_{op} = 36\text{A}$, $I_p = 221\text{A}$, $I_p/I_c = 6.13$	73
Figure 4-33. Sample SPCC-Cu-G: Run 11, $\tau = 300\text{ms}$, $t_{\text{hold}} = 7.0\text{s}$, $I_{op} = 36\text{A}$, $I_p = 335\text{A}$, $I_p/I_c = 9.10$	74
Figure 4-34. Critical current for sample SPCC-Cu-G after 11 th pulse. Measured using both 5-cm and 10-cm voltage taps; $I_{c\ 5\text{-cm}} = 39.3\text{A}$ and $I_{c\ 10\text{-cm}} = 39.3\text{A}$ with a $1\ \mu\text{V/cm}$ criterion.....	75
Figure 4-35. Sample SPCC-Cu-G: Run 12, $\tau = 300\text{ms}$, $t_{\text{hold}} = 7.0\text{s}$, $I_{op} = 36\text{A}$, $I_p = 370\text{A}$, $I_p/I_c = 9.48$	76
Figure 4-36. Experimental and simulated I_p/I_c ratios for each sample.....	77
Figure 4-37. Simulated results for each sample using a 100-ms pulse and 400K burnout criterion.....	78
Figure B-1. Specific Heat of Copper 100 for $10\text{K} < T < 200\text{K}$	94
Figure B-2. Specific Heat of Copper 100 for $200\text{K} < T < 1200\text{K}$	94
Figure B-3. Resistivity of Copper 100 for $20\text{K} < T < 190\text{K}$	95
Figure B-4. Resistivity of Copper 100 for $190\text{K} < T < 1300\text{K}$	95
Figure B-5. Specific Heat of Silver for $10\text{K} < T < 1200\text{K}$	96
Figure B-6. Resistivity of Silver for $0\text{K} < T < 293\text{K}$	96
Figure B-7. Resistivity of Silver for $293\text{K} < T < 1000\text{K}$	97
Figure B-8. Specific Heat of YBCO for $77.3\text{K} < T < 300\text{K}$	97
Figure C-1. LabVIEW code used to generate the pulse control for the power supplies. This was used with a voltage divider inline to the power supply signal.....	98
Figure C-2. LabVIEW code used to generate the pulse current signal. This figure is the left portion, continued in Figure C-3.....	99
Figure C-3. LabVIEW code used to generate the pulse current signal. This figure is the right portion, continued from Figure C-2.....	100
Figure D-1. Electrical Diagram for Sample to DAQ Connections.....	101

List of Tables

Table 3.1 SCXI chassis configuration and filters settings.....	33
Table 4-1. Specifications for 10-mm wide AMSC Ag stabilized samples.....	36
Table 4-2. Specifications for 4-mm SPI Ag stabilized samples.....	40
Table 4-3. Specifications for 1-cm wide Ag-Cu stabilized samples.....	46
Table 4-4. Specifications for 4-mm wide Ag-Cu stabilized samples.....	58
Table 4-5. Sample specifications for 4-mm SPI Ag-Cu stabilized samples.....	65

Chapter 1

Introduction

1.1 History of Superconductivity

1.1.1 Discovery

Kamerlingh Onnes first discovered superconductivity in 1911. After successfully liquefying helium in 1908, he was able to test the resistivity of several elements at 4.2 K [1]. While conducting these experiments, he first noticed that the resistivity of pure mercury was zero and went on to find the zero resistivity states for other elements, such as tin and lead, by 1914. Although this discovery was a major breakthrough, these early superconducting elements, designated Type I superconductors, exhibited several disadvantages, the most significant ones being their low critical magnetic field and low critical current densities.

1.1.2 Definition of Superconductivity

Superconductivity is defined as the ability to conduct current without resistive losses [2]. Superconductors are governed by a critical surface relating the three properties contributing to superconductivity: critical temperature (T_c), critical magnetic field (H_c), and critical current density (J_c). Although there are in-depth formulas governing their relations to each other, Figure 1-1 illustrates the general case.

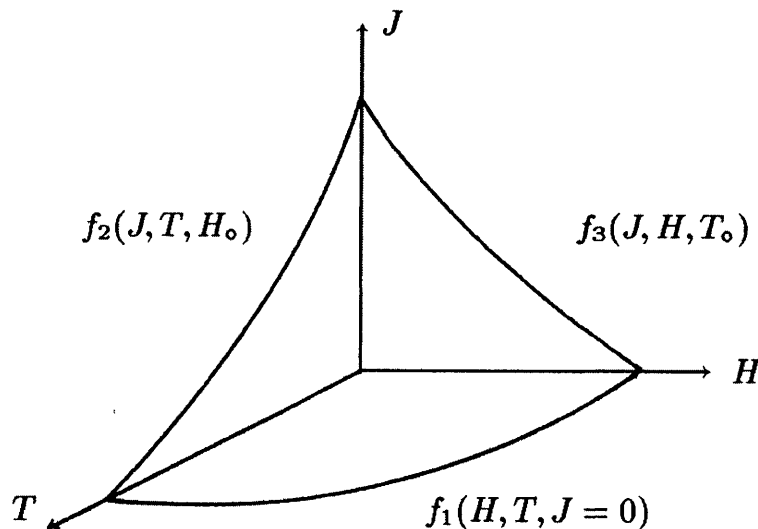


Figure 1-1. Typical critical surface for a superconductor [3].

From Figure 1-1, it can be seen that as one property is increased, the other two must decrease for the superconductor to remain superconducting. Although most superconductors have a critical temperature under 10K, modern research has developed the so-called “High Temperature Superconductors” (HTS), some of which have critical temperatures above 77K.

1.1.3 Type I Superconductors

Type I superconductors are often referred to as soft superconductors. A Type I superconductor is the classification given to those first discovered by Kamerlingh Onnes, and are generally pure metals. These superconductors are unsuitable for magnet design because they have extremely low critical fields, generally less than 10^5 A/m, and the absence of a trapped magnetic field. Known as the Meissner effect, these superconductors effectively shield out a magnetic field within the superconductor except over a thin layer at the surface [3].

1.1.4 Type II Superconductors

Often referred to as ‘hard’ superconductors, Type II superconductors were first discovered in 1930 by Haas and Voogd when they combined an alloy of lead and bismuth [4]. Type II superconductors have normal islands in a sea of superconductivity known as the Abrikosov Vortex Lattice [5]. Compared to Type I superconductors, they have very high critical magnetic field and current densities due to this mixed magnetic state. Most Type II superconductors such as the intermetallic compounds of niobium tin and alloys of niobium titanium have critical temperatures below 20K. Modern superconducting materials research continues to push the envelope higher, increasing the critical temperatures in HTS to as high as 140K.

1.2 High Temperature Superconductors

1.2.1 Types of High Temperature Superconductors

The advent of HTS came with the discovery of La-Ba-Cu-O in April of 1986 by Bednorz and Muller [5]. Their initial HTS had T_c of 35K, and although the temperature was not as high as later copper oxide perovskites, it started a boom to discover better superconductors with higher critical temperatures. Figure 1-2 shows the most common of the hundreds of HTS discovered since then.

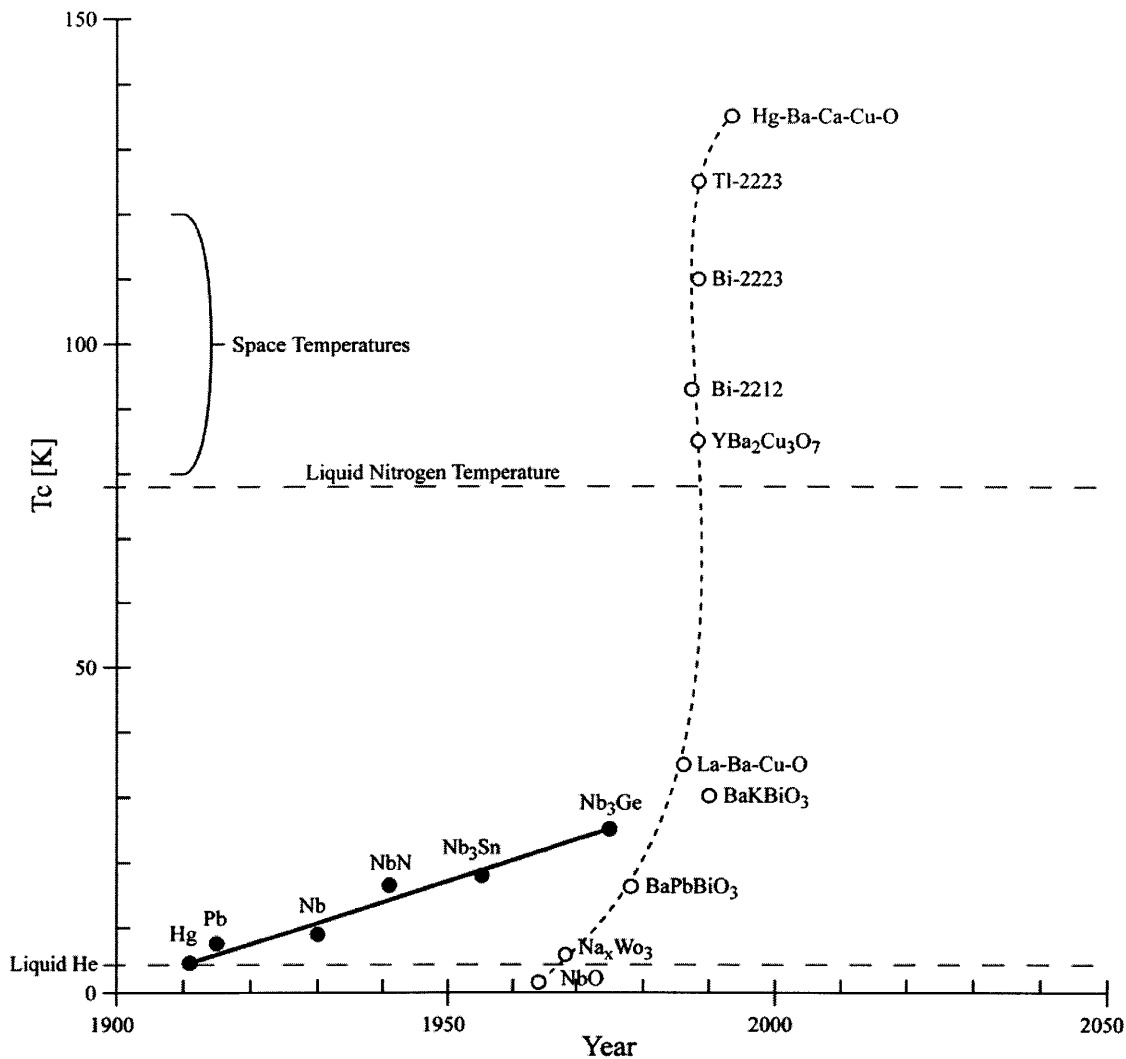


Figure 1-2. Evolution of T_c since the discovery of superconductivity [1 & 5].

1.2.2 Liquid Nitrogen Cooling

A significant advantage to HTS is that most can be used at a temperature as high as that of boiling liquid nitrogen, while most low temperature superconductors (LTS) require operation at liquid helium temperatures, of which the major disadvantage is greater cryogenic costs compared with operation at liquid nitrogen temperatures.

1.3 Thermal Stability

The superconductor must remain under its critical surface to remain superconducting. Although keeping the superconductor under its critical temperature is ideal, in typical applications, there are times when the temperature of the superconductor momentarily will rise above the critical temperature of the superconductor. Known as being driven

"normal" or "quenching", the superconductor becomes resistive. In this case, there must be some type of stabilization to the superconductor. Stabilization, often in the form of embedding the superconductor in a highly-conductive normal metal matrix, such as silver or copper, provides a resistive current path. Without this stabilization, the superconductor would burn out and the device would fail.

When a current-carrying superconductor is driven normal, it has two possible responses:

1. It recovers, meaning the quench-induced heating is balanced by the external cooling and the superconductor returns to the superconducting state.
2. It continues to generate heat, as heating exceeds cooling until the superconductor and metal matrix eventually burn out.

In a stabilized superconductor, as the temperature of the superconductor increases, "current sharing" will occur between the superconductor and the matrix alloys until eventually the matrix carries the entire current. In this case, the stabilizing matrix must be able to carry the entire load current until the conductor can recover without being burnt out. A heating-and-cooling balance must be achieved to ensure that the stabilization can carry the entire current of the sample if the superconductor is driven normal.

1.4 Overview

1.4.1 YBCO

This experiment will focus on coated YBCO, (yttrium barium copper oxide) with a critical temperature of 93 K. YBCO is the first superconductor to remain superconducting at liquid nitrogen temperatures. In the quest to develop better superconductors, this new ceramic has a higher critical current density than BSSCO superconductor.

The exponential slope of the V - I curve, referred to as the n -value of the superconductor, controls the rate at which the superconductor transitions to the resistive state. HTS, with lower n -values than LTS, are able to sustain current sharing over larger current ranges. The relations between current sharing, n -value, and temperature will be developed in Chapter 2.

1.4.2 Limits to Technology

Currently it is difficult to make coated YBCO conductors of length greater than 100 m. Efforts are being made to develop tape on the order of 1 km. Manufacturing difficulties include aligning the YBCO biaxially and ensuring a uniform textured buffer layer. For alignment control, several processes have been developed including ion-beam assisted deposition (IBAD), inclined substrate deposition (ISD), and rolling-assisted biaxially textured substrate (RABiTS).

Although YBCO has high current density its quenching phenomenon must be understood before YBCO can be used in power applications [6]. With so many advantages over BSSCO, companies are looking to use YBCO in magnets and other high current power applications. However, before YBCO can be used effectively, the stability of the superconductor must be well understood when it is driven normal.

1.4.3 Experimental Focus

To ensure that the superconductor remains stable, a balance must be obtained between the heating and cooling governed by the power equation. The general form of which is given in Equation 1-1 for a conductor cooled by liquid nitrogen [7].

$$V_{cd} \rho_{cd} C_{cd} \frac{\partial T}{\partial t} = V_{cd} \cdot \nabla (k_{cd} \nabla T) + G_j(T) - A_s \cdot q_{N_2}(T) \quad (1-1)$$

where,

V_{cd}	= Volume of the conductor	$[m^3]$
ρ_{cd}	= Density of the conductor	$\left[\frac{kg}{m^3} \right]$
C_{cd}	= Specific heat of the conductor	$\left[\frac{J}{kg \cdot K} \right]$
T	= Temperature	$[K]$
t	= Time	$[s]$
k_{cd}	= Thermal conductivity of the conductor	$\left[\frac{W}{m \cdot K} \right]$
G_j	= Joule heating of the conductor	$[W]$
A_s	= Surface area of the conductor exposed to liquid nitrogen	$[m^2]$
q_{N_2}	= Liquid nitrogen cooling flux	$\left[\frac{W}{m^2} \right]$

Using this equation as a base, we will develop a model to predict the limit at which YBCO conductors laminated with copper remains stable after an over-current pulse condition. An experiment will then be performed to verify the results developed in the model. In addition, we will explore the stability requirements for copper laminated YBCO superconductor.

Chapter 2

Model for Liquid Nitrogen Cooling

2.1 Model for Quench and Recovery in YBCO Superconductor

In order to develop an analytical model to predict the quench and recovery of YBCO, a simulation was developed using MATLAB. In the following sections, the equations used to generate the model are derived and explained, beginning with the power equation, then developing the heat transfer, and concluding with material properties. The actual program code for MATLAB is included in Appendix A.

2.1.1 Power Equation

The first place to begin with the development of a model for the thermodynamic behavior of a superconductor is through Equation 1-1. Expanding the conduction term for this equation in three dimensions yields Equation 2-1a:

$$V_{cd} \rho_{cd} C_{cd} \frac{\partial T}{\partial t} = V_{cd} k_{cd_x} \frac{\partial^2 T}{\partial x^2} + V_{cd} k_{cd_y} \frac{\partial^2 T}{\partial y^2} + V_{cd} k_{cd_z} \frac{\partial^2 T}{\partial z^2} + G_j(T) - A_s q_{N_2}(T) \quad (2-1a)$$

where,

$$k_{cd_i} = \text{Thermal conductivity of the entire conductor in the } i^{\text{th}} \text{ direction, } \left[\frac{\text{W}}{\text{m} \cdot \text{K}} \right]$$

The orientation of the superconductor with current terminals and coordinate axis is shown in Figure 2-1.

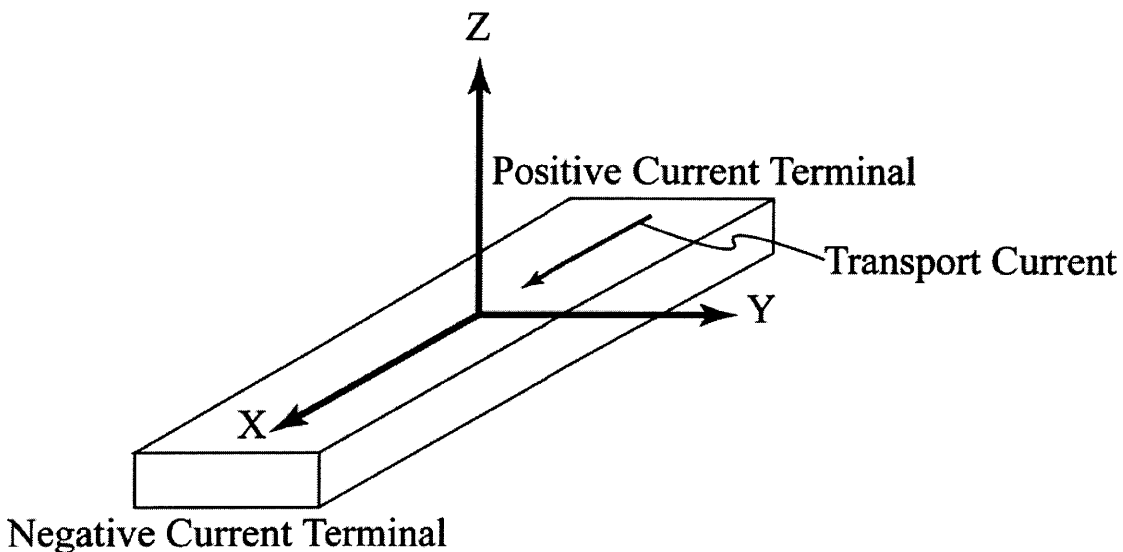


Figure 2-1. Coordinate axis orientation in sample with origin at midpoint of conductor.

For copper and silver stabilized samples, the rate of conduction given by the characteristic time constant in Equation 2-2 is controlled largely by the thermal diffusivity [8].

$$t_{c_i} = \frac{L^2}{\alpha} \quad (2-2)$$

where,

$$\begin{aligned} t_{c_i} &= \text{Characteristic time constant for conduction in the } i^{\text{th}} \text{ direction} && [\text{s}] \\ L &= \text{Length of the sample in the } i^{\text{th}} \text{ direction} && [\text{m}] \\ \alpha &= \text{Thermal diffusivity of conductor} && \left[\frac{\text{m}^2}{\text{s}} \right] \end{aligned}$$

Since silver and copper have extremely high thermal diffusivities, temperature changes in the entire conductor will propagate quickly. Consequently, the conductor is assumed to have uniform temperature in all three coordinate axes, and all the conduction terms cancel out of Equation 2-1a to produce Equation 2-1b.

$$V_{cd} \rho_{cd} C_{cd} \frac{\partial T}{\partial t} = G_j(T) - A_s q_{N_2}(T) \quad (2-1b)$$

With the simplified power equation, we can look specifically at the energy terms of the nitrogen cooling and joule heating. The cooling term given by $q_{N_2}(T)$ is comprised of a conduction and convection term as shown in Equation 2-1c:

$$V_{cd} \rho_{cd} C_{cd} \frac{\partial T}{\partial t} = G_j(T) - A_s h_{conv_{N_2}} \Delta T - V_{N_2} k_{N_2} \frac{\partial^2 T}{\partial i^2} \quad (2-1c)$$

where,

$$\begin{aligned} h_{conv_{N_2}} &= \text{Convective heat transfer coefficient} && \left[\frac{\text{W}}{\text{m}^2 \cdot \text{K}} \right] \\ V_{N_2} &= \text{Volume of liquid nitrogen} && [\text{m}^3] \\ k_{N_2} &= \text{Thermal conductivity of liquid nitrogen in the } i^{\text{th}} \text{ (x, y, z) direction} && \left[\frac{\text{W}}{\text{m} \cdot \text{K}} \right] \end{aligned}$$

Since the liquid nitrogen is boiling as a saturated liquid, the temperature of the nitrogen in the x and y directions are uniform; therefore, these two conduction terms are neglected. Similarly, the conduction term in the z-direction is neglected due to the formation of the liquid-vapor boundary layer during natural convection and ultimately boiling as conduction through this layer is very small. Eliminating these terms produces Equation 2-1d, leaving the dominating convective heat transfer term.

$$V_{cd} \rho_{cd} C_{cd} \frac{\partial T}{\partial t} = G_j(T) - A_s h_{conv_{N_2}} \Delta T \quad (2-1d)$$

Standard published data for the convective heat flux of liquid nitrogen was used in the numerical analysis and will be discussed in Section 2.2.

The second to the last term in Equation 2-1a is joule heating. This term comes from the dissipation of the current through the entire conductor matrix. If the current is less than the critical current of the superconductor, this term is zero. However, as the temperature of the conductor increases, current sharing with the resistive metal matrix produces Equation 2-1e.

$$V_{cd} \rho_{cd} C_{cd} \frac{\partial T}{\partial t} = I_{op} I_m R_m(T) - A_s h_{convN_2} \Delta T \quad (2-1e)$$

where

$$\begin{aligned} I_{op} &= \text{Total operating current in superconductor and metal matrix} && [\text{A}] \\ I_m &= \text{Current in the metal matrix} && [\text{A}] \\ R_m(T) &= \text{Resistance of the metal matrix} && [\Omega] \end{aligned}$$

2.1.2 Parallel Resistance Model

A superconductor must be stabilized with a metal matrix in order to provide current a conductive path to flow when the superconductor is not superconducting. For this experiment, the size and composition of the silver and copper laminates can vary. To understand the behavior of a superconductor and its interaction with the metal matrix, a parallel resistor circuit model is used to describe the current sharing that occurs as the superconductor is energized. The circuit model for this is shown in Figure 2-2. It includes all three modes of current distribution as the temperature of the superconductor increases.

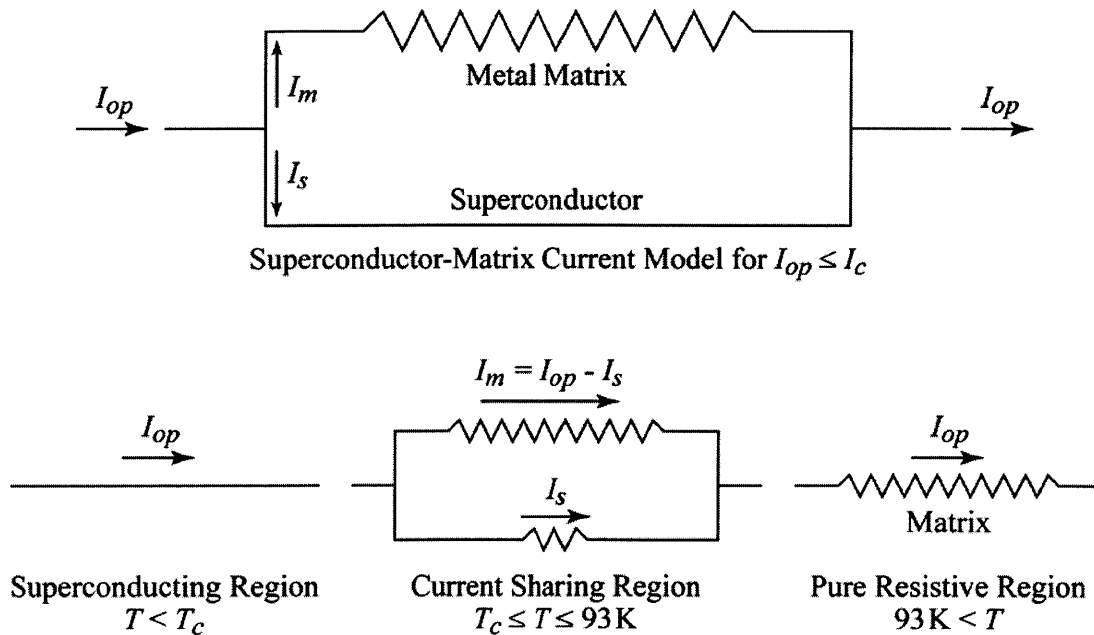


Figure 2-2. Circuit model for a composite superconductor. Above: Model for $I_t \leq I_c$.

Below: All three temperature ranges.

Below the critical temperature, the superconductor behaves like a short circuit as shown in the lower left most circuit model of Figure 2-2. As the current is increased above the superconductor's critical current, current sharing with the metal stabilizer occurs. As a result of the current sharing, there is resistive heating in the metal matrix, which, if not balanced by cooling causes the temperature of the conductor to rise. Due to increasing temperature, the voltage in the superconductor will rise with the onset resistivity. Since the superconductor is in parallel with the metal stabilizer, the voltage across the metal and superconductor must be the same, and is defined by Equation 2-3 [3].

$$V_s(T) = V_c \left[\frac{I_s}{I_c(T)} \right]^n \quad (2-3)$$

where,

$$\begin{aligned} V_s(T) &= \text{Voltage in superconductor} && [\text{V}] \\ V_c &= \text{Critical voltage parameter described as } 1\mu\text{V/cm} && [\text{V}] \\ I_s &= \text{Current in the superconductor} && [\text{A}] \\ I_c(T) &= \text{Critical current of the superconductor} && [\text{A}] \\ n &= \text{Index number for the superconductor} \end{aligned}$$

The critical current of the sample is measured experimentally in liquid nitrogen at 77.3 K, and for the simulation, is determined as a function of temperature using Equation 2-4 [9].

$$I_c(T) = - \left(\frac{I_{c77}}{0.1848} \right) \times \ln \left(\frac{T}{77.3} \right) \quad (2-4)$$

where,

$$I_{c77} = \text{Critical current measured in liquid nitrogen at } 77.3 \text{ K} \quad [\text{A}]$$

Due to the effect of the superconductors index number, the actual current in the superconductor can be higher than the critical current at 77.3 K. The index number, defined by the experimentally measured values in Equation 2-5, control the superconductor's voltage in the current sharing regime as the superconductor's current increases [3].

$$n = \frac{\ln(10)}{\ln \left(\frac{I_{5.0}}{I_{0.5}} \right)} \quad (2-5)$$

where,

$$\begin{aligned} I_{5.0} &= \text{Experimentally measured current when } V_s = 5.0\mu\text{V} && [\text{A}] \\ I_{0.5} &= \text{Experimentally measured current when } V_s = 0.5\mu\text{V} && [\text{A}] \end{aligned}$$

If the n -value is increased, the superconductor has a slower transition to the resistive state, and carries more current than a similar sample with a lower n -value at the same temperature. It is an important manufacturing goal to improve the n -value of HTS. Once the temperature of the YBCO rises above 93 K, due to its high resistivity, the

superconductor is neglected from the model and the voltage characteristics are controlled exclusively by the electrical resistivity of the metal stabilizer.

2.1.3 Numerical Solution

A solution to the model is obtained by fixing the time interval, $\Delta t = 0.001$ s. At any (k) time interval, the temperature of the conductor is determined by dividing the remaining heat not removed by the liquid nitrogen by the specific heat capacity of the conductor and adding this change in temperature to the previous interval's temperature. Due to the temperature dependence of the conductor's material properties, the resulting change in temperature produces a dynamic interaction that involves several iterations at each time interval to ensure the convergence of Equation 2-1e.

2.2 Heat Transfer

2.2.1 Overview

In this experiment, the heat flux through the surface of the conductor is a function of the temperature of the surface. The heat transfer mechanisms for liquid nitrogen cooling are divided into two categories: natural convection and pool boiling. Natural convection occurs until the temperature of the tape forces the heat transfer into a pool boiling regime.

Pool boiling is a complex heat transfer mechanism that can be divided into two regimes, nucleate and film boiling. Nucleate boiling starts when little droplets of vapor at the heater surface begin to nucleate on surface imperfections. As these vapor bubbles grow larger, they begin to depart from the surface of the heater when their buoyancy forces becomes significant.

As the heat flux from the heater is increased, the nucleate boiling will reach a maximum peak heat flux. This value occurs when the liquid down-flow to the surface cannot keep up with the rate at which the vapor bubbles leave the surface, resulting in the liquids inability to sustain a higher evaporation rate. Increasing the heat flux from the surface even slightly causes a dramatic jump in the surface temperature. Provided the input power remains constant, the maximum heat flux into the nitrogen will also remain constant. However, after a pulse, the power input decreases and as a result of this interruption in power flux, the nitrogen cooling can no longer sustain peak heat flux, and the cooling moves from the peak nucleate boiling regime into the film-boiling regime.

From the maximum change in temperature where the peak nucleate boiling heat flux stops, the nitrogen cooling follows a gradual decrease through the film-boiling regime, which occurs when the nucleating bubbles begin to form a vapor layer satisfying Taylor wave criteria across the surface of the conductor. Although stable, the convective heat transfer from the film regime does not decrease all the way to zero. There is a minimum heat flux where the film regime will revert back to the nucleate boiling regime through a state of constant minimum heat flux. Figure 2-3 illustrates the typical published heat transfer data from liquid nitrogen as a function of the change in temperature of the heater surface.

2.2.2 Simulation Model for Liquid Nitrogen Heat Transfer

To model the heat transfer for a pulsed heat flux, an algorithm was developed using MATLAB. When the current is held constant before the pulse, the sample is cooled through natural convection. In order to simplify the calculations for the natural convection heat transfer, the straight line shown in Equation 2-6a was adapted from the data of Merte and Clark to approximate the cooling through this regime [10].

$$q_{NC} = 901.3115 \times (\Delta T \times 1.8) \quad 77.3\text{K} \leq T < 79.2\text{K} \quad (2-6a)$$

where,

$$q_{NC} = \text{Natural convection heat transfer of liquid nitrogen,} \quad \left[\frac{\text{W}}{\text{m}^2} \right]$$

$$\Delta T = \text{Difference in temperature between sample and liquid nitrogen} \quad [\text{K}]$$

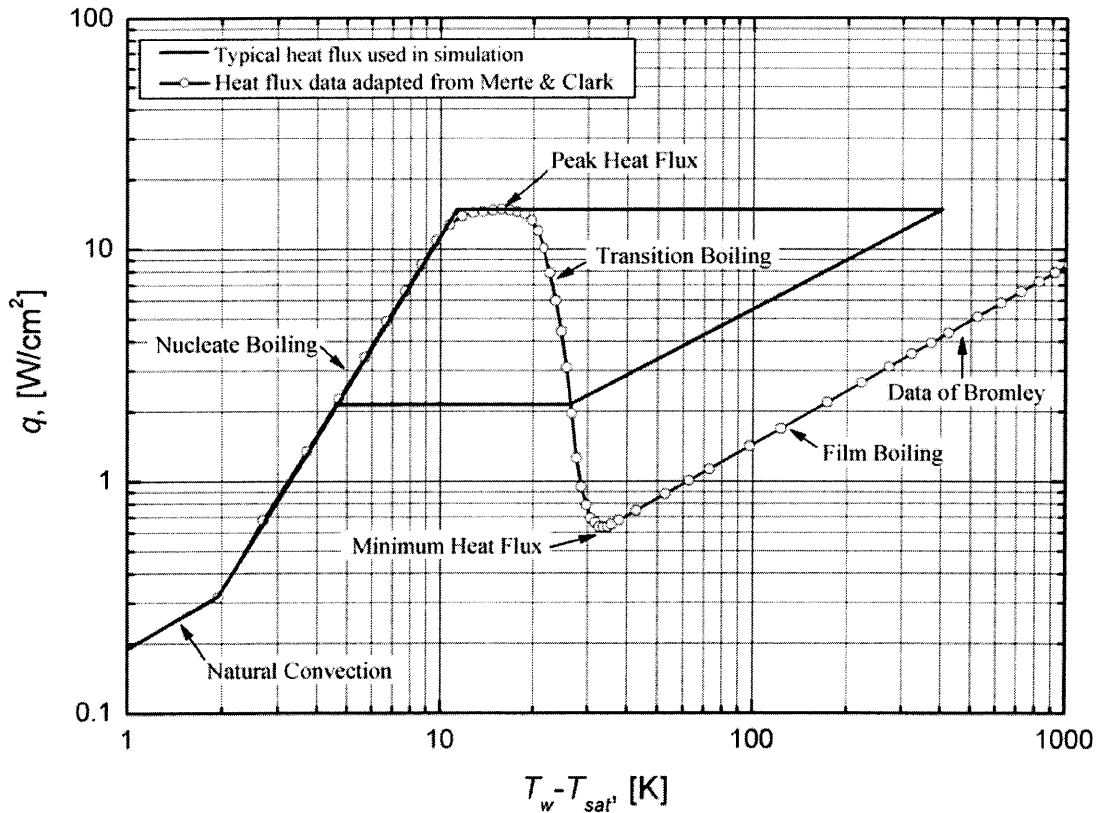


Figure 2-3. Standard liquid nitrogen heat flux adapted from the data of Merte and Clark with a typical curve from the simulation superimposed [10].

When the pulse is large, the natural convection regime transitions to the nucleate boiling regime. Since the maximum heat flux changes with pulse amplitude, it was determined that the temperature where the transition from nucleate boiling to the peak heat flux could range between 85-90 K. Using 88 K as a reference transition temperature to the maximum

heat flux $\left(\frac{I_p}{I_c} - 3\right)$ was added to this temperature. Adapted from the data of Merte and Clark, Equation 2-6b was used to define the nucleate boiling regime of the heat transfer [10].

$$q_{NB} = 207.8875 \times (\Delta T * 1.8)^{2.1709} \quad 79.2\text{K} \leq T < \left[88 + \left(I_p/I_c - 3\right)\right]\text{K} \quad (2-6b)$$

where,

$$q_{NB} = \text{Nucleate boiling heat transfer of liquid nitrogen} \quad \left[\frac{\text{W}}{\text{m}^2}\right]$$

Once the temperature of the sample exceeds the transition temperature for the peak heat flux, the temperature will continue to rise, but cooling will remain constant until there is an interruption in power or the sample burns out. The peak nucleate boiling heat flux, shown in Equation 2-6c, was adapted from the data presented by Merte and Clark [10].

$$q_{NB_{Peak}} = 207.8875 \times \left\{1.8 \times \left[10.7 + \left(I_p/I_c - 3\right)\right]\right\}^{2.1709} \quad \left[88 + \left(I_p/I_c - 3\right)\right] \leq T < T_{Peak} \quad (2-6c)$$

where,

$$q_{NB_{Peak}} = \text{Peak nucleate boiling heat transfer of liquid nitrogen}, \quad \left[\frac{\text{W}}{\text{m}^2}\right]$$

$$T_{Peak} = \text{Peak Temperature after pulse ends} \quad [\text{K}]$$

After the pulse, the power is interrupted and a maximum temperature is reached. At this point, the liquid nitrogen is unable to sustain peak heat flux and transitions to the film-boiling regime. Based on the material presented by Titus, I have chosen a film-boiling curve that follows a line parallel to the data presented by Bromely et al., but starts at the peak heat flux and maximum temperature immediately after the pulse [11]. The heat transfer to the liquid nitrogen for the film-boiling regime, described by Equation 2-6d, was adapted from the data presented by Merte and Clark [10].

$$q_{Film} = 3.15459 \times \frac{q_{NB_{Peak}}}{T_{Peak}^{0.7686}} \times (\Delta T \times 1.8)^{0.7686} \quad T_{Peak} \geq T > T_{Trans_1} \quad (2-6d)$$

where,

$$q_{Film} = \text{Film boiling heat transfer for liquid nitrogen} \quad \left[\frac{\text{W}}{\text{m}^2}\right]$$

$$T_{Trans_1} = \text{Transition temperature where Equation 2-6d and 2-7 intersect} \quad [\text{K}]$$

As the sample cools the heat transfer will remain in the film-boiling regime until it intersects the transition heat flux line defined by Equation 2-7, adapted from the standard boiling data of Merte and Clark [10]:

$$q_{Trans} = 2.52367 \times 10^{24} (\Delta T \times 1.8)^{-11.958} \quad 99\text{K} \geq T > 108\text{K} \quad (2-7)$$

where,

$$q_{Trans} = \text{Transition boiling heat transfer} \quad \left[\frac{\text{W}}{\text{m}^2} \right]$$

When Equation 2-6d intersects Equation 2-7, the heat flux will remain constant at the minimum film boiling heat flux for the temperature range shown in Equation 2-6e, which was adapted from the data presented by Merte and Clark [10].

$$q_{Film_{min}} = 3.15459 \times \frac{q_{NB_{Peak}}}{T_{Peak}^{0.7686}} \times \left[(T_{Trans_1} - 77.3) \times 1.8 \right]^{0.7686} \quad T_{Trans_1} \geq T > T_{Trans_2} \quad (2-6e)$$

where,

$$q_{Film_{min}} = \text{Minimum film boiling heat transfer for liquid nitrogen} \quad \left[\frac{\text{W}}{\text{m}^2} \right]$$

$$T_{Trans_2} = \text{Transition temperature where Equation 2-6e and 2-6b intersect} \quad [\text{K}]$$

Minimum film boiling heat flux will continue until Equation 2-6e intersects Equation 2-6b. From that intersection, the sample will continue to cool and the heat flux to the liquid nitrogen will pass back through the nucleate boiling and natural convection regimes, eventually reaching zero.

Equation 2-6 was incorporated into the MATLAB code. However, the equations for the material properties as functions of temperature were designed to run as stand-alone scripts that could be called in the main MATLAB program. Isolating these components streamlined the code to run efficiently, and they were easily modified as more accurate material data became available.

2.3 Copper Properties

This section presents piecewise equations for copper properties created from published data.

2.3.1 Specific Heat of Copper

The following equations, based on published data [8, 12] are used for specific heat of copper, $CuCp$ [J/kg · K].

$$CuCp = 368.53324(1 - e^{-0.02322T})^{3.65205} \quad 10K \leq T < 200K \quad (2-8a)$$

$$CuCp = 2.3181 \times 10^{-7} T^3 - 0.00052T^2 + 0.44648T + 287.47602 \quad 200K \leq T < 1200K \quad (2-8b)$$

Reference data and the supporting curve fit from OriginPro are provided as a supplement in Appendix B.

2.3.2 Resistivity of Copper

The resistivity of copper, $CuRes$ [$n\Omega \cdot m$] was also tabulated from cryogenic and room temperature sources [3, 13].

$$CuRes = -1.1787 \times 10^{-6} T^3 + 0.00067T^2 - 0.02399T + 0.3855 \quad 20K \leq T < 190K \quad (2-9a)$$

$$CuRes = 34.4038e^{\left(\frac{T+2715.04572}{2191.4633}\right)} - 118.11359 \quad 190K \leq T < 1300K \quad (2-9b)$$

Reference data and the supporting curve-fit from OriginPro are provided as a supplement in Appendix B.

2.4 Silver Properties

2.4.1 Specific Heat of Silver

Tabulated data for the specific heat of silver, $AgCp$ [$J/kg \cdot K$] were curve-fit from cryogenic and room temperature sources to produce Equation 2-10 [8, 14].

$$AgCp = 571302.22046T^{0.00011} - 571442.51725 \quad 10K < T < 1200K \quad (2-10)$$

Reference data and the supporting curve-fit from OriginPro are provided as a supplement in Appendix B.

2.4.2 Resistivity of Silver

Similarly, Equation 2-11, a piecewise function for the resistivity of silver, $AgRes$ [$n\Omega \cdot m$] was determined from a curve-fit of cryogenic and room temperature data [3, 13].

$$AgRes = -1.0796 \times 10^{-6} T^3 + 0.00046T^2 + 0.01555T - 0.38874 \quad 0K \leq T < 293K \quad (2-11a)$$

$$AgRes = 00685T - 3.77476 \quad 293K \leq T < 1000K \quad (2-11b)$$

Reference data and the supporting curve-fit from OriginPro are provided as a supplement in Appendix B.

2.5 Material Properties of Substrate

The substrate used in both the American Superconductor Inc. (AMSC) and SuperPower Inc. (SPI) tapes were derived from nickel alloys. The AMSC substrate was composed of nickel with 5%W RABiTS, while the SPI substrate was composed of Hastaloy C. The specific heat of nickel, $C_{p_{Ni}}$ [J/kg·K] is used for both substrates because of their high nickel content. Equation 2-12 is a piecewise construction of the specific heat of nickel, comprised from cryogenic and room temperature data [8, 15].

$$C_{p_{Ni}} = 8890 \times 10^{15,503.108 - 37,280.377 \text{Log}(T) + 26,788.417 \text{Log}(T)^2 + 7,010.0877 \text{Log}(T)^3 \dots}$$

$$-22,731.651 \text{Log}(T)^4 + 15,386.526 \text{Log}(T)^5 - 5,175.7968 \text{Log}(T)^6 \dots$$

$$+896.97274 \text{Log}(T)^7 - 64.055866 \text{Log}(T)^8 \quad 55\text{K} \leq T \leq 300\text{K} \quad (2-12a)$$

$$C_{p_{Ni}} = 8,890 \times (0.1581T + 410.24) \quad 300\text{K} < T \quad (2-12b)$$

Since Equation 2-12a was provided by NIST, the curve-fit data associated with the material properties is not required whereas Equation 2-12b was derived from the linear interpolation of the tabulated data from Mills [8, 15].

2.5.1 AMSC Substrate Resistivity

The resistivity, $SubRes_{AMSC}$ [nΩ·m] shown in Equation 2-13 for nickel with 5%W RABiTS substrate, was provided by AMSC [9].

$$SubRes_{AMSC} = 4.717 \times 10^{-10} T + 2.28491 \times 10^{-7} \quad 77\text{K} \leq T < 1000\text{K} \quad (2-13)$$

2.5.2 SPI Substrate Resistivity

In contrast, for the SPI samples, the resistivity was measured in the lab at both liquid nitrogen and room temperatures. However, since there was very little variation between the cryogenic and room temperature resistivity, a constant value of $SubRes_{SPI} = 1.30 \times 10^{-6}$ [nΩ·m] was used for all temperature ranges.

2.6 Material Properties of YBCO

2.6.1 Specific Heat of YBCO

Due to the effect of the short coherence lengths YBCO superconductor can have local fluctuations in and out of the superconducting state without affecting the entire tape. The effects of the local fluctuations in and out of the superconducting state can be seen in the specific heat, thermal conductivity, and magnetic susceptibility of the sample. Each of these properties change anomalously around the superconducting transition temperature of the sample [16]. In particular, the specific heat of YBCO has two distinct jumps near its superconducting transition temperature.

Aravind and Fung attribute the dip in the thermal diffusivity at the onset of resistivity to an abrupt increase in the electron specific heat as the sample moves from the resistive to superconducting states within the individual grains. They further speculate that the increase in the thermal diffusivity below the critical temperature is due to the increase in the mean free path of photons, which occurs as the charge carriers condense to form Cooper pairs [16].

Aravind and Fung have developed the most thorough results for the cryogenic specific heat of YBCO, $C_{p_{YBCO}}$ [J/kg · K]. Equation 2-14a-f is a piecewise curve-fit combining their data with the data of Roulin et al. [16, 17].

$$C_{p_{YBCO}} = 1.2173T + 91.659 \quad 77.4\text{K} < T \leq 80.5\text{K} \quad (2-14a)$$

$$C_{p_{YBCO}} = -19.423T + 1752.4 \quad 80.5\text{K} < T \leq 84\text{K} \quad (2-14b)$$

$$C_{p_{YBCO}} = 5.0661T - 304.24 \quad 84\text{K} < T \leq 90\text{K} \quad (2-14c)$$

$$C_{p_{YBCO}} = -3.9285T + 504.7 \quad 90\text{K} < T \leq 92\text{K} \quad (2-14d)$$

$$C_{p_{YBCO}} = -456.60151 \times e^{\frac{-T}{65.99887}} + 260.40759 \quad 92\text{K} < T \leq 200\text{K} \quad (2-14e)$$

$$C_{p_{YBCO}} = -0.0183T^2 + 11.254T - 1281.1 \quad 200\text{K} < T \leq 300\text{K} \quad (2-14f)$$

Equally important to the specific heat data at cryogenic properties are those between 300-1000K. Most studies into YBCO stability neglect these room temperature properties, but the present study shows that these are in fact the most relevant values for the heat transfer from a pulsed conductor. Through the pulse induced quench process, the sample exceeds the cryogenic temperature range within a few milliseconds. After reaching room temperatures, the sample then remains well above cryogenic temperatures for more than a few seconds. Consequently, these room temperature material property values dramatically influence the quench recovery criteria.

Matskevich and Stenin show an additional anomaly in the specific heat near 500K [18]. The behavior of the specific heat in this region may explain why the superconductor appears to degrade around this temperature range. The anomalies in these measurements coincide with previous data taken for the linear-expansion coefficient by White et al. [19]. Matskevich and Stenin propose that the additional phase transition at 500K is due to the elongation of the bonds in the $\text{Cu}_2\text{-O}_4$ layers. They also concluded that the temperature for these anomalies change depending on the amount of apical oxygen doping in the CuO_2 plane.

On the range of 300-900K, Matskevich and Stenin define the specific heat by Equation 2-14g-h [18]:

$$C_{p_{YBCO}} = 334.68 - 0.28854T + 5.7220 \times 10^{-4}T^2 \quad 300\text{K} < T \leq 500\text{K} \quad (2-14g)$$

$$C_{p_{YBCO}} = 316.92 - 0.10258T + 1.9478 \times 10^{-4}T^2 \quad 500\text{K} < T \leq 900\text{K} \quad (2-14h)$$

For the specific heat of YBCO, the supporting curve-fit for the cryogenic values from OriginPro are provided as a supplement in Appendix B.

Chapter 3

Experimental Verification of Model

3.1 Experimental Setup

3.1.1 Sample and Fixture

To ensure that each sample had the same orientation during each experiment, a fixture was fabricated to hold the samples in a liquid nitrogen bath. Copper current leads were connected to the sample. These leads, shown in Figure 3-1, allow the power supply cables to be bolted to the sample. The copper current leads provide a 1.5-cm overlap for the power supply cable lugs and a 1.2-cm overlap on the YBCO tape.

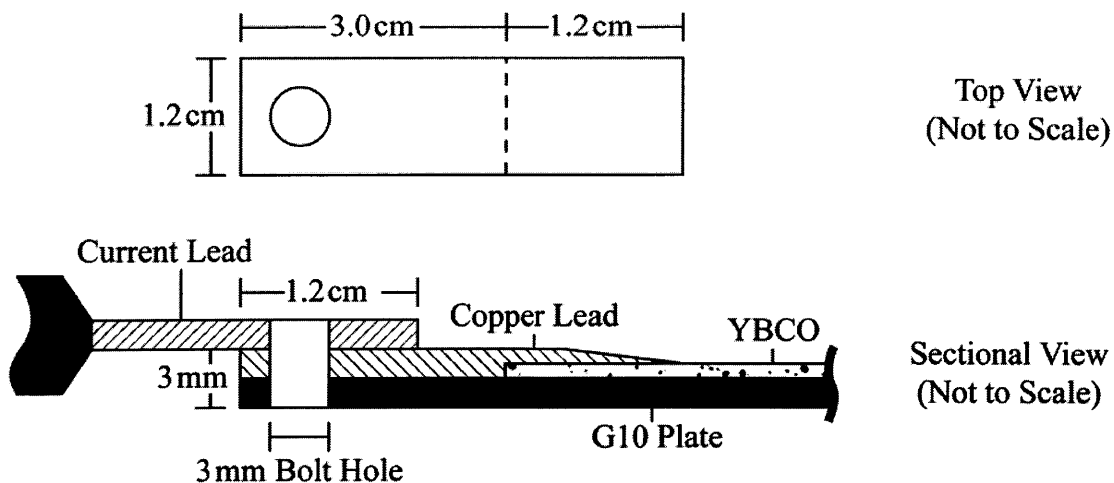


Figure 3-1. Copper leads to connect power supply lugs to YBCO sample.

In order to mount the sample to the copper current leads and minimize the contact resistance, the following procedure was used, as adapted from AMSC [20]:

1. Set soldering iron to 200°C to prevent overheating and damage to sample
2. Using Tix flux, tin the copper leads and the top of YBCO sample with Indium (66%) and Bismuth (33%) solder
3. Wipe leads and sample to remove excess flux with alcohol
4. Applying heat to the back of the sample, press it into the solder on the copper leads
5. Re-swab sample and current leads with alcohol to remove excess flux

After the sample was mounted onto the current leads, it was reinforced with a G-10 plate. The G-10 plate provided a stable base for the sample and allowed additional space for other components including the thermocouples and voltage tabs. The complete assembly,

shown in Figure 3-2, illustrates the three large clamps for the thermocouples, a thermocouple reference node, and the power supply's copper current leads. It is also important to note that the G-10 plate acts as a thermal insulator to the backside sample, which is treated as adiabatic.

Gold-Chromel thermocouples were used for the temperature measurements of the sample. Each thermocouple was clamped on the sample's surface and electrically insulated with a 25- μm layer of Kapton tape. To insulate the thermocouple from the liquid nitrogen, it was covered with a 2-mm thick Styrofoam sheet.

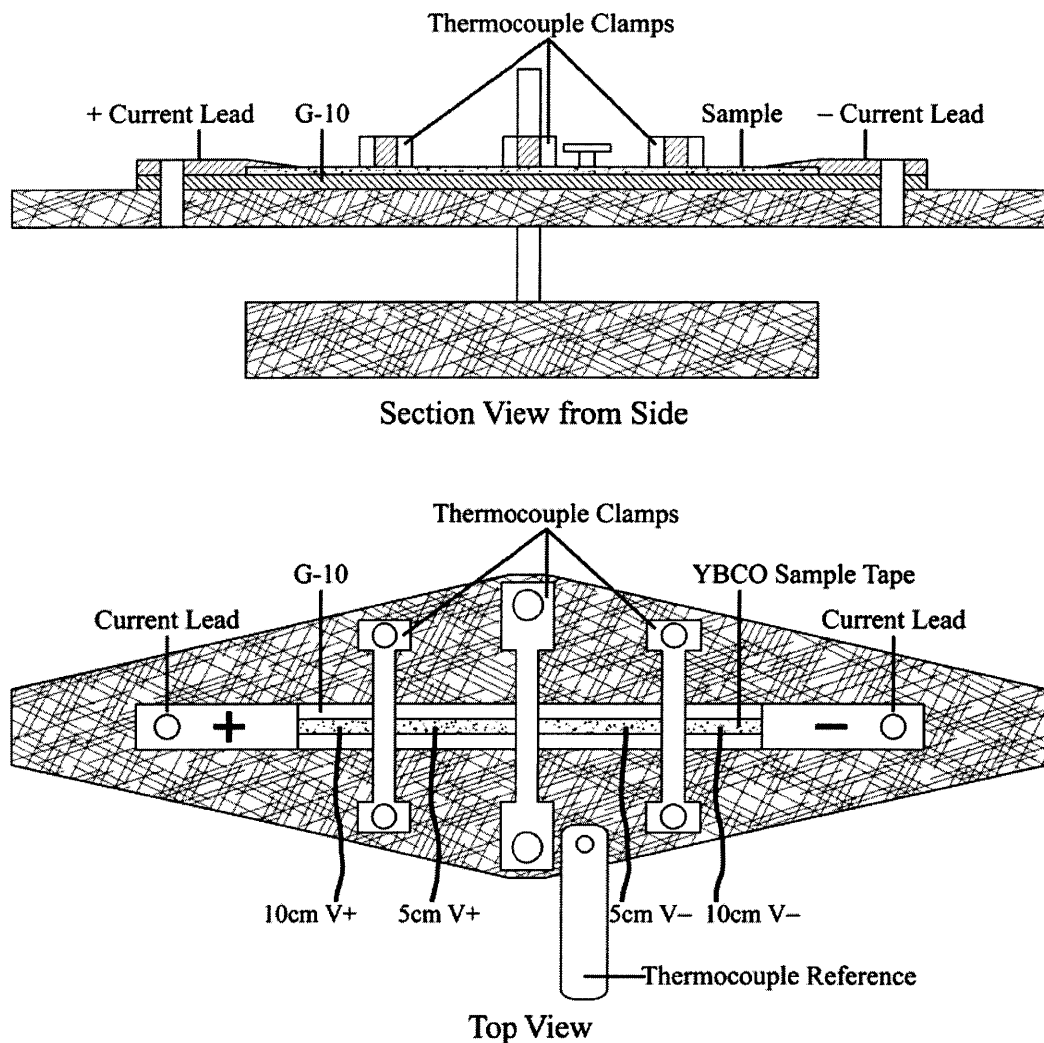


Figure 3-2. Complete sample holder and test assembly for liquid nitrogen cooling, shown in approximate scale except sample thickness, which has been exaggerated to show detail.

Trillaud et al. note that clamping the thermocouples would cause tiny imperfections in the surface of the YBCO that reduce the current capacity of the tape [21]. However, our test samples have shown there is no degradation in the current capacity. The absence of current degradation may be attributable to the presence of the copper lamination. The clamp assembly is shown in Figure 3-3 with enlarged details of the individual components. To achieve uniform clamping pressure between experiments, screws holding the thermocouple clamps were hand tightened to approximately the same torque.

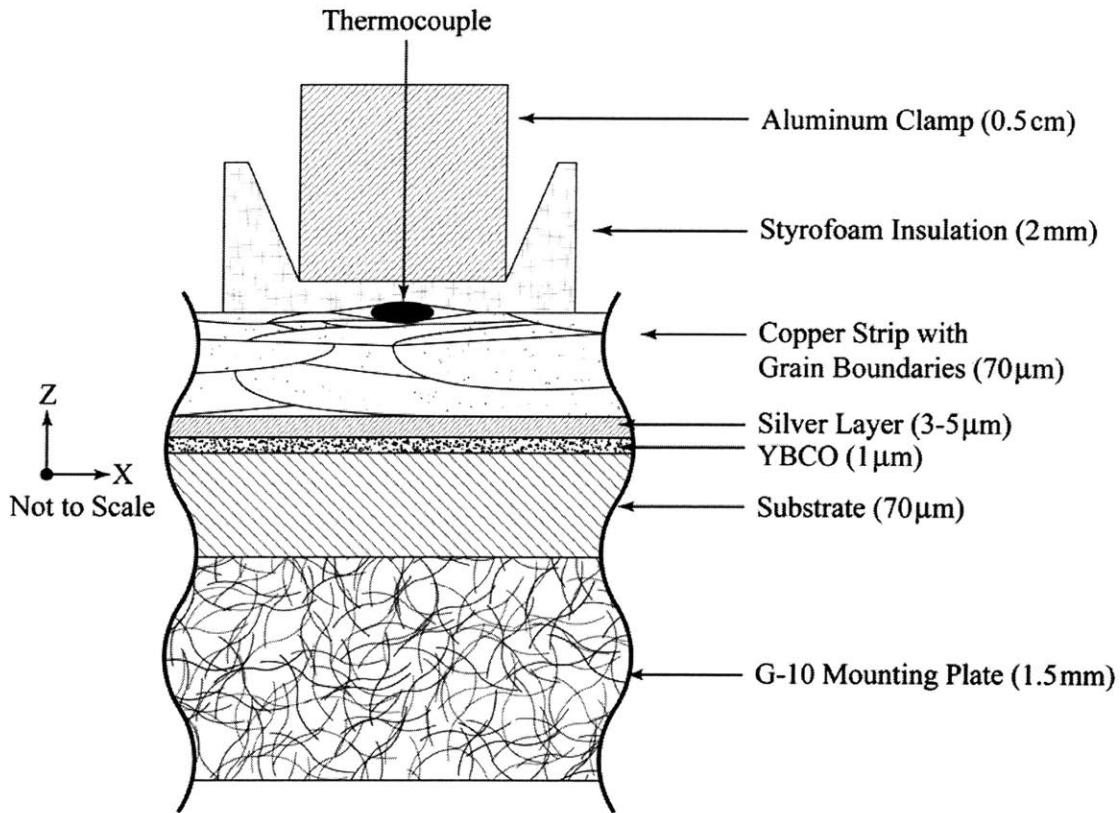
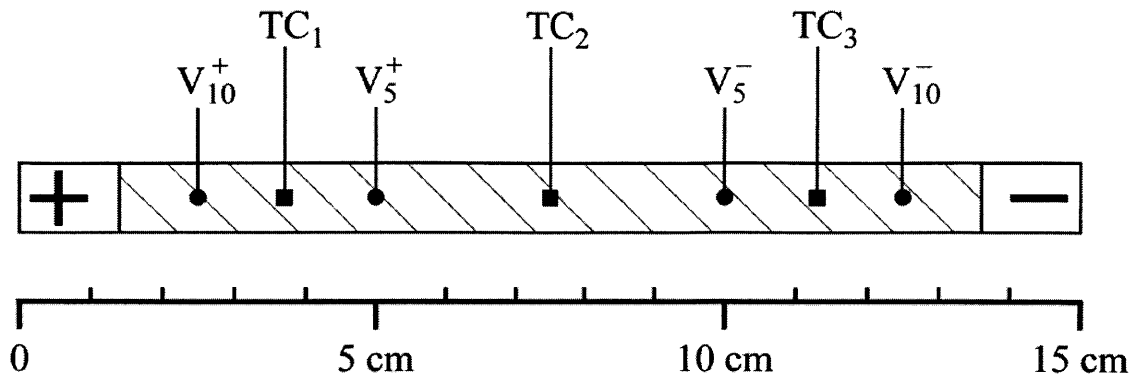


Figure 3-3. Detailed sectional side view of thermocouple clamp system and the absorption of the pressure from the thermocouple into copper stabilizer and Styrofoam.

A reference temperature node for each thermocouple, at boiling liquid nitrogen (77.3K), was attached to the side of the G-10 sample holder. At these reference nodes, the thermocouples were attached to the copper signal wires that are connected to the data acquisition (DAQ) system.

Two sets of voltage taps were soldered to the samples, one set 5-cm apart and the other 10-cm apart. The location of the voltage taps and thermocouples mounted on the YBCO sample are schematically shown in Figure 3-4.



Hatched surface exposed to liquid nitrogen cooling

Figure 3-4. Location of voltage taps and thermocouples on 15-cm long YBCO sample.

3.1.2 Experimental Procedure

In order to quench the YBCO sample it was subjected to an over-current pulse. First, the sample remains superconducting at an operating current, set at 90% of the critical current. This represents a typical operating condition. The sample is then subjected to an over-current pulse that drives the entire length of the sample to a normal resistive state. After the pulse, the current is reduced to the initial operating current. The pulse amplitude ranged 2-12 times the critical current.

Before each pulse run, the sample's critical current, an electric field criterion of $1 \mu\text{V}/\text{cm}$, was measured. From this, we determined the n -value of the superconductor [3]. The critical current was measured before each pulse run to determine if the sample experienced degradation during the previous run.

Figure 3-5, shows a typical current vs. time function used in the measurement. In this experiment, a square pulse of duration (τ_{pulse}) in the range 100-1000ms was used. The quench behavior during and after the current pulse was recorded. In order to generate an over-current pulse of up to 600 A, six 100-A power supplies (HP6260B) were connected in parallel.

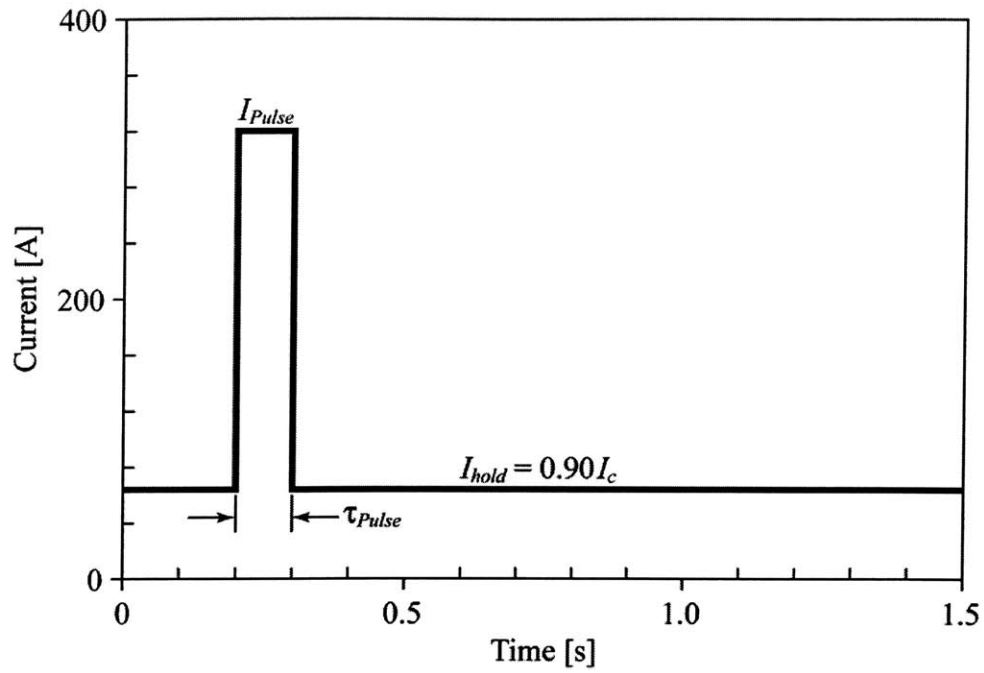


Figure 3-5. Typical current pulse generated by HP6260B power supplies for experiment.

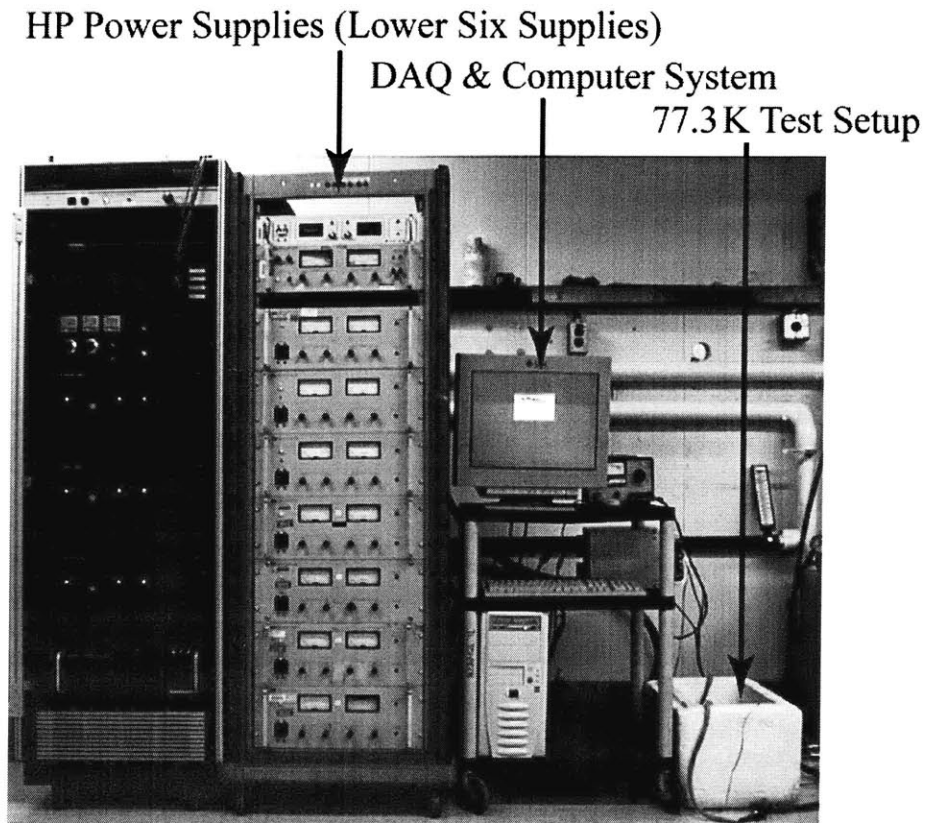


Figure 3-6. Experimental setup with power supplies, DAQ, and test setup.

The power supplies were controlled with a voltage-programming signal generated in LabVIEW. LabVIEW was set up to allow synchronous power supply programming with data acquisition. The LabVIEW system is detailed in the following sections and an overview of the experimental setup is shown in Figure 3-6.

3.2 Data Acquisition System

3.2.1 Equipment and Setup

A National Instruments 12-bit PCI-AT-MIO-16E data acquisition (DAQ) card was used to synchronize and control the analog input and output for the experiment. With this DAQ card, two separate control systems were created for the analog output. The first provided a slow current ramp signal to the power supplies, while the second provided the programmable holding current and pulse.

For the current ramp program, a signal wire with a voltage divider was used to connect the DAQ output to the power supply's programming signal. By using the full DAQ output scale and a voltage divider, we were able to ramp the current as slow as 0.5 A per second. The voltage divider introduced an RC interaction within the programming circuit that caused the power supplies to compensate and ramp according to the program requirements [22]. To control the pulse current, a regular signal wire without a voltage divider was used, and this had to be switched with the other signal wire depending on the desired test mode. A separate LabVIEW code was also generated to ensure the proper output voltage signal.

Together with an SCXI-1000 chassis, LabVIEW 7.1 software was used to collect and interpret the experimental data. The SCXI chassis was configured with one SCXI-1120D and two SCXI-1120 modules, which allowed the user to configure individual gain and filter settings for each channel. Connected to these modules, SCXI-1320 terminal blocks were used for input connections. Table 3.1 lists the configurations used for this experiment and their corresponding signal sources.

Although there were only two input voltage signals from the voltage taps, one 5-cm taps and the other 10-cm taps, eight channels were used to record a set of data. The signal from each channel was recorded at four amplification settings to avoid saturation of the DAQ channels. For the over-current pulse experiments, it was determined that the best filtering was a 10-kHz low-pass filter on each voltage signal. In contrast, a 4-Hz filter with a gain of 1000 was used for the voltage measurements in determining the critical current, however, the rest of the signals were measured with a 10-kHz low-pass filter. To verify the signal range and acquired values, Keithley 155 multimeters were used to monitor the signals in addition to the LabVIEW system.

Table 3.1 SCXI chassis configuration and filters settings.

Module 1 SCXI-1120D			
Channel	Gain	Low-Pass Filter Frequency	Signal
1-1	100	4.5kHz	Shunt resistor across power supplies
Module 2 SCXI-1120			
Channel	Gain	Low-Pass Filter Frequency	Signal
2-0	1	10kHz	5-cm Voltage tap - Pulse experiment
2-1	10	10kHz	5-cm Voltage tap - Pulse experiment
2-2	100	10kHz	5-cm Voltage tap - Pulse experiment
2-3	1000	10kHz	5-cm Voltage tap - Pulse experiment
2-4	1	10kHz	10-cm Voltage tap - Pulse experiment
2-5	10	10kHz	10-cm Voltage tap - Pulse experiment
2-6	100	10kHz	10-cm Voltage tap - Pulse experiment
2-7	1000	10kHz	10-cm Voltage tap - Pulse experiment
Module 3 SCXI-1120			
Channel	Gain	Low-Pass Filter Frequency	Signal
3-0	1000	4Hz	5-cm Voltage tap - Ramp experiment
3-1	1000	4Hz	10-cm Voltage tap - Ramp experiment
3-2	100	10kHz	Thermocouple one
3-3	1000	10kHz	Thermocouple one
3-4	100	10kHz	Thermocouple two
3-5	1000	10kHz	Thermocouple two
3-6	100	10kHz	Thermocouple three
3-7	1000	10kHz	Thermocouple three
Module 4 Analog Output Hardwired from DAQ Card			
Channel	Gain	Filter Frequency	Signal
AO-0	-	-	Analog output voltage for pulse control
AO-1	-	-	Analog output voltage for ramp control

3.2.2 Software Analysis

Both the LabVIEW control programs for the ramp and over-current pulse were designed to write an analog output for each point the DAQ acquired. The scan and output rate was set to 1.0-kHz, which allowed the use of 0.001 s discretizations in the simulation. The code used for each of these LabVIEW applications are provided in Appendix C. Once the data were written to a text file, OriginPro was used to plot the data. To enhance the clarity the thermocouple data were smoothed with a 100-point adjacent averaging technique.

3.3 Block Diagram

The block diagram for the experiment is shown in Figure 3-7. The components and their connections to each other are illustrated, but the specific wiring diagram between the sample and the DAQ system are shown in Appendix D.

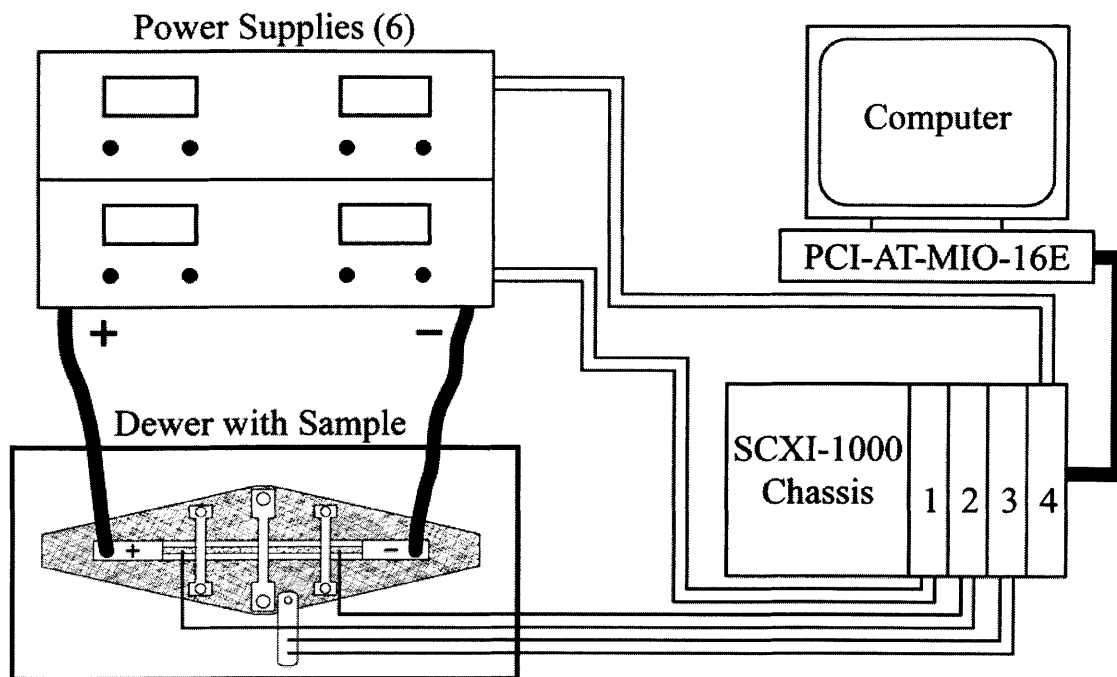


Figure 3-7. Overall block diagram for experimental setup.

Chapter 4

Experimental Results

4.1 Silver Only Stabilized Conductor: AMSC 10-mm Width

4.1.1 Sample Specifications

Bare YBCO samples from American Superconductor Inc. (AMSC) were provided in 10-mm widths. Each sample was laminated with a 3-8 μ m layer of silver. The laminate compositions for the AMSC silver-only samples, shown in Figure 4-1, were measured by AMSC to have the dimensions and critical currents listed in Table 4-1. All AMSC samples were prepared by the RABiTS method.

4.1.2 Experimental and Simulated Results

Sample BDOE-L590 burned out after 6 pulses, but due to saturation problems near the burnout voltage with the preliminary DAQ system settings, only experimental data for the fourth pulse was compared to the simulation. Figure 4-2 shows the virgin critical current for the sample.

Figure 4-3 shows the fourth pulse with the corresponding simulated voltage and temperature. Although the experimental and simulated voltages agree well, the experimental and simulated temperatures do not. The experimental results did not record a temperature rise; this absence of a temperature rise is likely caused by poor thermal insulation of the thermocouple from the liquid nitrogen. In these initial measurements, the thermocouples were not well-insulated.

Figure 4-4 shows a simulation result that predicts the non-recovery limit for this sample. The simulated quench current of 225 A differs from the observed experimental burnout value of 221 A observed in run 5, however, since sample burned out immediately after the pulse, the experimental results cannot be compared with the simulated result.

For silver-only samples, if the Joule dissipation remains below the peak nucleate flux, the sample will recover. On the other hand, if the Joule dissipation exceeds the peak nucleate heat flux, the sample will quench.

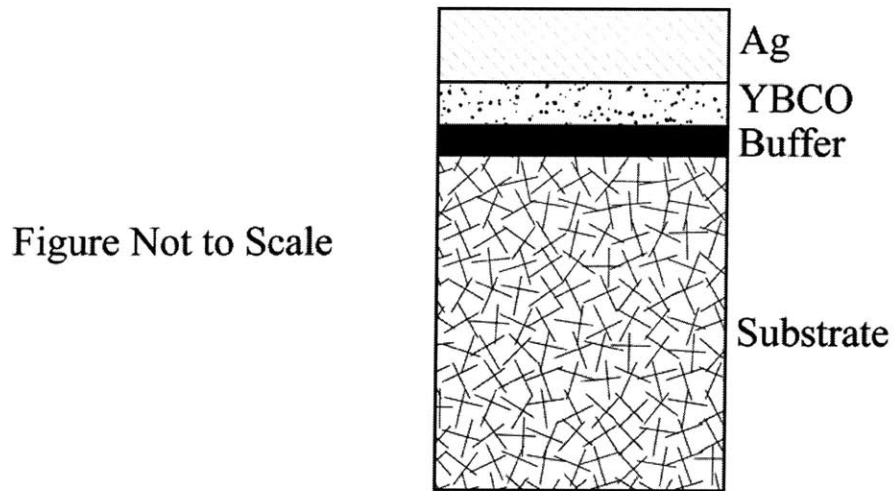


Figure 4-1. Layer arrangements in sample for silver-only laminated superconductor.

Table 4-1. Specifications for 10-mm wide AMSC Ag stabilized samples.

Sample	BDOE-L590
Manufacturer	AMSC
Ag Thickness	3-8 μm
YBCO Thickness	1 μm
Buffer Thickness	0.3 μm
Substrate Thickness	76 μm
Width	10 mm
Length	9.5 cm
I_c^*	138.0 A ¹

* 77.3K self field with a 1- $\mu\text{V}/\text{cm}$ criterion

¹ Measured by AMSC

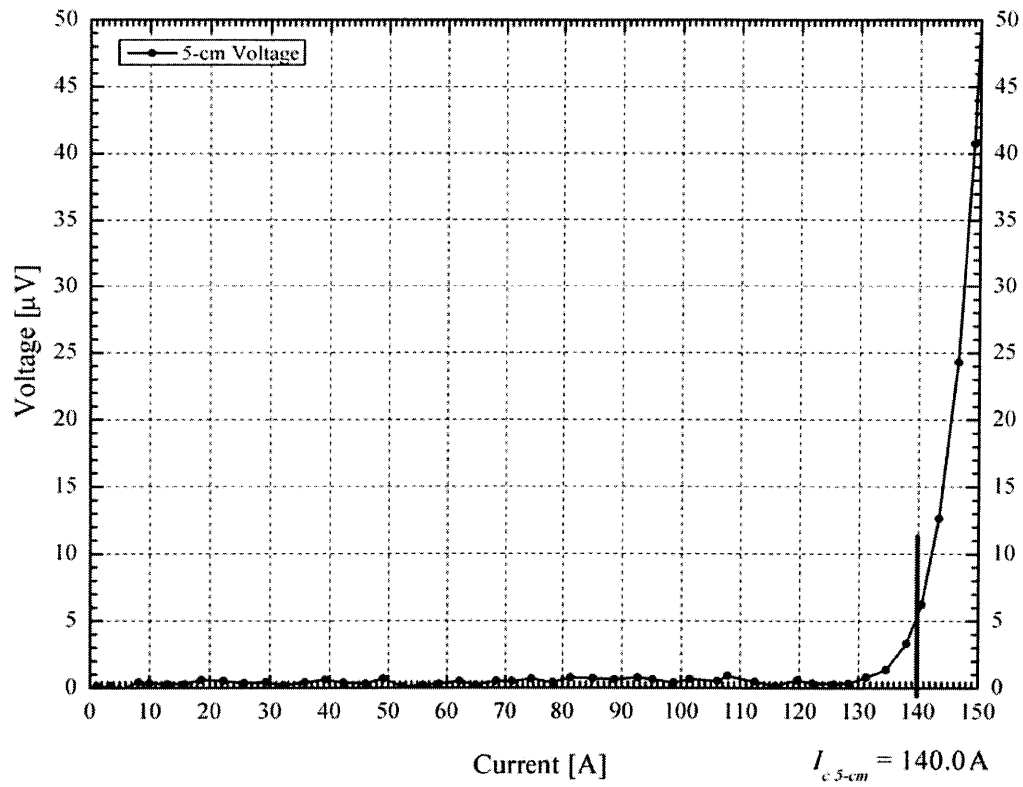


Figure 4-2. Virgin run for sample BDOE-L590. Measured using 5-cm voltage taps; $I_c = 140\text{ A}$ with a $1\ \mu\text{V}/\text{cm}$ criterion.

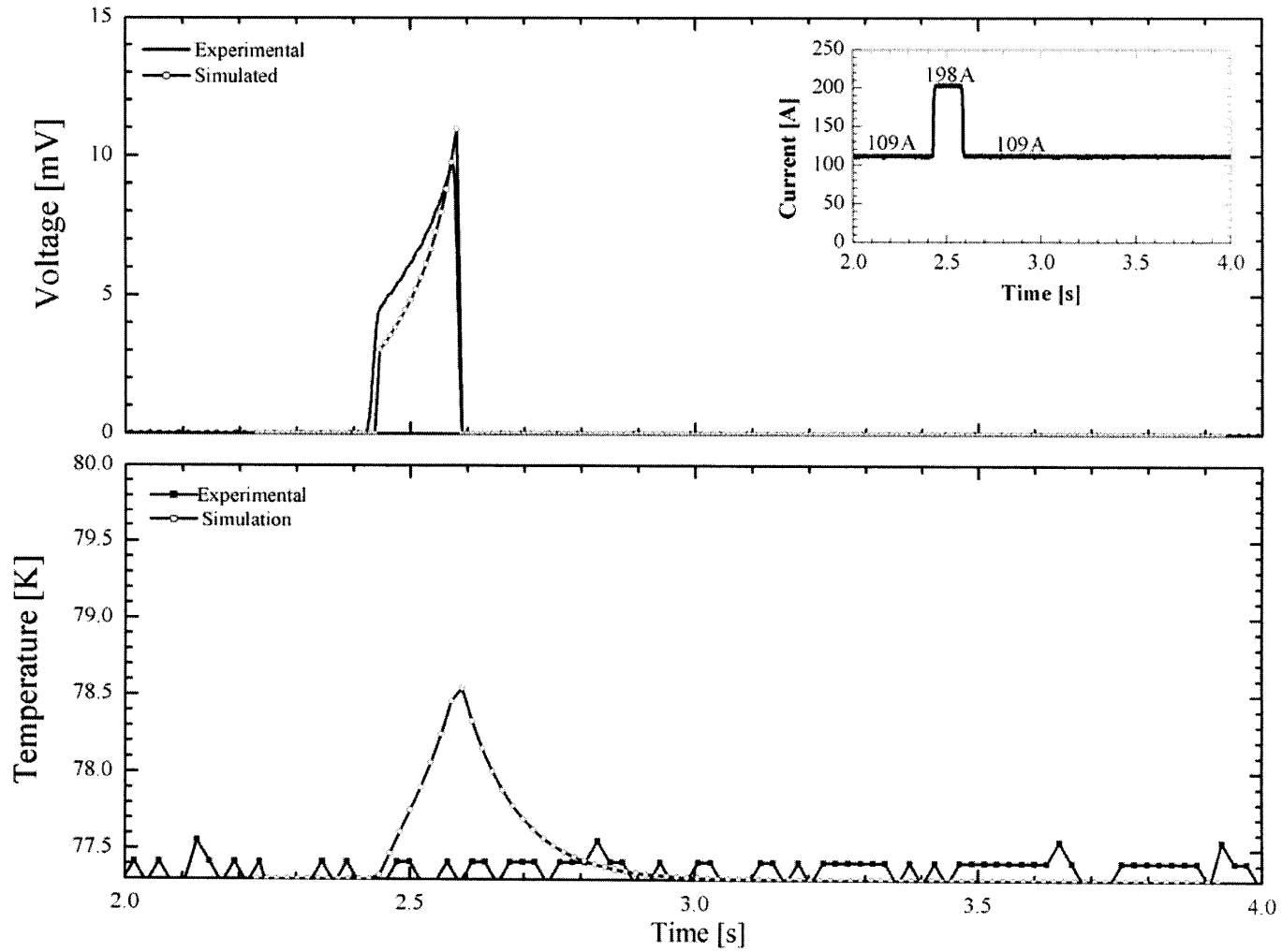


Figure 4-3. Sample BDOE-L590: Run 4, $\tau = 150\text{ms}$, $t_{\text{hold}} = 7.0\text{s}$, $I_{op} = 109\text{A}$, $I_p = 198\text{A}$, $I_p/I_c = 1.41$.

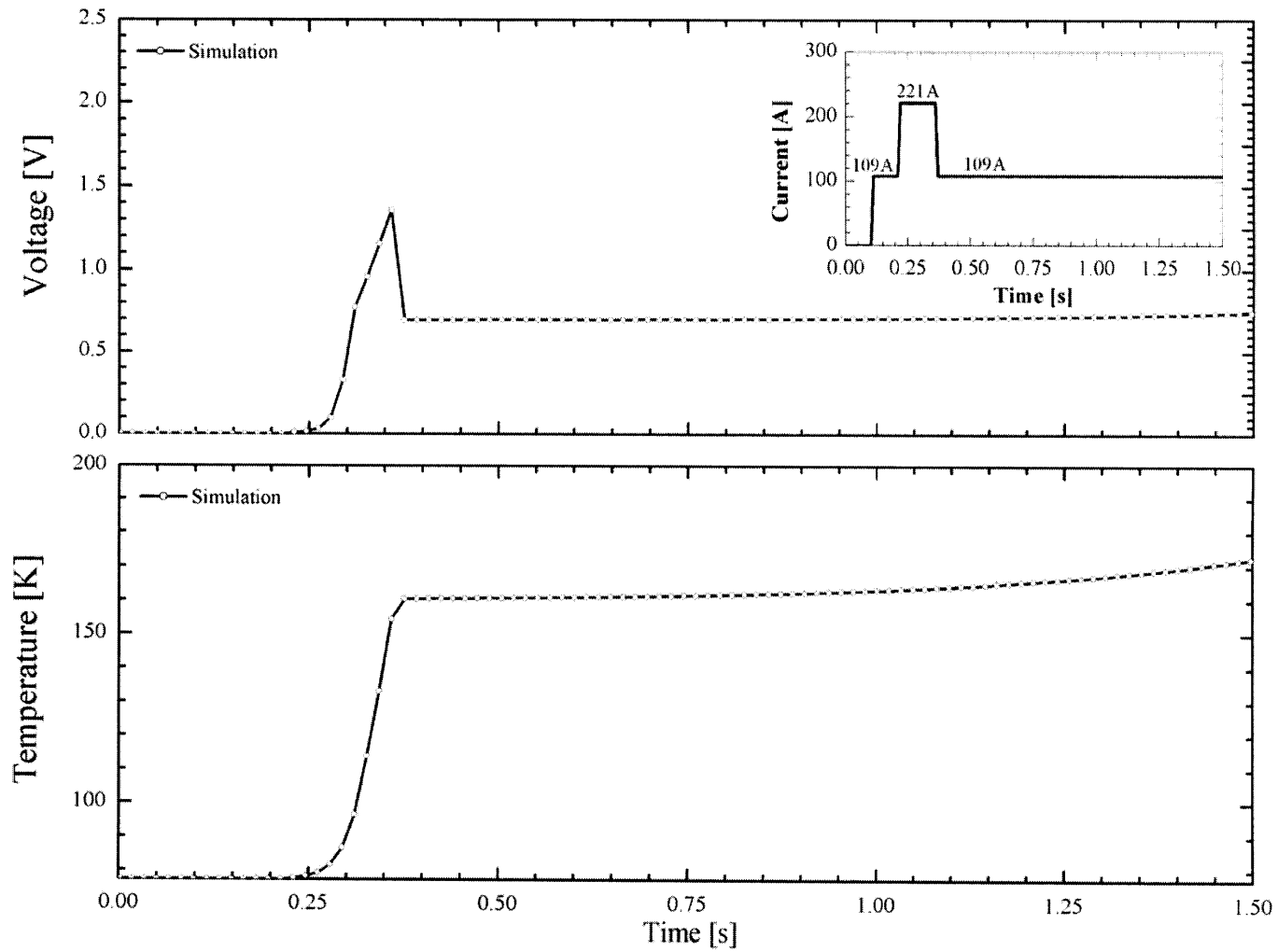


Figure 4-4. Sample BDOE-L590: Simulated results showing non-recovery. $\tau = 150\text{ms}$, $t_{hold} = 7.0\text{s}$,
 $I_{op} = 109\text{A}$, $I_p = 221\text{A}$, $I_p/I_c = 1.58$.

4.2 Silver Only Stabilized Conductor: SPI 4-mm Width

4.2.1 Sample Specifications

The samples provided by SPI, manufactured with the IBAD buffering technique were each 30-cm in length. They were cut in half to prepare two 15-cm long samples, designated 1 and 2, for each half of the alphabetical sample. The typical cross sectional view of these samples is shown in Figure 4-1 and the corresponding layer dimensions are shown in Table 4-2.

4.2.2 Experimental and Simulated Results

Sample SPCC-Ag-A-2 burned out during the first pulse with a I_p/I_c ratio of 1.52, illustrating the vulnerability for non-copper stabilized samples to fail as a result of an over-current pulse. Similarly, sample SPCC-Ag-B-1 burned out after the fourth pulse with a I_p/I_c ratio of 1.36.

The virgin critical current for sample SPCC-Ag-B-2, shown in Figure 4-5, was measured with both 5-cm and 10-cm voltage taps. Experimental results from the 4th run are compared to simulation in Figure 4-6, showing that the 5-cm voltage trace agrees quite well with the simulated voltage. In this figure, although similar to the simulation, each experimental temperatures trace shows a slight delay and smaller amplitude, most likely due to the effects of the thermocouple's Kapton 25- μm thick insulation layer, placed between the thermocouple and the sample's surface for electrical insulation. Figure 4-7 shows that the sample was not degraded after the 6th pulse.

Finally, although not physically open circuited, the YBCO in sample SPCC-Ag-B-2 was significantly degraded after the 7th pulse, shown in Figure 4-8. Here, the simulation predicts an unrecoverable quench within 2A of the experimental value. However, at the point of quench, experimental and simulated voltages did not agree well. Uncertainty in the measured n -value, which is used in the simulation is likely to be the primary cause of this disagreement. After the 7th pulse, the critical current was no longer measurable as the sample was purely resistive.

Table 4-2. Specifications for 4-mm SPI Ag stabilized samples.

Sample	SPCC-Ag-A-2	SPCC-Ag-B-1	SPCC-Ag-B-2
Manufacturer	SPI	SPI	SPI
Ag Thickness	3.3 μm	3.5 μm	3.5 μm
YBCO Thickness	2.4 μm	1.4 μm	1.4 μm
Buffer Thickness	2 μm	2 μm	2 μm
Substrate Thickness	100 μm	100 μm	100 μm
Width	4.0 mm	4.0 mm	4.0 mm
Length	15.0 cm	15.0 cm	15.0 cm
I_c^*	77A ¹	56A ¹	56A ¹

* 77.3K self field with a 1- $\mu\text{V}/\text{cm}$ criterion

¹ Measured by SPI

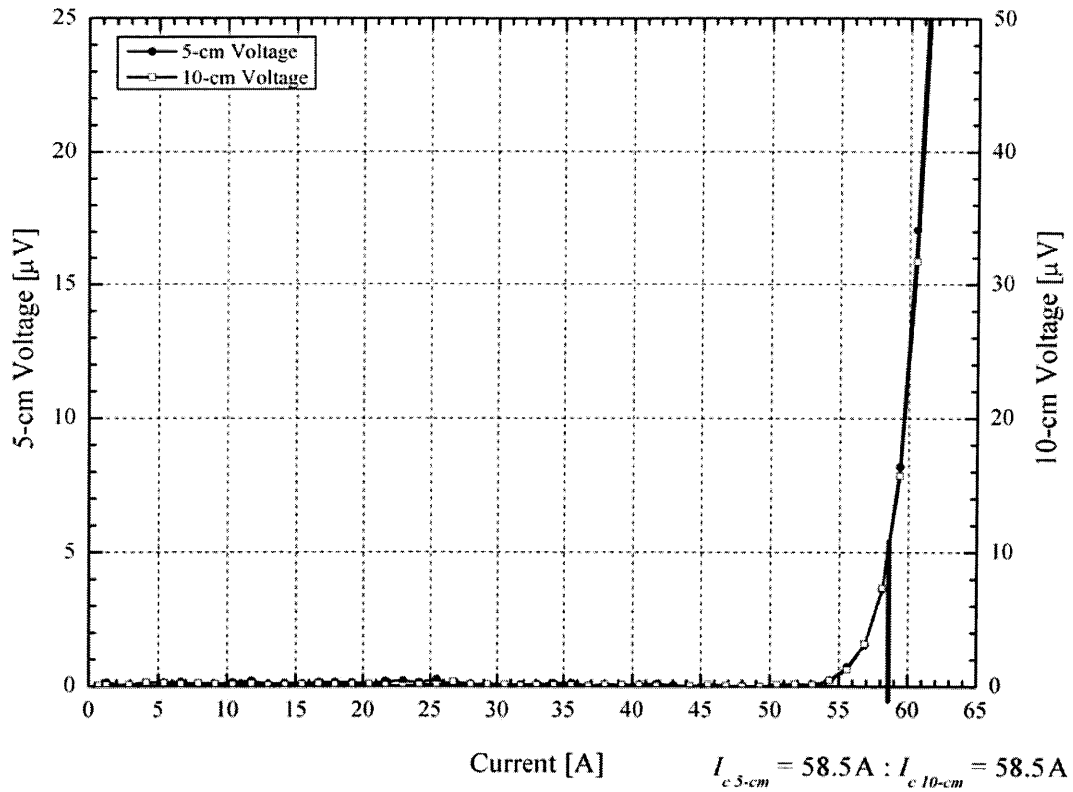


Figure 4-5. Virgin run for sample SPCC-Ag-B-2. Measured using both 5-cm and 10-cm voltage taps; $I_{c\ 5\text{-cm}} = 58.5\text{ A}$ and $I_{c\ 10\text{-cm}} = 58.5\text{ A}$ with a $1\ \mu\text{V}/\text{cm}$ criterion.

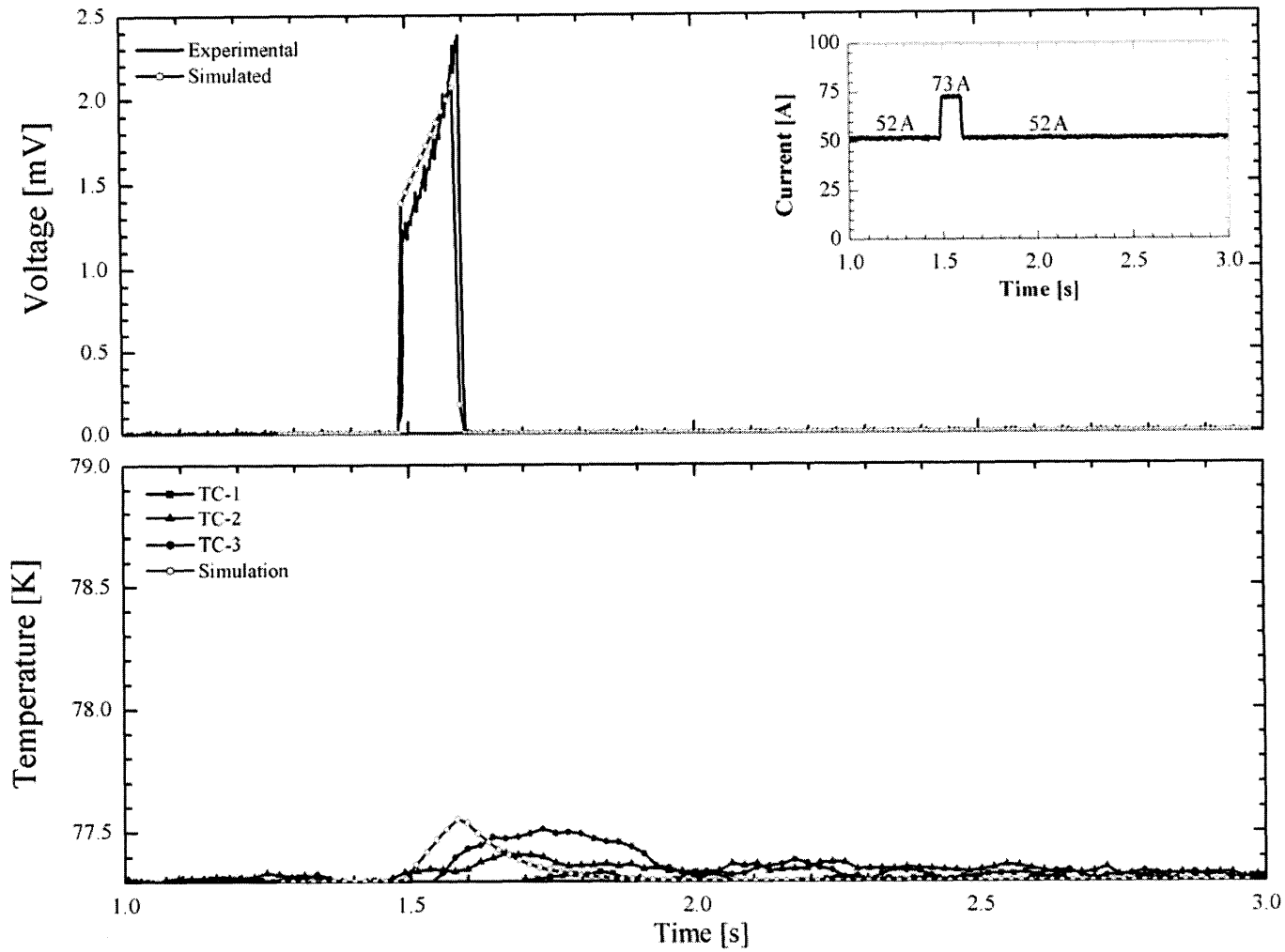


Figure 4-6. Sample SPCC-Ag-B-2: Run 4, $\tau = 100\text{ms}$, $t_{hold} = 7.0\text{s}$, $I_{op} = 52\text{A}$, $I_p = 73\text{A}$, $I_p/I_c = 1.24$.

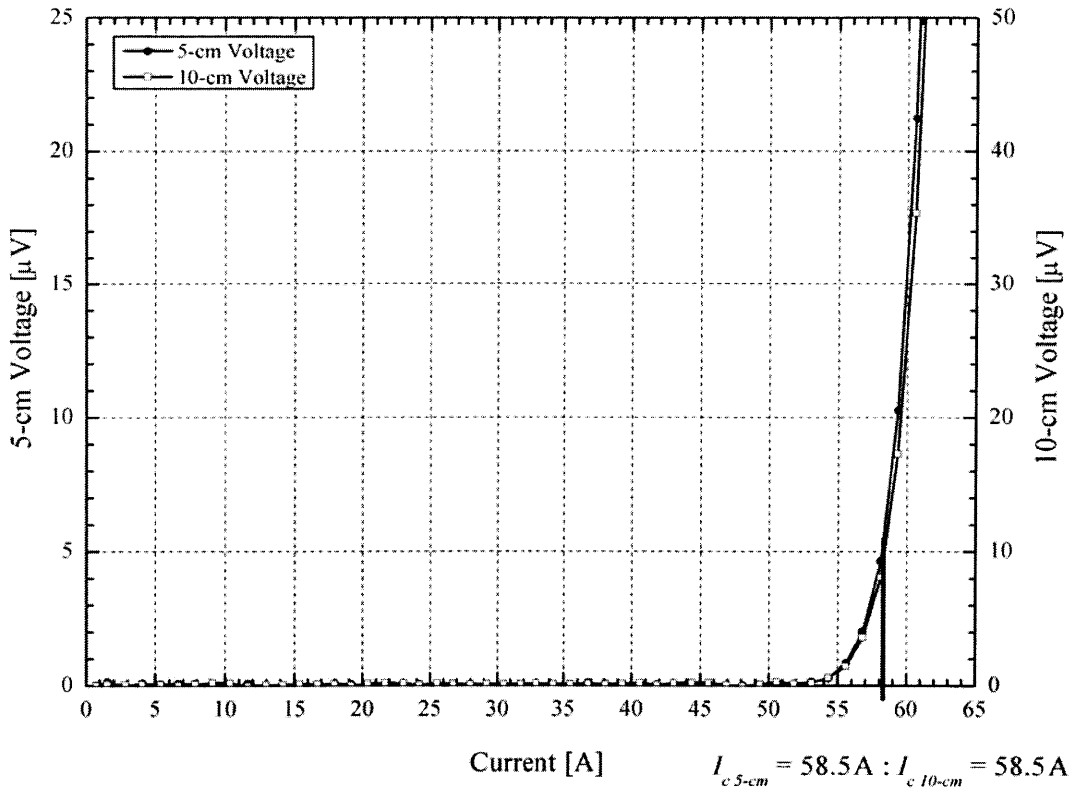


Figure 4-7. Critical current for sample SPCC-Ag-B-2 after 6th pulse. Measured using both 5-cm and 10-cm voltage taps; $I_{c\ 5\text{-cm}} = 58.5\text{ A}$ and $I_{c\ 10\text{-cm}} = 58.5\text{ A}$ with a $1\ \mu\text{V}/\text{cm}$ criterion.

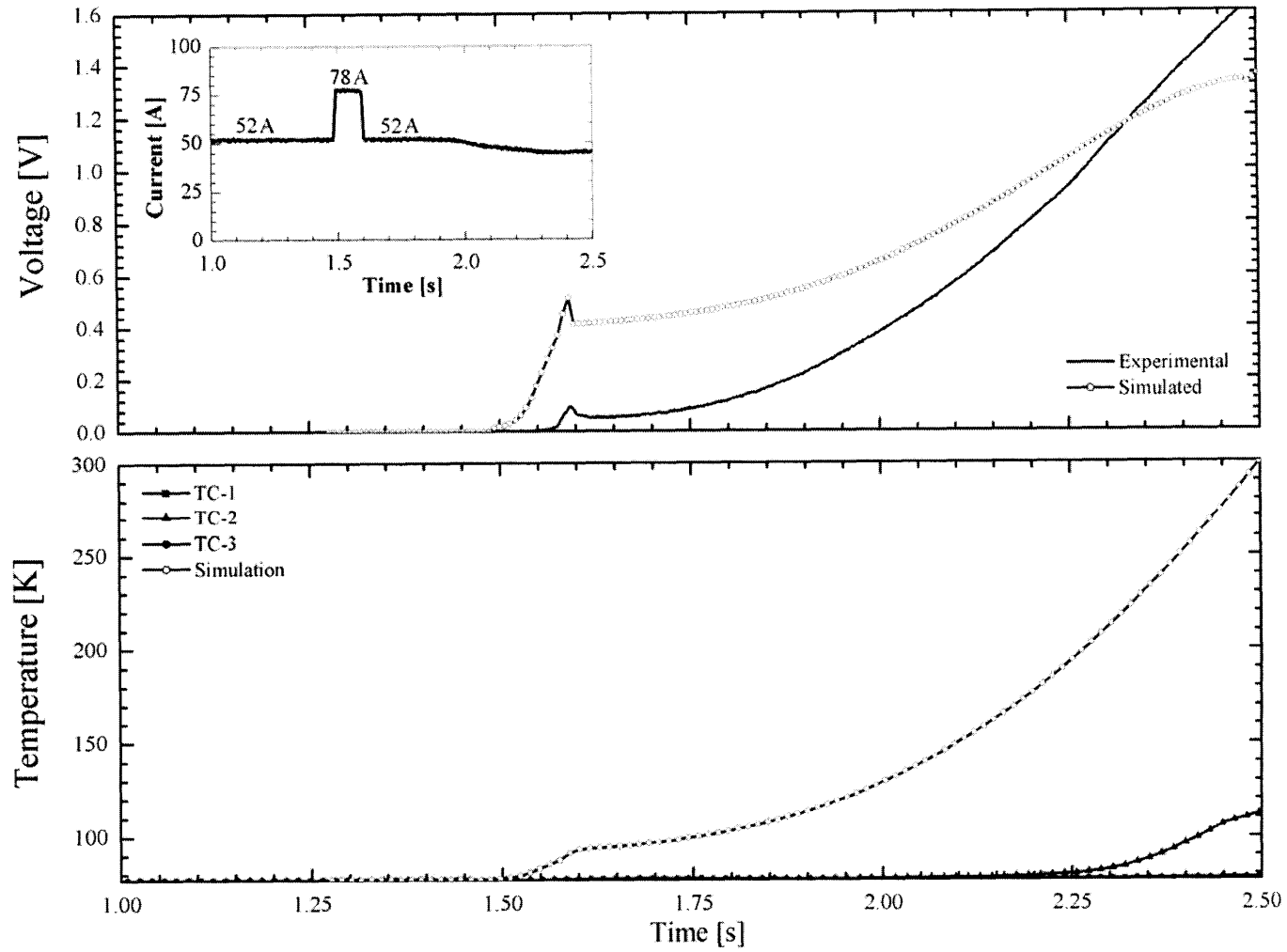


Figure 4-8. Sample SPCC-Ag-B-2: Run 7, $\tau = 100\text{ms}$, $t_{hold} = 7.0\text{s}$, $I_{op} = 52\text{A}$, $I_p = 78\text{A}$, $I_p/I_c = 1.33$.

4.3 Ag-Cu Stabilized Conductor: AMSC 10-mm Width

4.3.1 Sample Specifications

Several 10-mm wide samples were provided by AMSC with 50- μm and 76- μm thick copper lamination and were either 10-cm or 15-cm long. Layer arrangements are shown in Figure 4-9, while sample specifications and layer dimensions are provided in Table 4-3.

4.3.2 Experimental and Simulated Results: 50- μm Thick Copper Lamina

For the 50- μm thick copper laminated samples, various pulse durations were used to try to induce a runaway quench; however, for these samples the simulation indicated that the YBCO would be damaged due to heating before a quench occurred.

The virgin critical current for sample CC52-335-LAM, measured with 5-cm voltage taps, is shown in Figure 4-10. The voltage trace for the 15th run is shown in Figure 4-11, which shows a difference at the peak voltage point of less than 4 mV (40% of the peak voltage) between the experimental and simulated voltages. This difference is due to an error of ~ 1 A in the current signal. In addition, temperature data for this sample were not recorded due to improper DAQ configuration.

Figure 4-12 shows the results for the 35th pulse without temperature data. In this figure, heating after the pulse is shown by the extended recovery time for the voltage. The critical current was measured after the 35th pulse and does not indicate any YBCO degradation, as demonstrated by the V - I plot shown in Figure 4-13.

Due to limitations of the power supply, we were unable to generate enough current to quench the tape and as a result, only the simulated traces at a minimum predicted quench current are presented in Figure 4-14. Here a pulse amplitude that produced a 400 K temperature in the tape was defined as the minimum quench current, because YBCO suffered I_c degradation when heated to this temperature. Despite numerous pulsing, because of the low pulse current amplitude sample CC52-335-LAM did not exhibit degradation, nor was it quenchable. Similarly, we were unable to quench sample CC52-345-LAM.

Table 4-3. Specifications for 1-cm wide Ag-Cu stabilized samples.

Sample	CC52-335-LAM	CC52-345-LAM	CC51-R540-0-10	CC51-R540-10-20	CC51-R540-20-35	CC51-R540-65-80
Manufacturer	AMSC	AMSC	AMSC	AMSC	AMSC	AMSC
Cu Thickness	50 μm	50 μm	76 μm	76 μm	76 μm	76 μm
Ag Thickness	3-8 μm	3-8 μm	3-8 μm	3-8 μm	3-8 μm	3-8 μm
YBCO Thickness	1 μm	1 μm	1 μm	1 μm	1 μm	1 μm
Buffer Thickness	0.3 μm	0.3 μm	0.3 μm	0.3 μm	0.3 μm	0.3 μm
Substrate Thickness	76 μm	76 μm	76 μm	76 μm	76 μm	76 μm
Width	10mm	10mm	10mm	10mm	10mm	10mm
Length	10cm	10cm	10cm	10cm	10cm	10cm
I_c^*	129.0A ¹	120.0A ¹	107.5A ²	99.1A ²	113.0A ¹	107.0A ¹

* 77.3K self field with a 1- $\mu\text{V}/\text{cm}$ criterion

¹ Measured at MIT

² Measured by AMSC

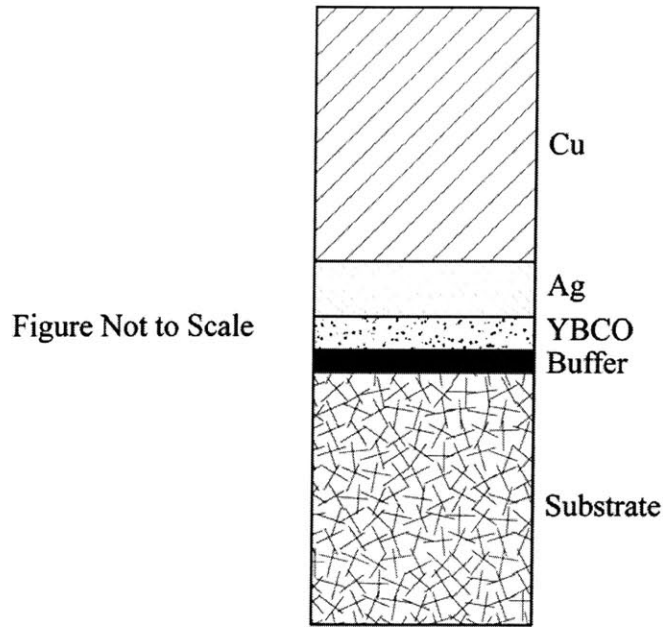


Figure 4-9. Layer arrangements in sample for AMSC Ag-Cu laminated superconductor.

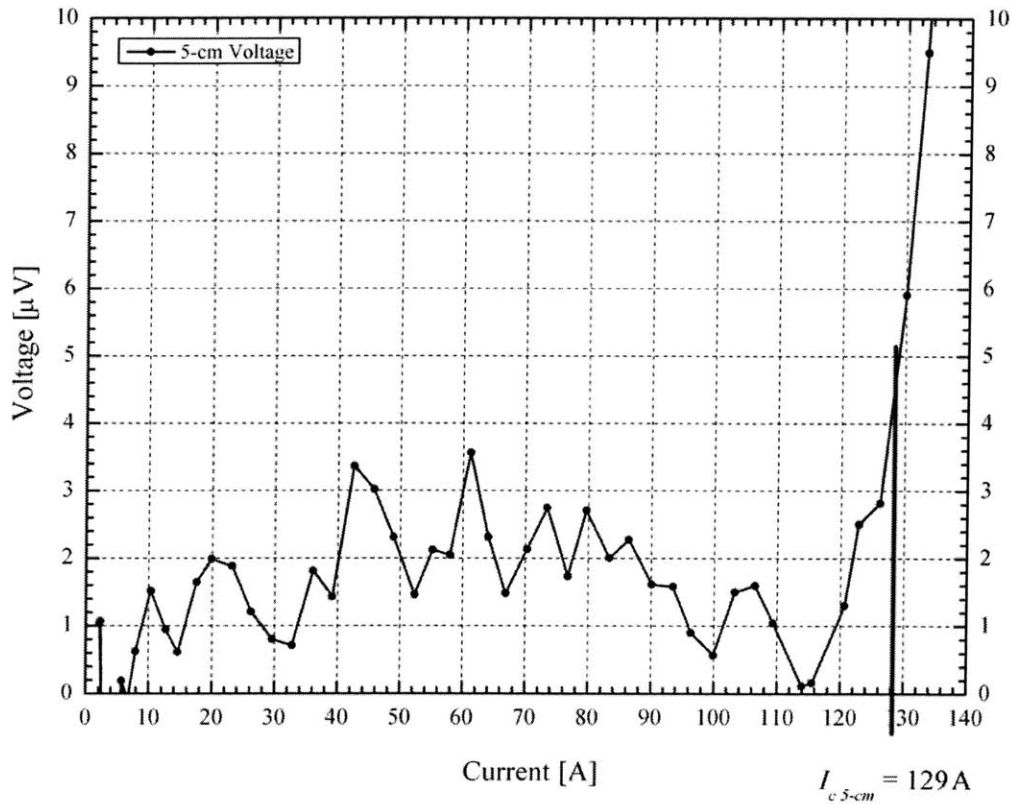


Figure 4-10. Virgin run for sample CC52-335-LAM. Measured using 5-cm voltage taps;
 $I_{c\ 5\text{-cm}} = 129\text{A}$ with a $1\ \mu\text{V}/\text{cm}$ criterion.

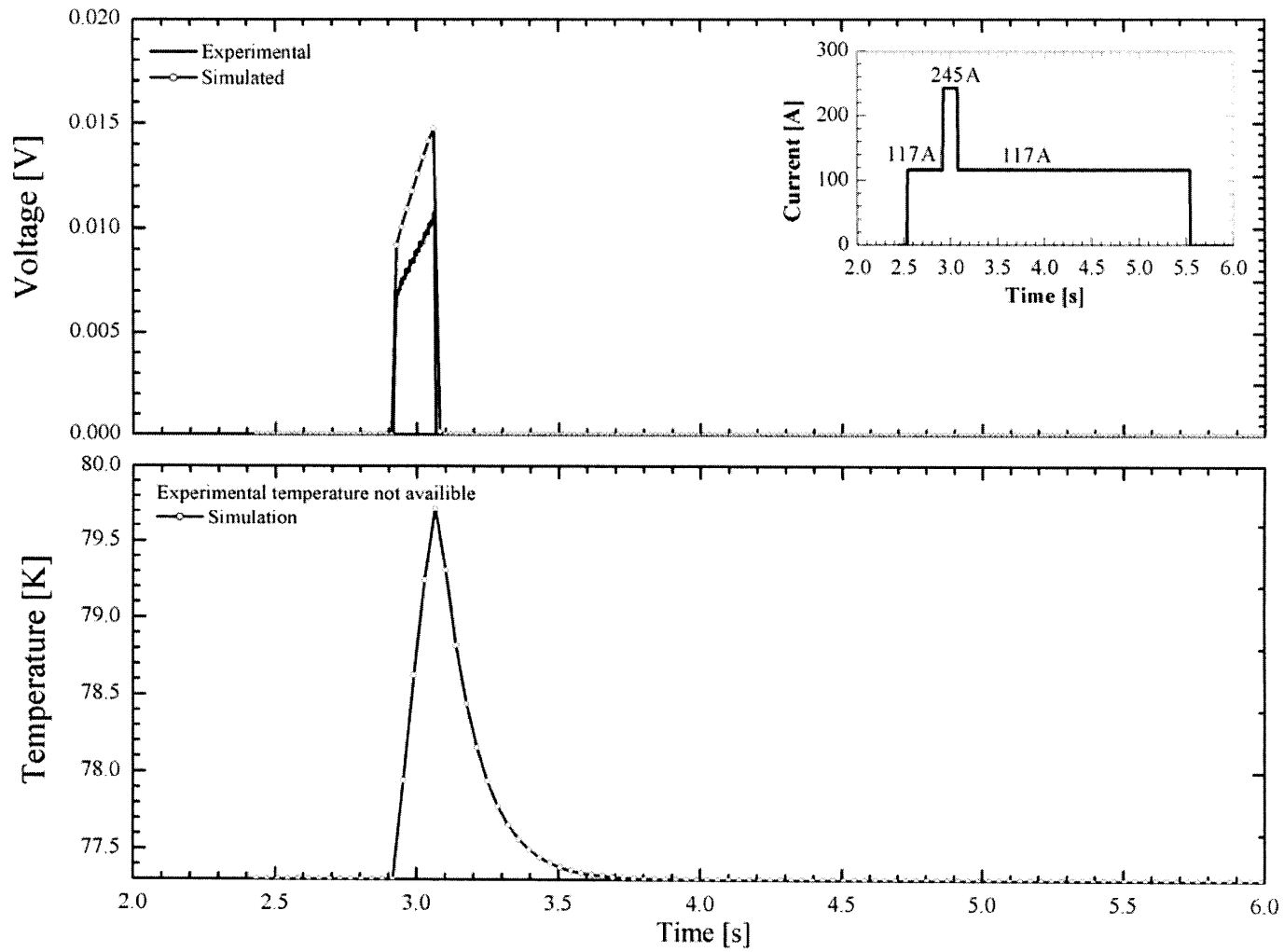


Figure 4-11. Sample CC52-335-LAM: Run 15, $\tau = 150\text{ms}$, $t_{hold} = 7.0\text{s}$, $I_{op} = 117\text{A}$, $I_p = 245\text{A}$, $I_p/I_c = 1.90$.

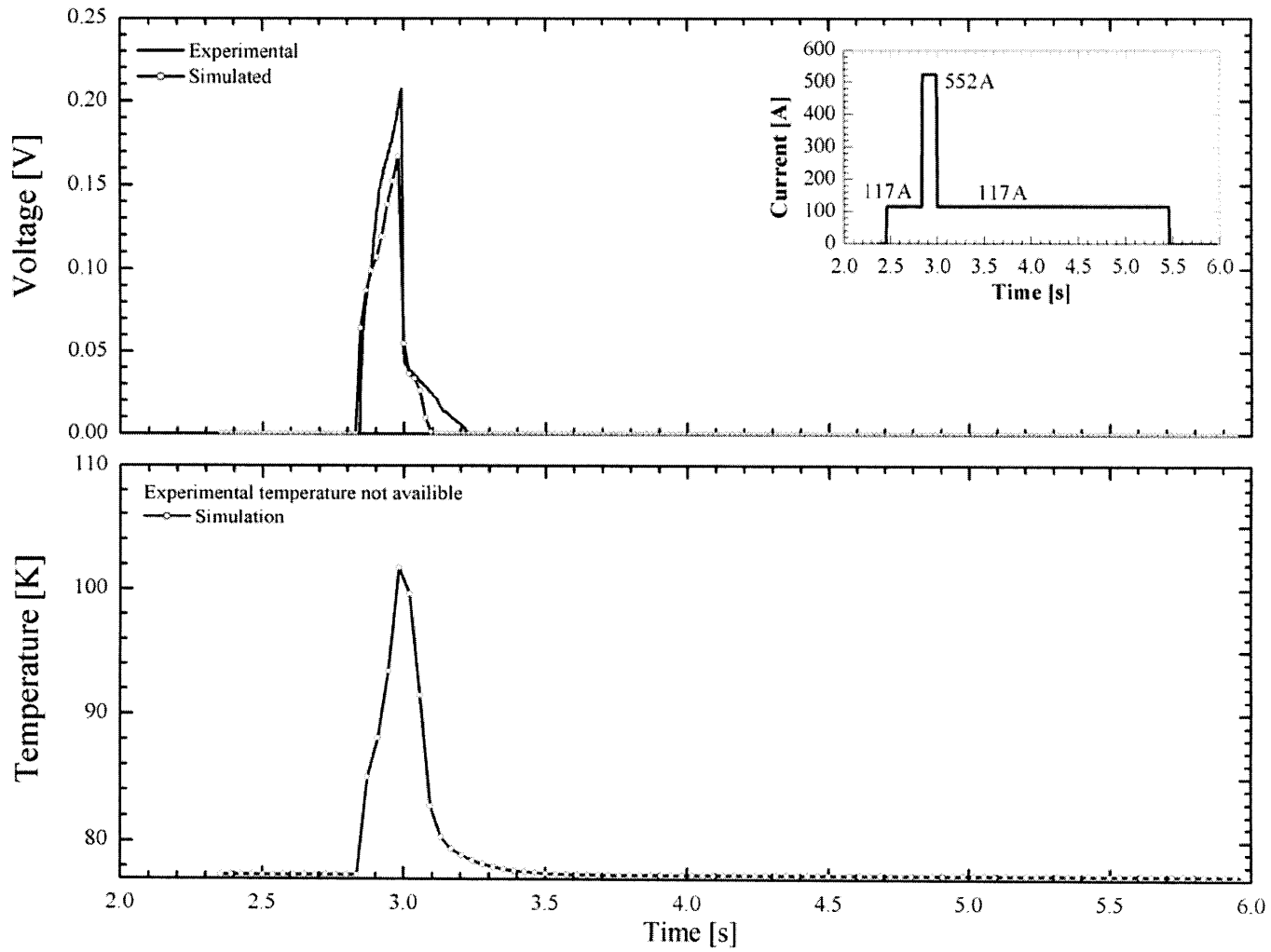


Figure 4-12. Sample CC52-335-LAM: Run 35, $\tau = 150\text{ms}$, $t_{hold} = 7.0\text{s}$, $I_{op} = 117\text{A}$, $I_p = 552\text{A}$, $I_p/I_c = 4.30$.

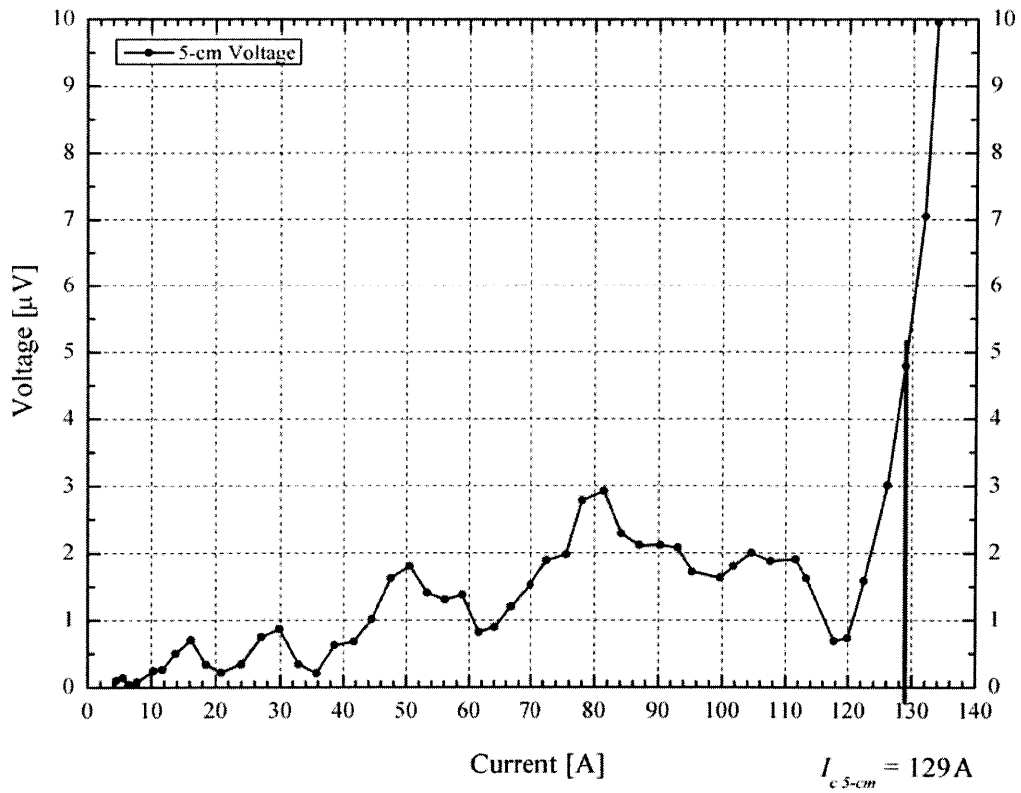


Figure 4-13. Critical current for sample CC52-335-LAM after 35th pulse. Measured using only 5-cm voltage taps; $I_{c\ 5-cm} = 129\text{A}$ with a $1\ \mu\text{V}/\text{cm}$ criterion.

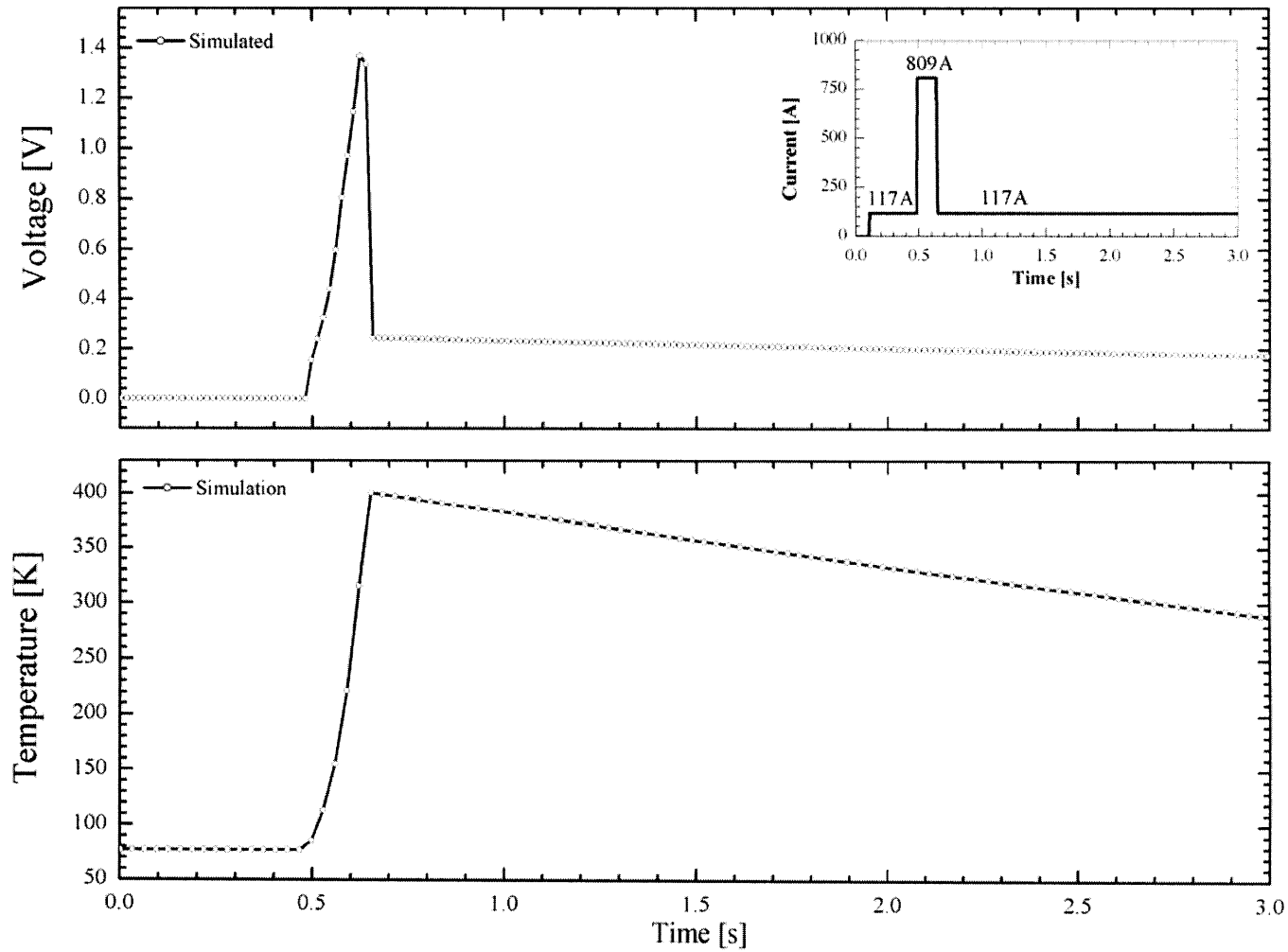


Figure 4-14. Sample CC52-335-LAM: Predicted YBCO burnout. $\tau = 150\text{ms}$, $t_{hold} = 7.0\text{s}$, $I_{op} = 117\text{A}$, $I_p = 809\text{A}$, $I_p/I_c = 6.27$.

4.3.3 Experimental and Simulated Results: 76- μm Thick Copper Lamina

The remaining 10-mm wide AMSC samples had a copper lamina thickness of 76- μm and, as with the 50- μm thick copper lamina samples, we were unable to produce a quench or superconductor damage in any of them. In general, the simulations for the 50- μm thick copper samples indicate that failure will result from excessive heating. However, the simulations for the 76- μm thick copper laminated samples indicate that a runaway voltage is possible near the current required cause a rise in temperature hot enough to damage the YBCO. As a result, the 76- μm thick copper laminated samples may fail either through degradation or quench, but this is dependant on the n-values and critical current of the sample.

Results for the virgin critical current measurement of sample CC51-R540-0-10 are shown in Figure 4-15. The results for the 21st pulse are shown in Figure 4-16. In this figure, the simulated voltage flattens out after the pulse demonstrating that at this pulse current level Joule dissipation is balanced by liquid nitrogen cooling. If the pulse duration was extended, the experimental voltage would also flatten out . When the Joule dissipation remains below the peak nucleate boiling heat flux, the sample remains at a constant voltage. Again, the difference between the experimental and simulated temperature is most likely attributed to the effects of the Kapton insulation.

From Figure 4-17, it can be seen that there is no degradation in the superconductor after the 21st pulse. The simulation traces with a 400K criterion is shown in Figure 4-17. Note that because the sample is being cooled in the film boiling regime, it takes a long while for the sample to return to the superconducting state.

The other 76- μm thick copper laminated samples listed in Table 4-3 were subject to different over-current sequences such as multiple pulses and 1-s pulse durations in order to verify the simulations.

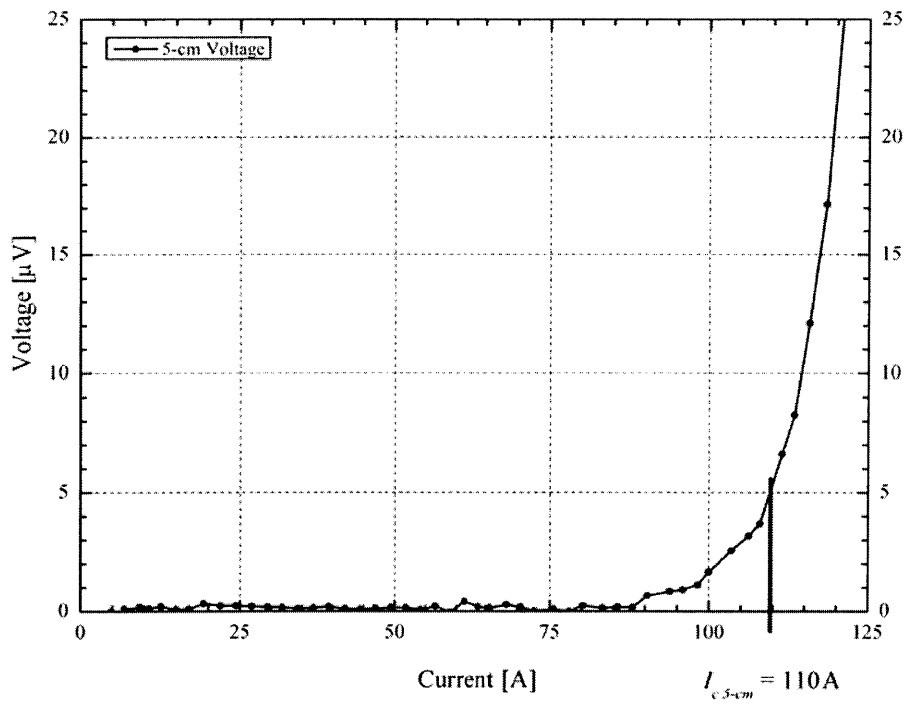


Figure 4-15. Virgin run for sample CC51-R540-0-10. Measured using only 5-cm voltage taps; $I_{c\ 5\text{-cm}} = 110\text{A}$ with a $1\ \mu\text{V}/\text{cm}$ criterion.

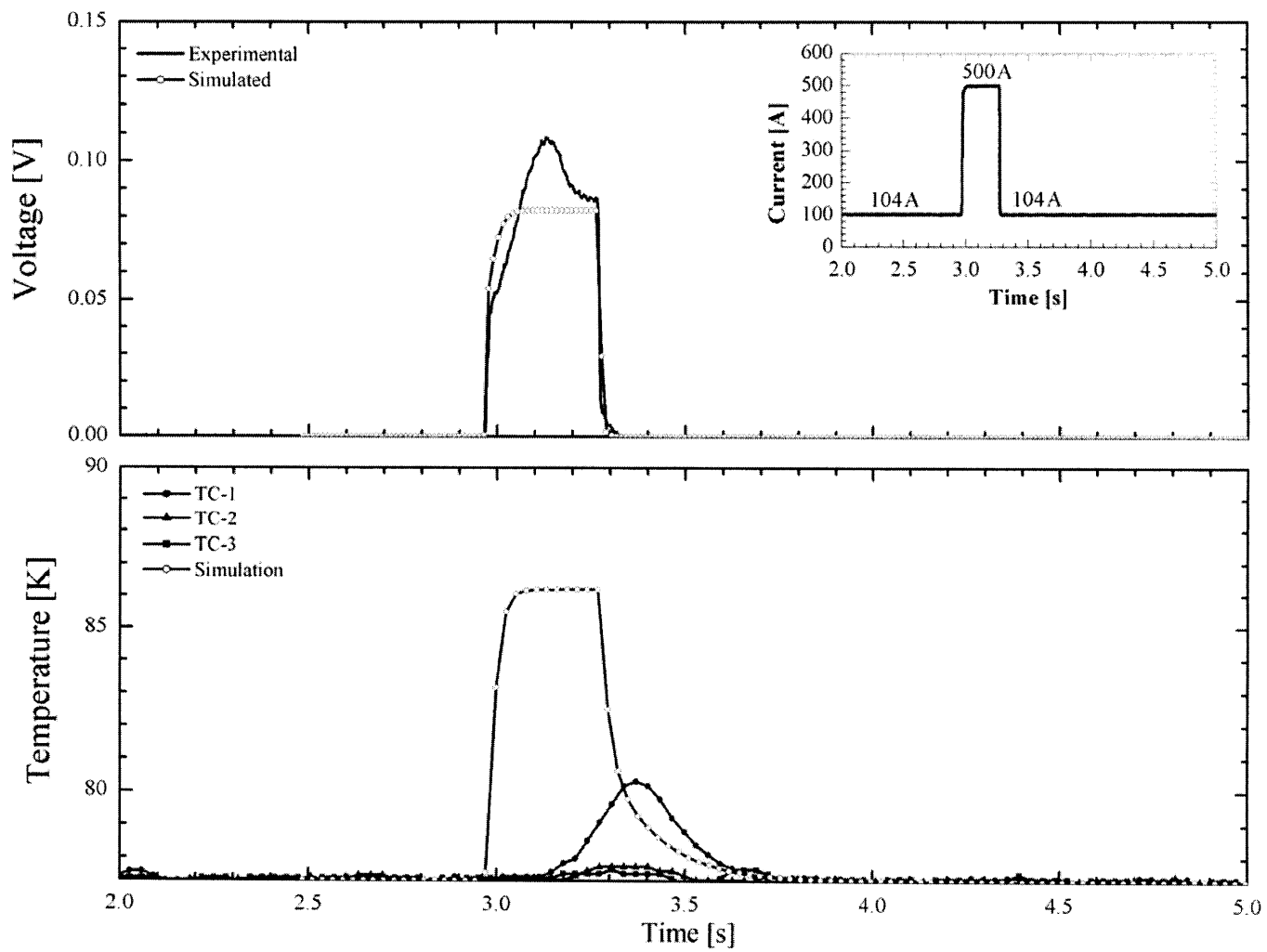


Figure 4-16. Sample CC51-R540-0-10: Run 21, $\tau = 300\text{ms}$, $t_{hold} = 7.0\text{s}$, $I_{op} = 104\text{A}$, $I_p = 500\text{A}$, $I_p/I_c = 4.55$.

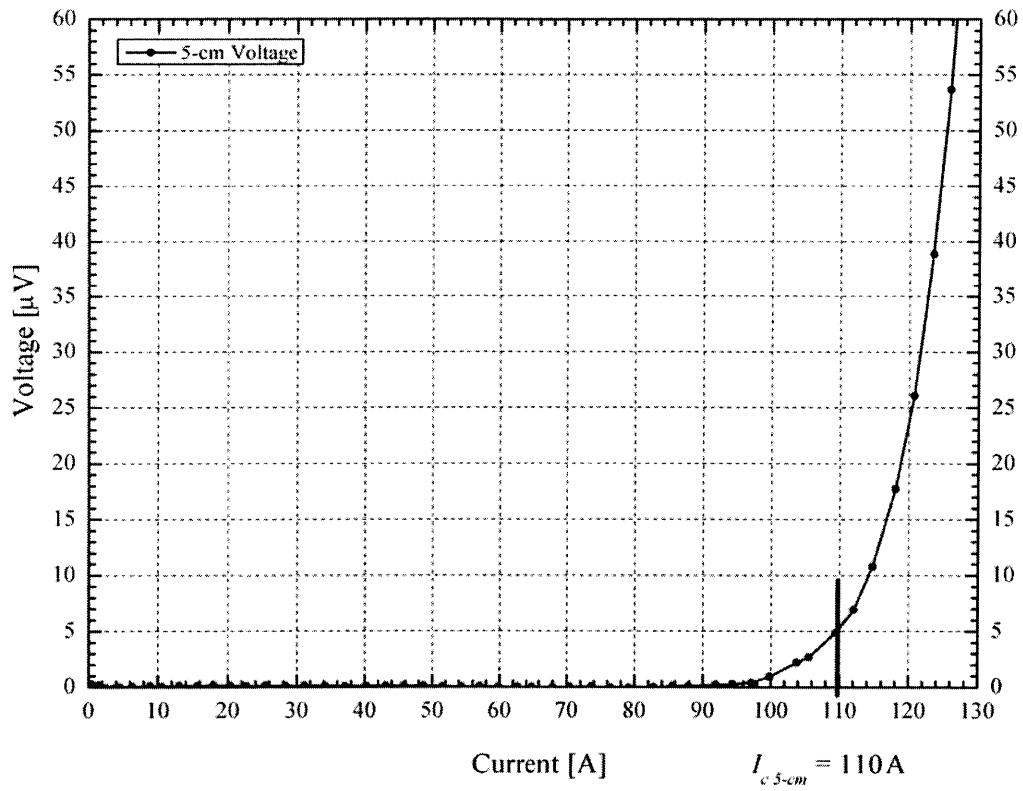


Figure 4-17. Critical current for sample CC51-R540-0-10 after 21st pulse. Measured using only 5-cm voltage taps; $I_{c\ 5-cm} = 110\text{A}$ with a $1\ \mu\text{V}/\text{cm}$ criterion.

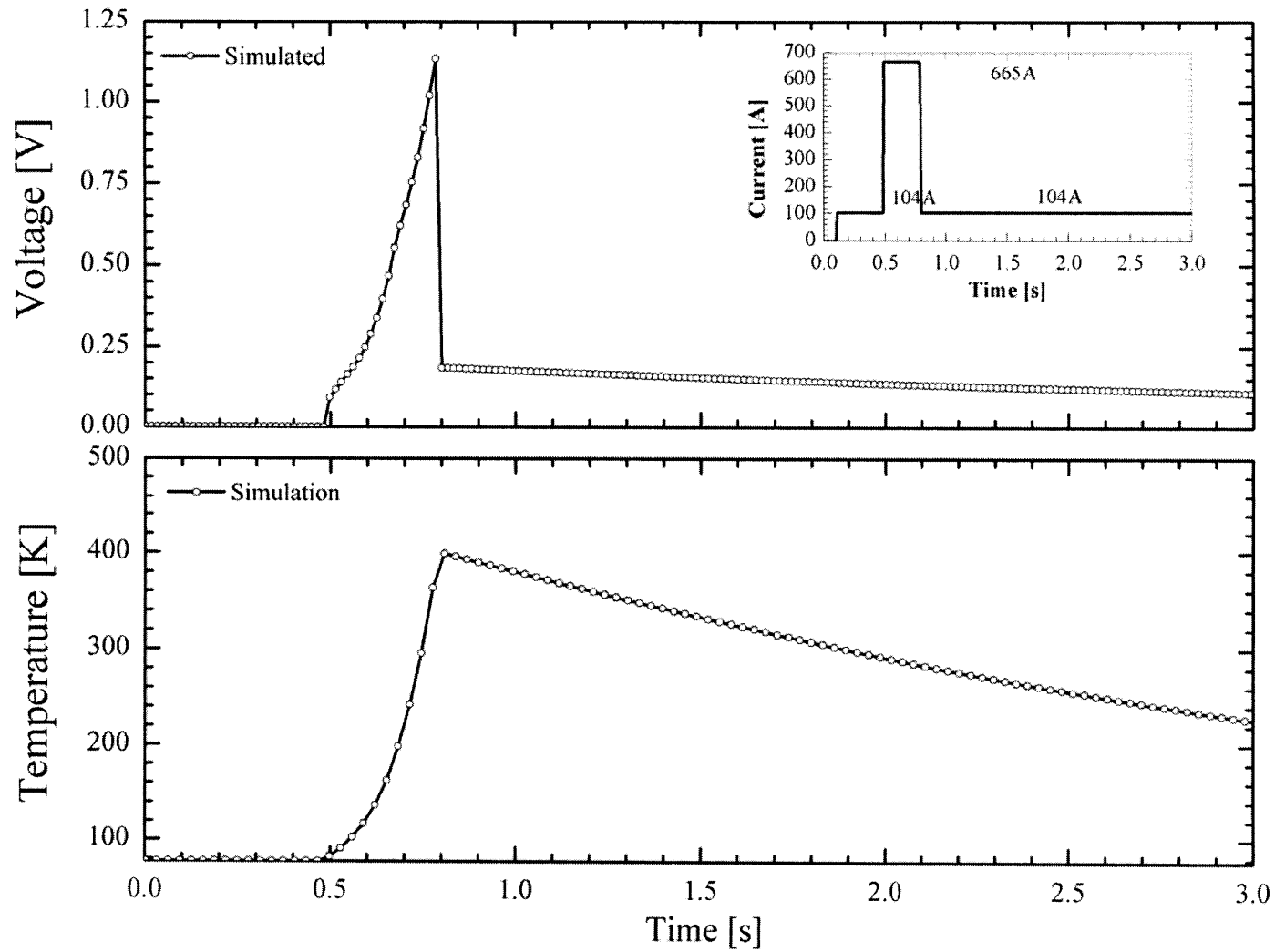


Figure 4-18. Sample CC51-R540-0-10: Predicted YBCO burnout, $\tau = 300$ ms, $t_{hold} = 7.0$ s, $I_{op} = 104$ A, $I_p = 665$ A, $I_p/I_c = 6.04$.

4.4 Ag-Cu Stabilized Conductor: AMSC 4-mm Width

4.4.1 Sample Specifications

In addition to 10-mm wide, 76- μm thick copper laminated samples, AMSC produced 4-mm wide samples by slitting 10-mm wide tapes. The critical currents of these 4-mm wide tapes were about 40% of those of the original 10-mm wide tape. Reduction in I_c allowed us to subject these narrow samples to I_p/I_c ratios high enough to quench them. Layer arrangements for these samples are identical to those shown in Figure 4-9 for 10-mm wide samples, The sample specifications are provided in Table 4-4.

4.4.2 Experimental and Simulated Results

With the thick copper stabilizer it was possible to produce a constant recovery voltage after the pulse, but to determine if the sample quenched, a longer hold time for the operating current after the pulse was required. For these experiments, the longest hold time was 10s.

The virgin critical current measured for sample CC84-755-8, shown in Figures 4-19, was 94A. After the first pulse, with a I_p/I_c ratio of 2.0, the critical current dropped to 91A, however, it remained at this value until the YBCO became degraded due to heating. To illustrate that the critical current indeed remained constant at 91A, the V vs. I trace measured after the 31st pulse is shown in Figure 4-20.

The results from 32nd pulse are shown in Figure 4-21. In this figure, the experimental and simulated voltage traces agree very well during the pulse; the simulated voltage recovers slightly faster the experimental voltage after the pulse. Although the simulation assumes the entire sample to be at the same temperature, the experimental traces clearly indicate this is not the case: each end of the sample (as indicated by TC_1 and TC_3) is cooling much faster than the center (TC_2), due most likely to the conduction of heat to each copper electrode. The critical current after the 37th pulse is shown in Figure 4-22, indicating that the sample still remained essentially intact.

The superconductor did not show signs of degradation before the 38th pulse. More importantly, the voltage for the sample up to this point remained constant after the pulse, indicating a balance between the cooling and joule dissipation. However, during the 38th pulse, shown in Figure 4-23, a runaway voltage was detected. After the pulse, the sample continued to heat up, exceeding 400K and the superconductor was degraded to the point that the sample remained resistive.

The experimental and simulated temperature traces shown in Figure 4-23 suggest that the peak heating during the pulse was sufficient to raise the sample temperature – 370K (simulation), 200K (TC_3), 150K (TC_2) – and hence the film boiling heat transfer flux to

be slightly less than Joule dissipation of the sample even at a operating current of 80 A. Apparently, this imbalance in cooling and Joule heating was sufficient to cause a gradual heating of the sample, indicated by both the experimental and simulated temperature traces.

Sample CC84-755-9 showed a similar temperature runaway at a I_p/I_c ratio of 4.64 and also suffered degradation. In contrast, sample EC-530-45 burned out at a I_p/I_c ratio of 4.49.

Table 4-4. Specifications for 4-mm wide Ag-Cu stabilized samples.

Sample	CC84-755-8	CC84-755-9	EC10-530-45
Manufacturer	AMSC	AMSC	AMSC
Cu	76 μm	76 μm	76 μm
Ag	3-8 μm	3-8 μm	3-8 μm
YBCO	1 μm	1 μm	1 μm
Buffer	0.3 μm	0.3 μm	0.3 μm
Substrate	76 μm	76 μm	76 μm
Width	4 mm	4 mm	4 mm
Length	15 cm	15 cm	15 cm
I_c^*	94 A ¹	88 A ¹	58 A ¹

* 77.3 K self field with a 1- $\mu\text{V}/\text{cm}$ criterion

¹ Measured at MIT

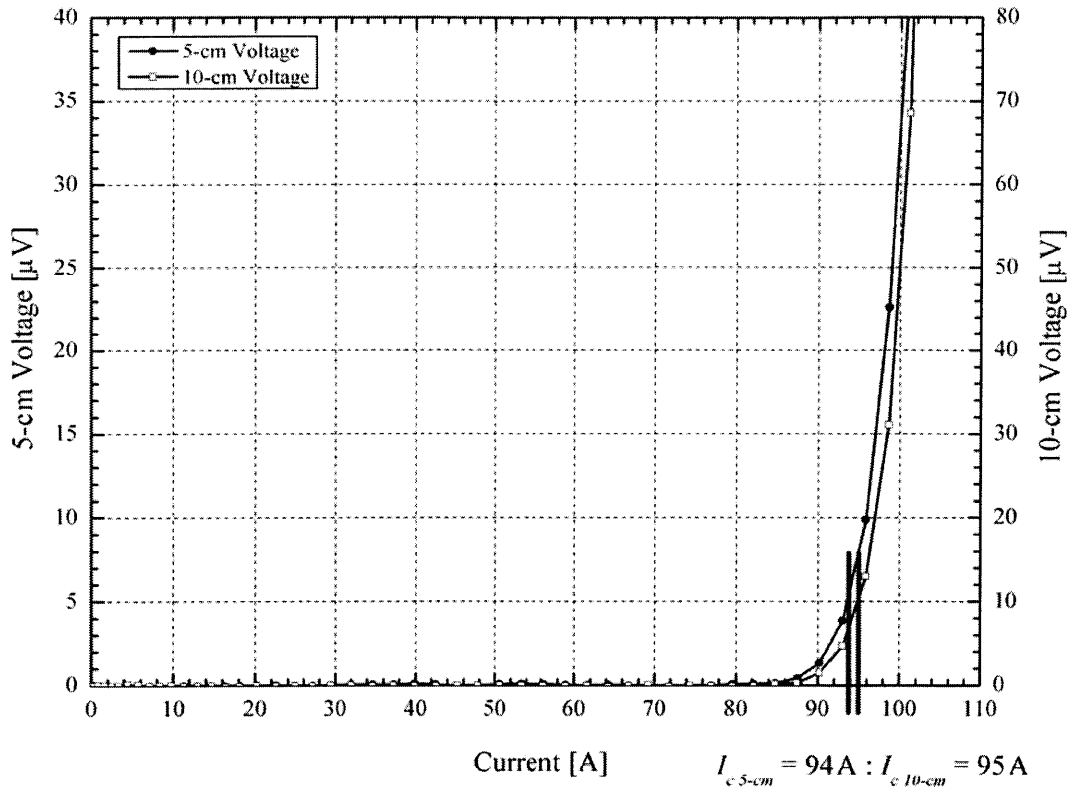


Figure 4-19. Virgin run for sample CC84-755-8. Measured using both 5-cm and 10-cm voltage taps; $I_{c\ 5\text{-cm}} = 94\text{ A}$ and $I_{c\ 10\text{-cm}} = 95\text{ A}$ with a $1\ \mu\text{V}/\text{cm}$ criterion.

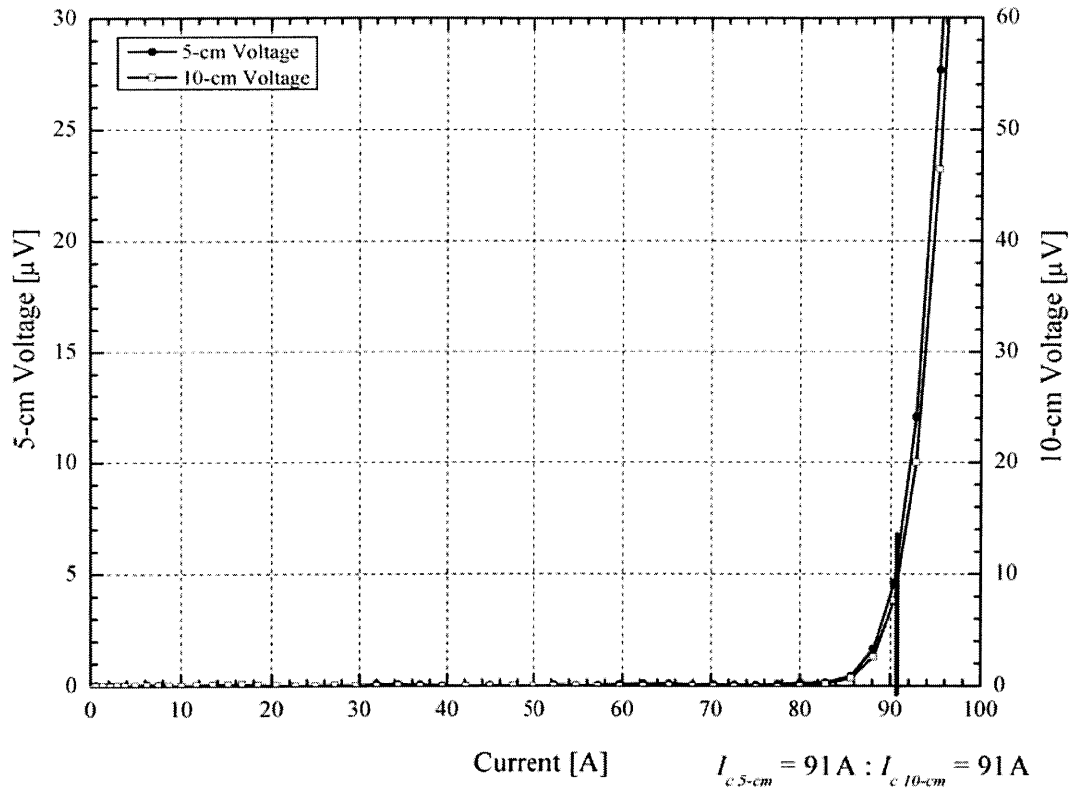


Figure 4-20. Critical current for sample CC84-755-8 after 31st pulse. Measured using both 5-cm and 10-cm voltage taps; $I_{c\ 5\text{-cm}} = 91\ \text{A}$ and $I_{c\ 10\text{-cm}} = 91\ \text{A}$ with a $1\ \mu\text{V}/\text{cm}$ criterion.

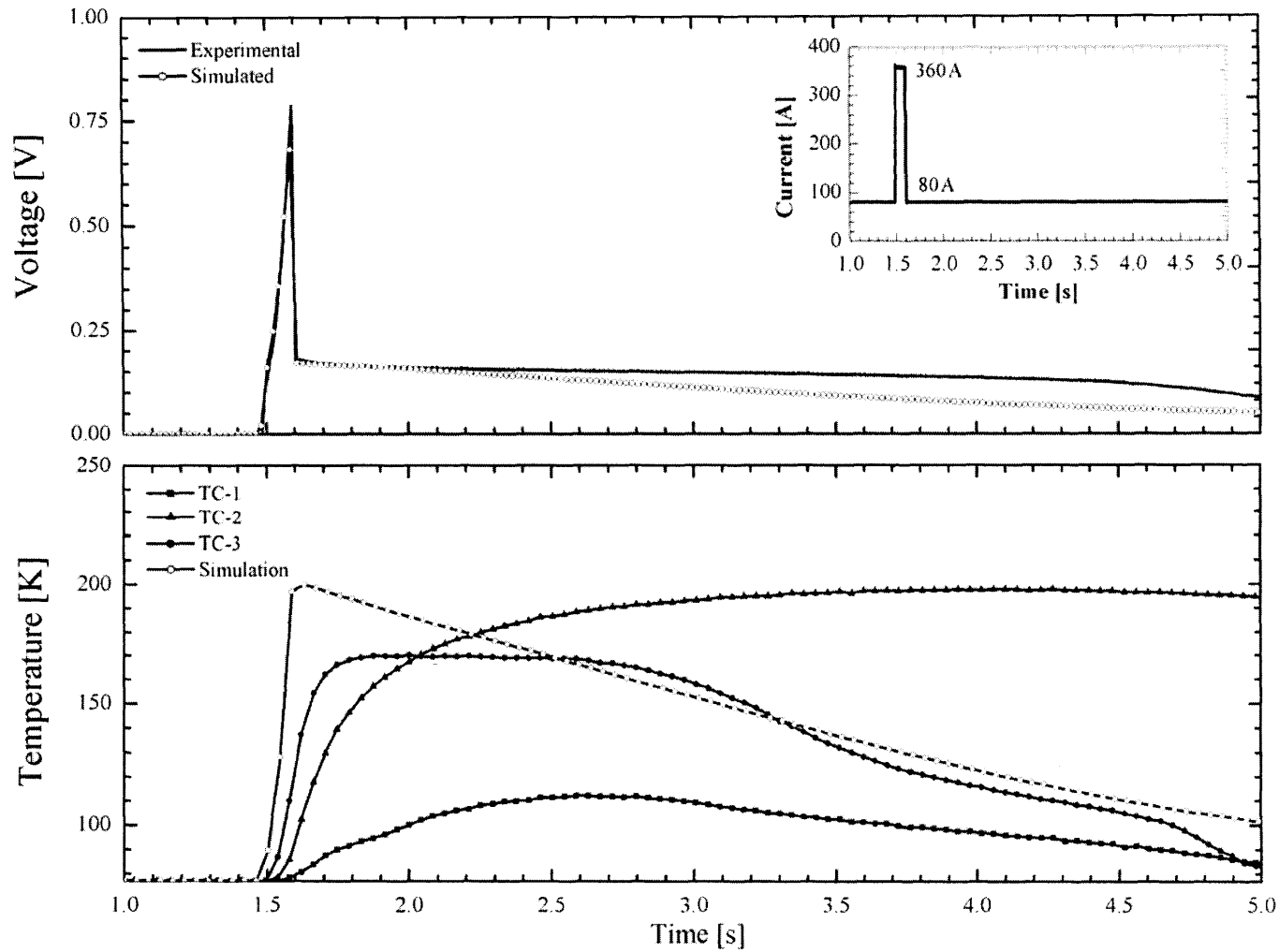


Figure 4-21. Sample CC84-755-8: Run 32, $\tau = 100\text{ms}$, $t_{\text{hold}} = 7.0\text{s}$, $I_{\text{op}} = 80\text{A}$, $I_p = 360\text{A}$, $I_p/I_c = 3.96$.

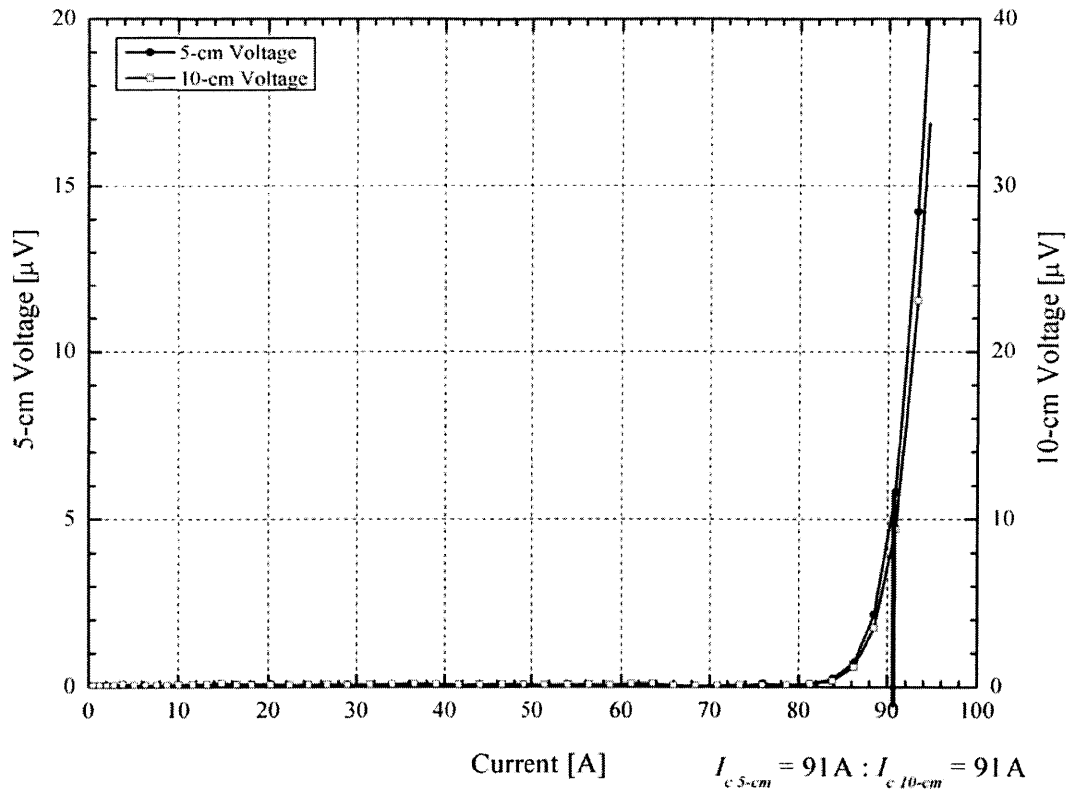


Figure 4-22. Critical current for sample CC84-755-8 after 37th pulse. Measured using both 5-cm and 10-cm voltage taps; $I_{c\ 5\text{-cm}} = 91\ \text{A}$ and $I_{c\ 10\text{-cm}} = 91\ \text{A}$ with a $1\ \mu\text{V}/\text{cm}$ criterion.

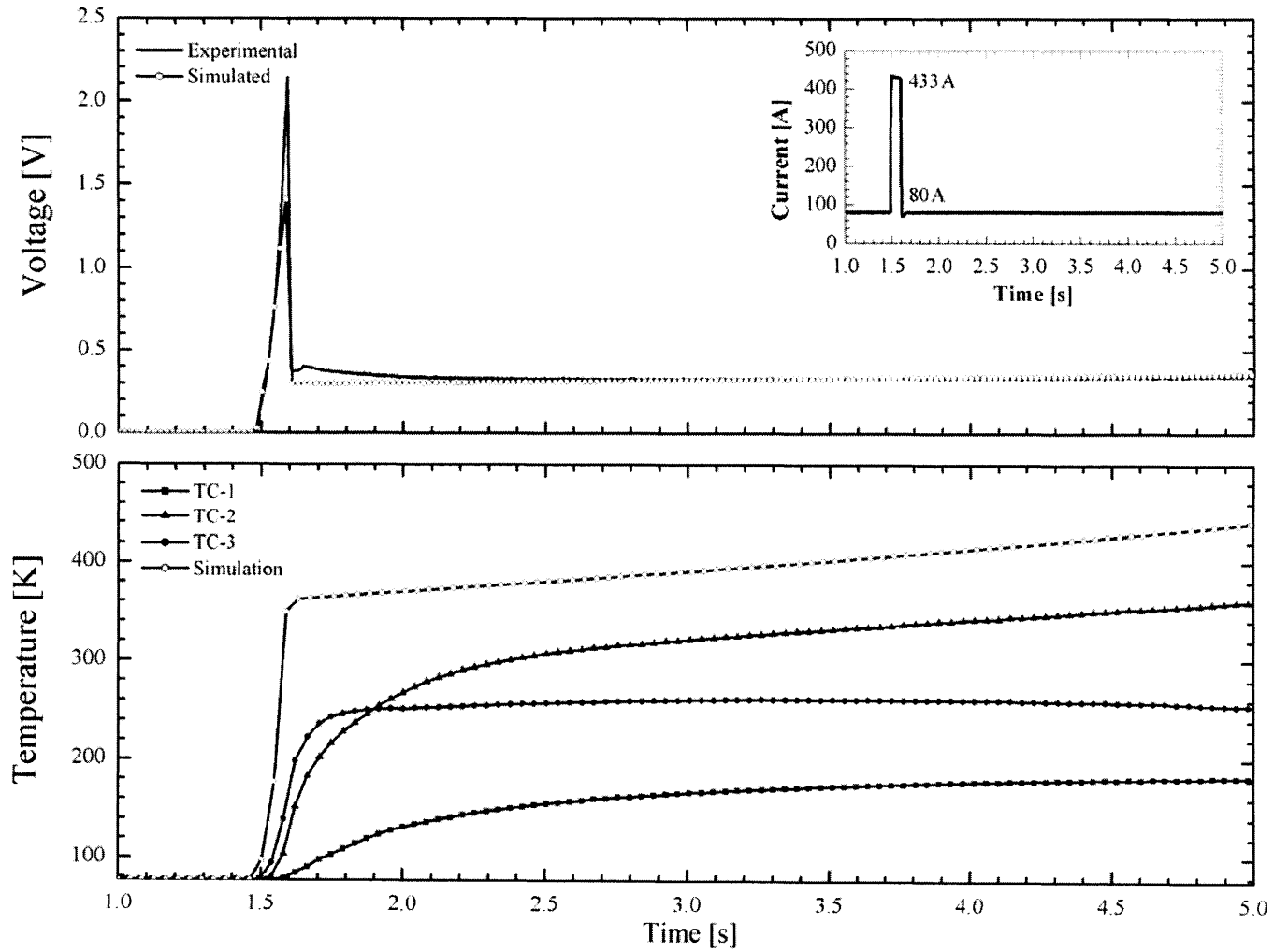


Figure 4-23. Sample CC84-755-8: Run 38, $\tau = 100\text{ms}$, $t_{hold} = 7.0\text{s}$, $I_{op} = 80\text{A}$, $I_p = 433\text{A}$, $I_p/I_c = 4.76$.

4.5 Ag-Cu Stabilized Conductor: SPI 4-mm Width

4.5.1 Sample Specifications

SPI provided 4-mm wide samples with both 46- μm and 75- μm thick copper lamination thickness. The electroplating technique was used to deposit layers of copper on both the top (silver) and bottom (substrate) surfaces, as shown schematically in Figure 4-24. Specifications for the SPI copper laminated samples are provided in Table 4-5.

4.5.2 Experimental and Simulated Results: 46- μm Thick Copper Lamina

Results for sample SPCC-Cu-A-1 begin with the virgin critical current shown in Figure 4-25. In this figure, the critical current based on the 10-cm voltage taps is 3.5-A less than that based on the 5-cm voltage taps. The difference between these two values illustrates the non-homogeneity in the critical current of the YBCO superconductor. Starting with a low I_p/I_c ratio of 1.68, shown in Figure 4-26, the experimental and simulated voltages agree almost exactly. Despite the presence of a 2-mm thick layer of Styrofoam insulating each thermocouple from direct cooling of liquid nitrogen, disagreement between experiment and simulation is still significant – although the actual difference is within 1 K, percentage-wise it is nearly 100%.

Pulsing the sample to a I_p/I_c ratio of 5.92, as shown in Figure 4-27, both the experimental and simulated voltages recovered. The experimental temperatures are lower than the simulated temperature, but the cooling rates similar. The critical current after the 12th pulse, shown in Figure 4-28, does not indicate degradation in the YBCO. However, when the sample was subjected to a I_p/I_c ratio of 6.85 shown in Figure 4-29, the temperature of the superconductor exceeded 400K. For the 13th pulse the experimental data shows recovery and the simulation predicts a quench. The discrepancy between the two indicates that the liquid nitrogen cooling for the sample is better than the simulation predicts.

The decreased critical currents of Figure 4-30 show degradation as a result of overheating. With each subsequent pulse, the critical current of the sample continued to fall, until it became purely resistive. Unfortunately, the voltage data from the 13th pulse (Figure 4-29) was not recorded because the voltage taps melted away from the conductor. Instead, the simulated values for 13th pulse are presented.

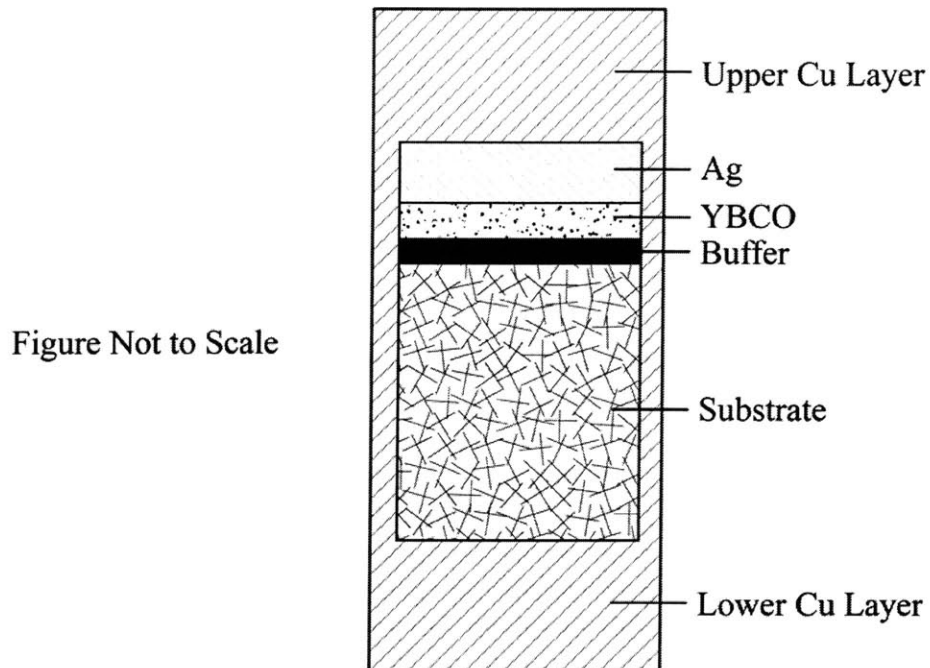


Figure 4-24. Layer arrangements in sample for SPI Ag-Cu laminated superconductor. Side copper layers electrically short upper and lower layers. The thickness of each side copper layer is not known exactly, though it is on the order of $\sim 10\text{-}\mu\text{m}$.

Table 4-5. Sample specifications for 4-mm SPI Ag-Cu stabilized samples.

Sample	SPCC-Cu-A-1	SPCC-Cu-A-2	SPCC-Cu-E	SPCC-Cu-F	SPCC-Cu-G
Manufacturer	SPI	SPI	SPI	SPI	SPI
Upper Cu Thickness	23 μm	23 μm	52 μm	52 μm	52 μm
Ag Thickness	2 μm	2 μm	2 μm	2 μm	2 μm
YBCO Thickness	1.4 μm	1.4 μm	1.4 μm	1.4 μm	1.4 μm
Buffer Thickness	2 μm	2 μm	2 μm	2 μm	2 μm
Substrate Thickness	100 μm	100 μm	100 μm	100 μm	100 μm
Lower Cu Thickness	23 μm	23 μm	23 μm	23 μm	23 μm
Width	4 mm	4 mm	4 mm	4 mm	4 mm
Length	15 cm	15 cm	15 cm	15 cm	15 cm
I_c^*	59 A ¹	46 A ¹	50 A ¹	53 A ¹	40 A ¹

* 77.3K self field with a 1- $\mu\text{V}/\text{cm}$ criterion

¹ Measured at MIT

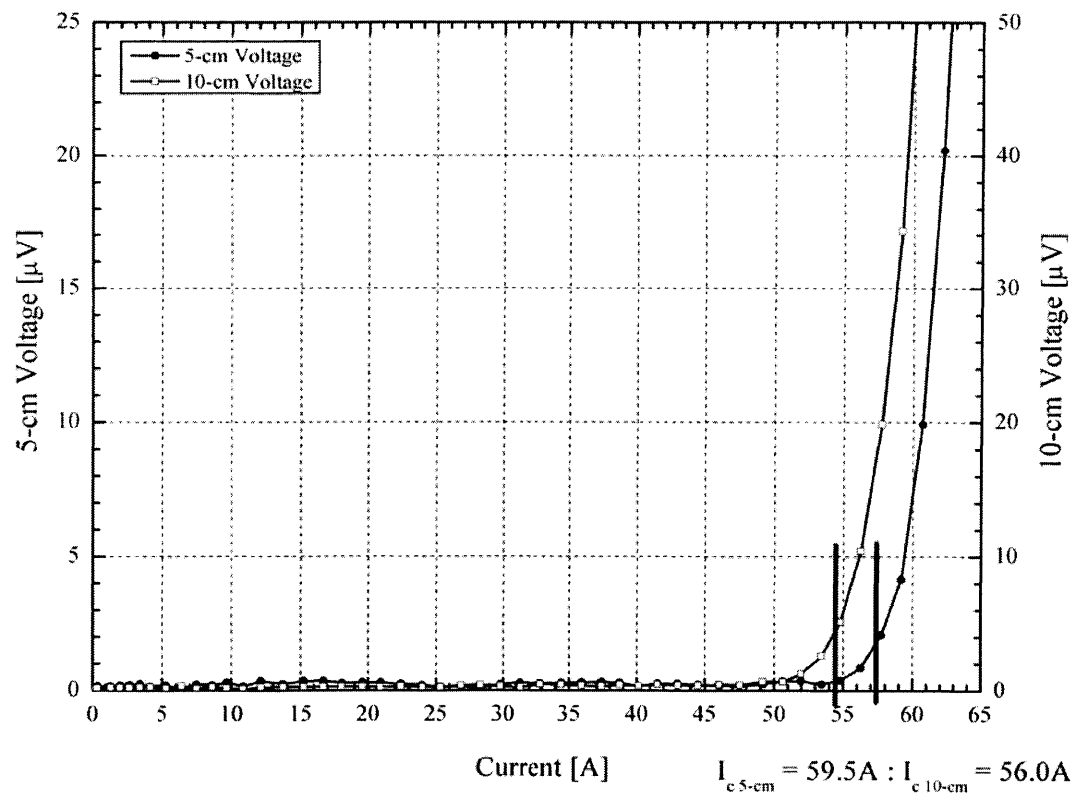


Figure 4-25. Virgin run for sample SPCC-Cu-A-1. Measured using both 5-cm and 10-cm voltage taps; $I_{c\ 5\text{-cm}} = 59.5\text{ A}$ and $I_{c\ 10\text{-cm}} = 56.0\text{ A}$ with a $1\ \mu\text{V}/\text{cm}$ criterion.

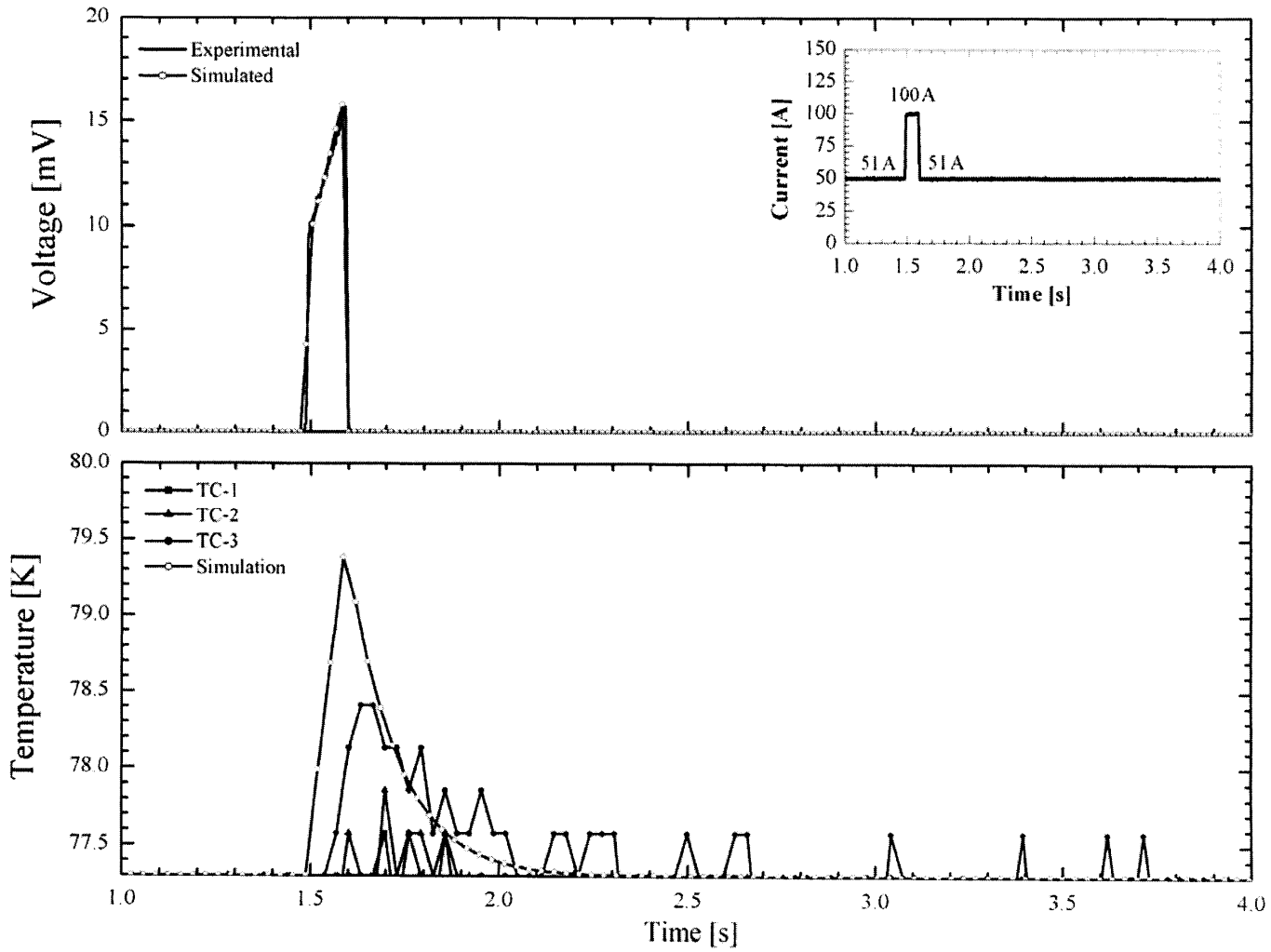


Figure 4-26. Sample SPCC-Cu-A-1: Run 2, $\tau = 100\text{ms}$, $t_{hold} = 7.0\text{s}$, $I_{op} = 51\text{A}$, $I_p = 100\text{A}$, $I_p/I_c = 1.68$.

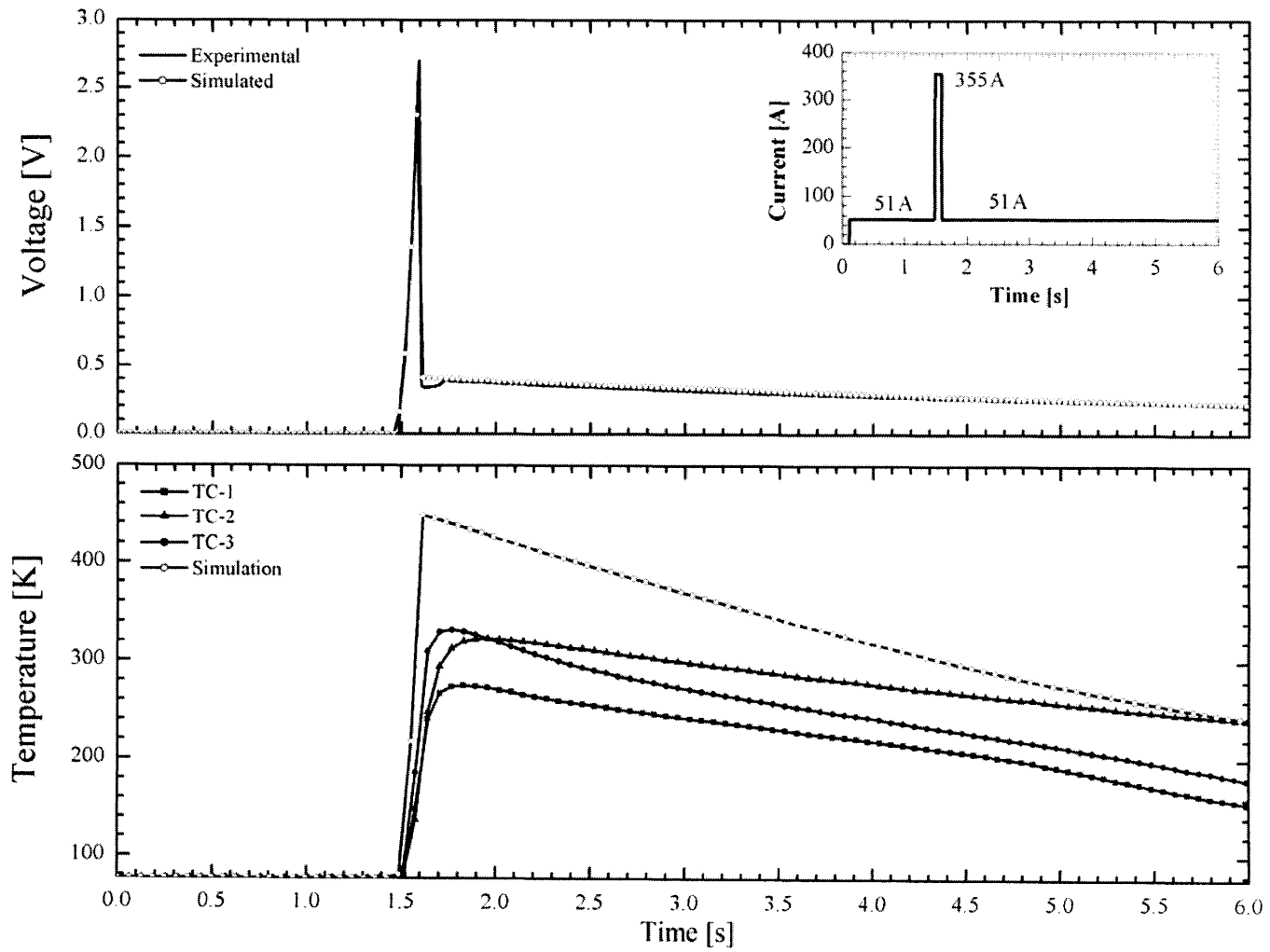


Figure 4-27. Sample SPCC-Cu-A-1: Run 12, $\tau = 100\text{ms}$, $t_{hold} = 7.0\text{s}$, $I_{op} = 51\text{A}$, $I_p = 355\text{A}$, $I_p/I_c = 5.92$.

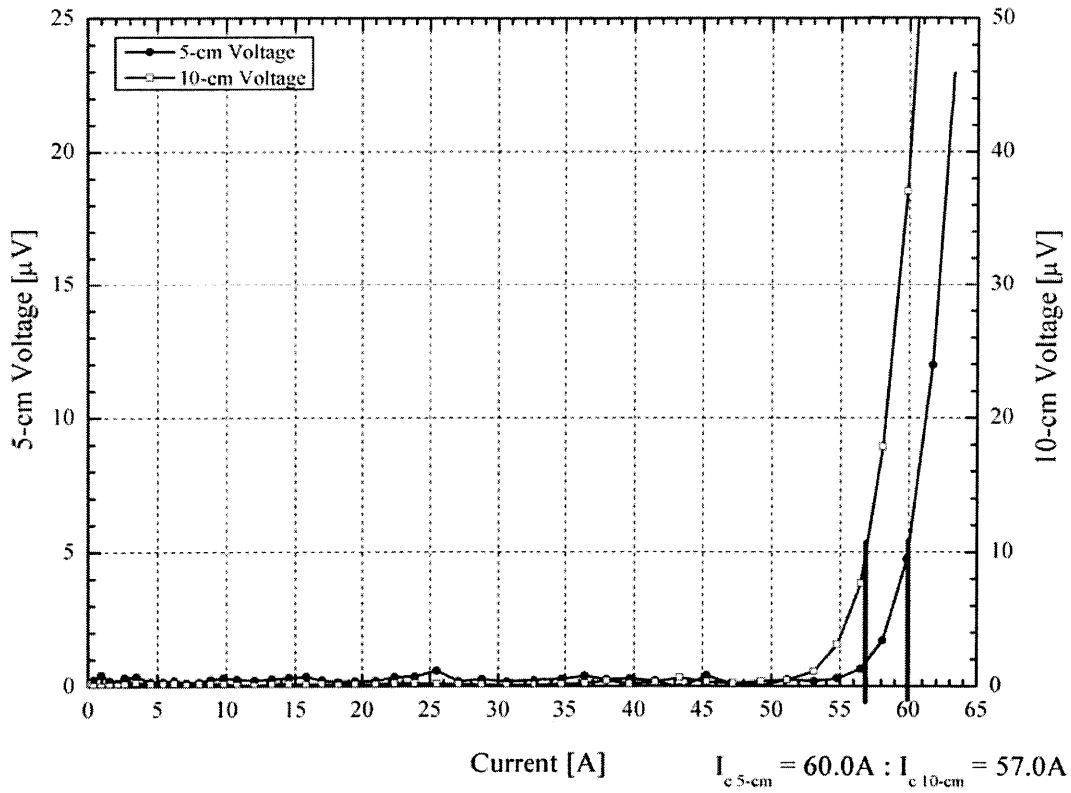


Figure 4-28. Critical current for sample SPCC-Cu-A-1 after 12th pulse. Measured using both 5-cm and 10-cm voltage taps; $I_{c\ 5\text{-cm}} = 60.0\text{A}$ and $I_{c\ 10\text{-cm}} = 57.0\text{A}$ with a $1\ \mu\text{V}/\text{cm}$ criterion.

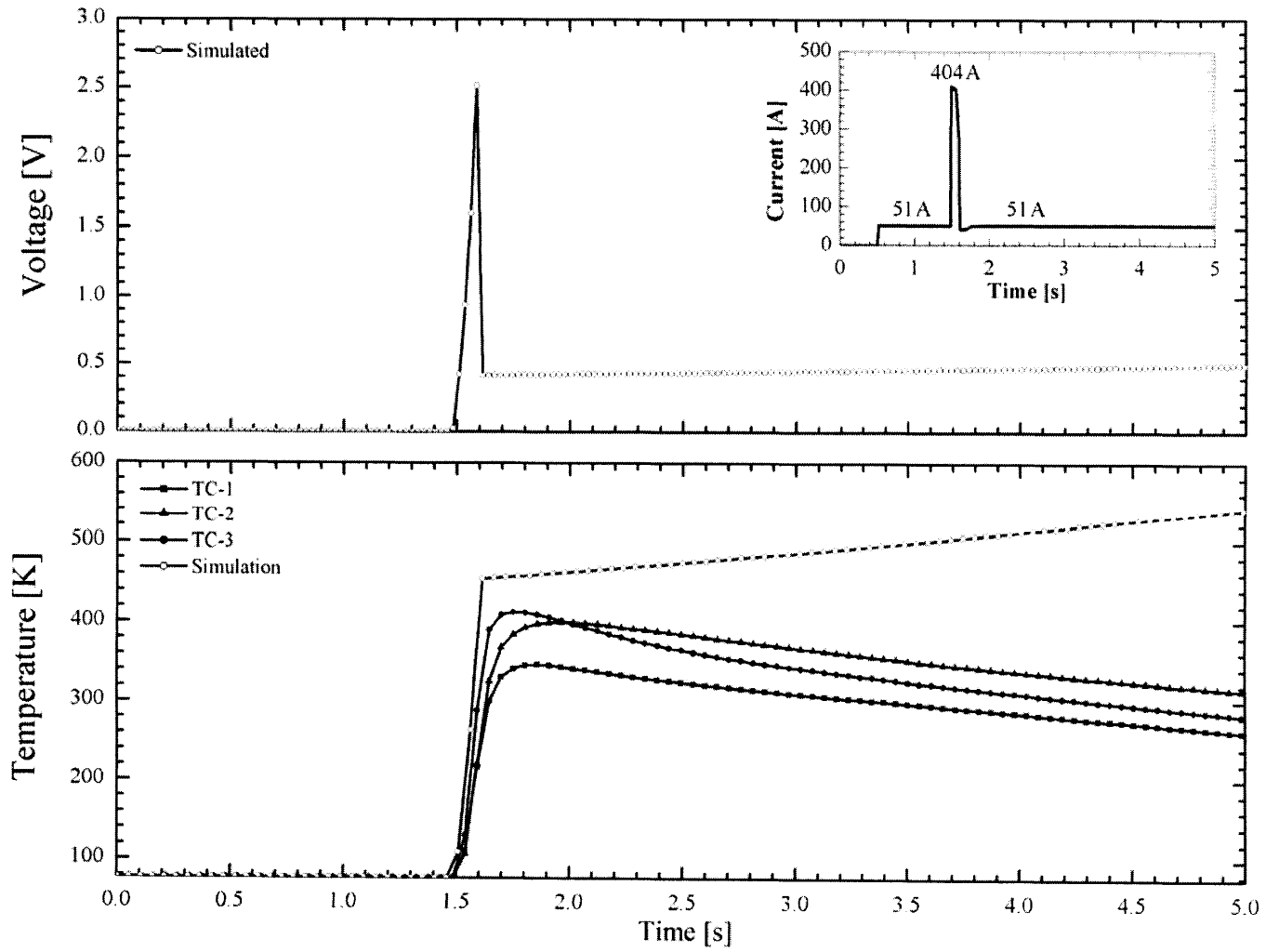


Figure 4-29. Sample SPCC-Cu-A-1: Run 13, $\tau = 100\text{ms}$, $t_{hold} = 7.0\text{s}$, $I_{op} = 51\text{A}$, $I_p = 404\text{A}$, $I_p/I_c = 6.85$.

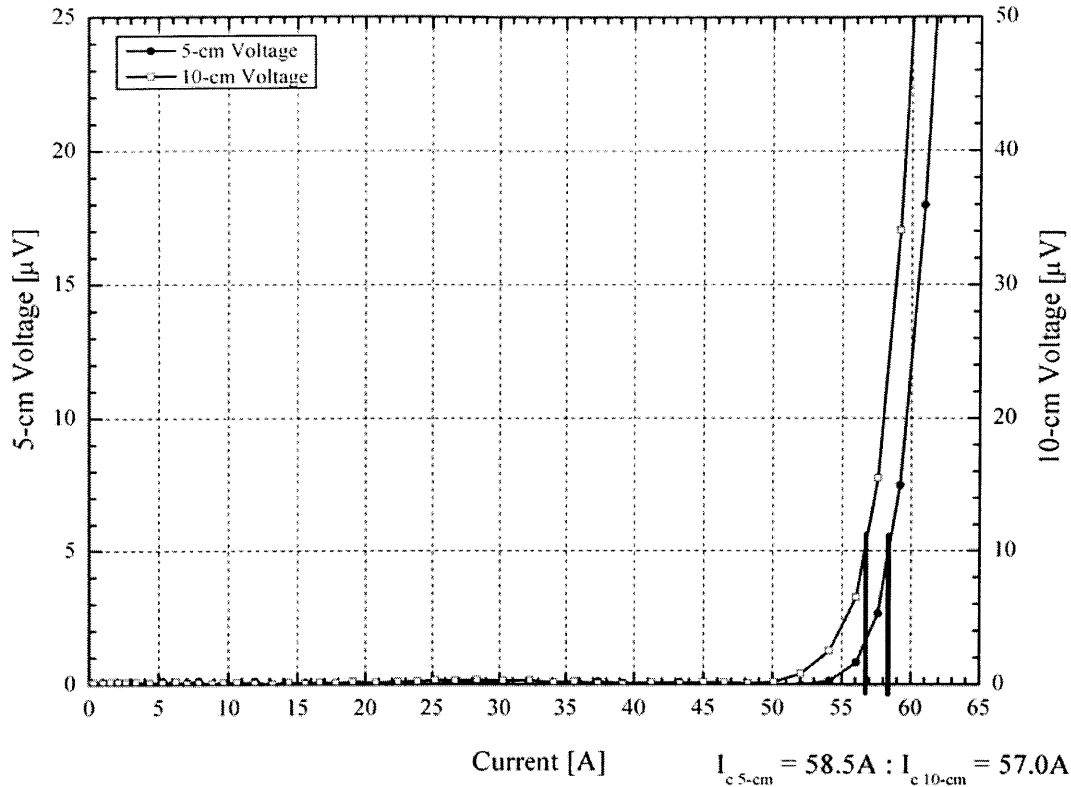


Figure 4-30. Critical current for sample SPCC-Cu-A-1 after 13th pulse. Measured using both 5-cm and 10-cm voltage taps; $I_{c\ 5\text{-cm}} = 58.5\text{ A}$ and $I_{c\ 10\text{-cm}} = 57.0\text{ A}$ with a $1\ \mu\text{V/cm}$ criterion.

4.5.3 Experimental and Simulated Results: 75- μm Thick Copper Lamina

Using the 75- μm thick copper laminated samples from SPI, several pulse durations were tested, including a 300-ms and 1-s pulse. For sample SPCC-Cu-G, the virgin critical current is shown in Figure 4-31. In Figure 4-32, the 4th pulse not only shows agreement in voltage traces between the experiment and simulation, but also very good agreement on temperatures. Shown in Figure 4-33, the sample was pulsed to a I_p/I_c ratio of 9.10 without degradation. The experimental (500K) and simulated (750K) temperatures were hot enough to damage the YBCO, but the sample managed to recover as indicated by both voltage and temperature traces. In addition, although the experimental temperature exceeded 400K, the critical current measurement after the 11th pulse did not indicate degradation; this is shown in Figure 4-34. However, sample SPCC-Cu-G became purely resistive after the 12th pulse with the I_p/I_c ratio of 9.48, shown in Figure 4-34.

The other two 75- μm thick copper laminated samples also suffered degradation to the superconductor from overheating. For sample SPCC-Cu-E this occurred at a I_p/I_c ratio of 8.0, while a burnout of sample SPCC-Cu-F occurred at a I_p/I_c ratio of 4.5 and pulse duration of 1-s.

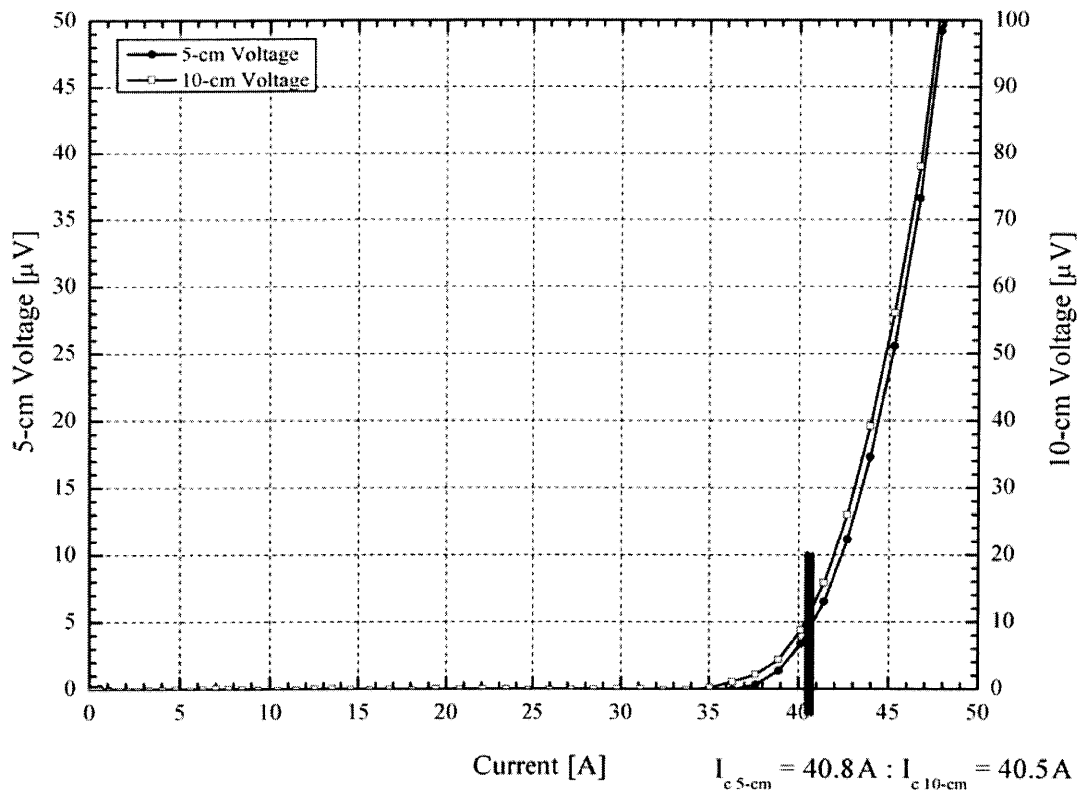


Figure 4-31. Virgin run for sample SPCC-Cu-G. Measured using both 5-cm and 10-cm voltage taps; $I_{c\ 5\text{-cm}} = 40.8\text{ A}$ and $I_{c\ 10\text{-cm}} = 40.5\text{ A}$ with a $1\ \mu\text{V}/\text{cm}$ criterion.

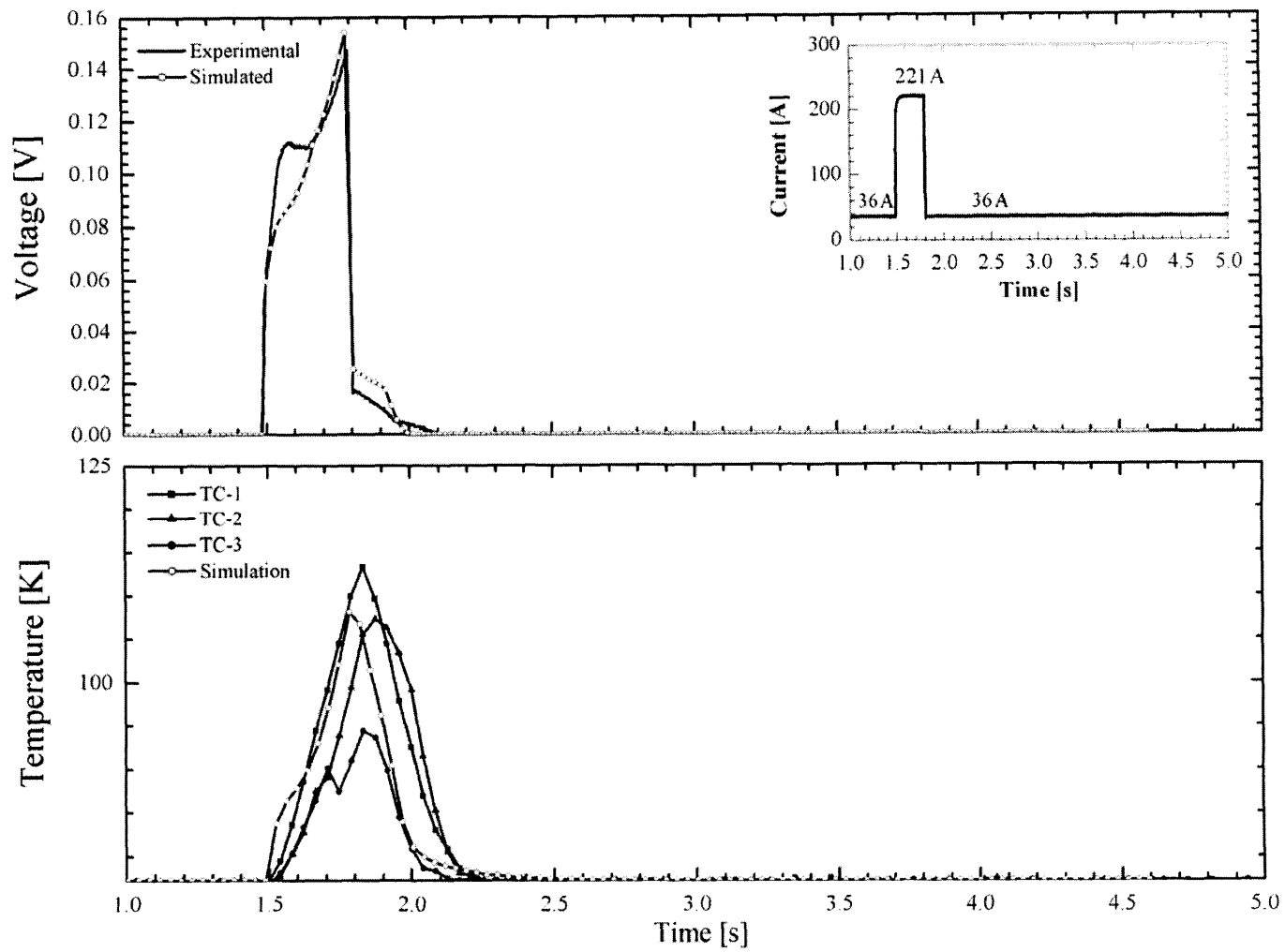


Figure 4-32. Sample SPCC-Cu-G: Run 4, $\tau = 300\text{ms}$, $t_{\text{hold}} = 7.0\text{s}$, $I_{\text{op}} = 36\text{A}$, $I_p = 221\text{A}$, $I_p/I_c = 6.13$.

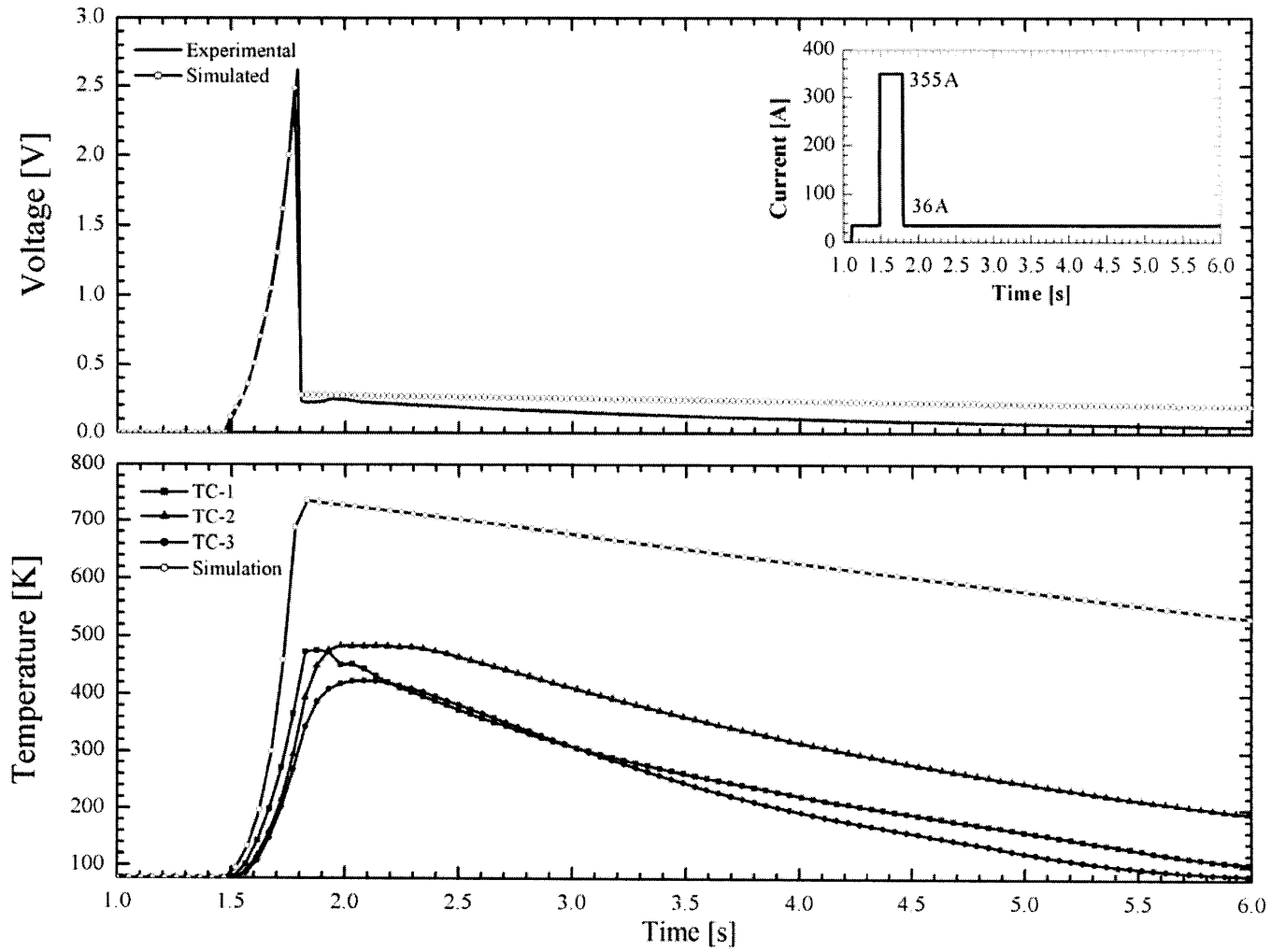


Figure 4-33. Sample SPCC-Cu-G: Run 11, $\tau = 300\text{ms}$, $t_{hold} = 7.0\text{s}$, $I_{op} = 36\text{A}$, $I_p = 355\text{A}$, $I_p/I_c = 9.10$.

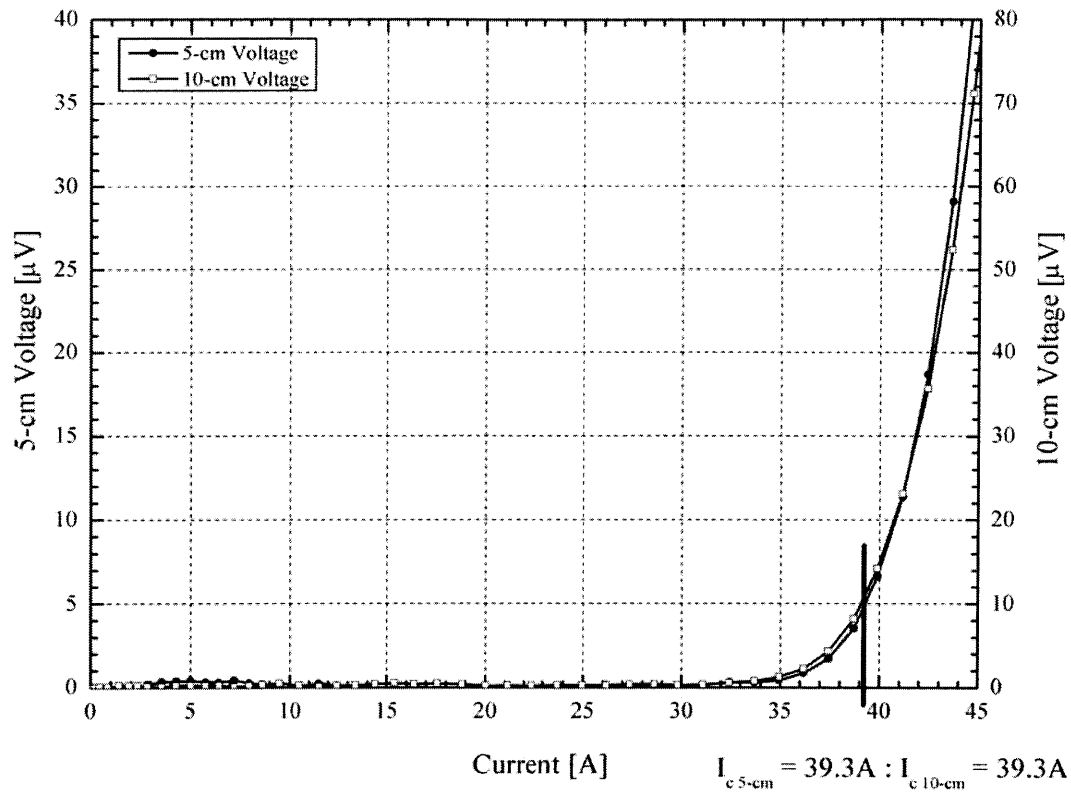


Figure 4-34. Critical current for sample SPCC-Cu-G after 11th pulse. Measured using both 5-cm and 10-cm voltage taps; $I_{c\ 5\text{-cm}} = 39.3\text{ A}$ and $I_{c\ 10\text{-cm}} = 39.3\text{ A}$ with a $1\ \mu\text{V}/\text{cm}$ criterion.

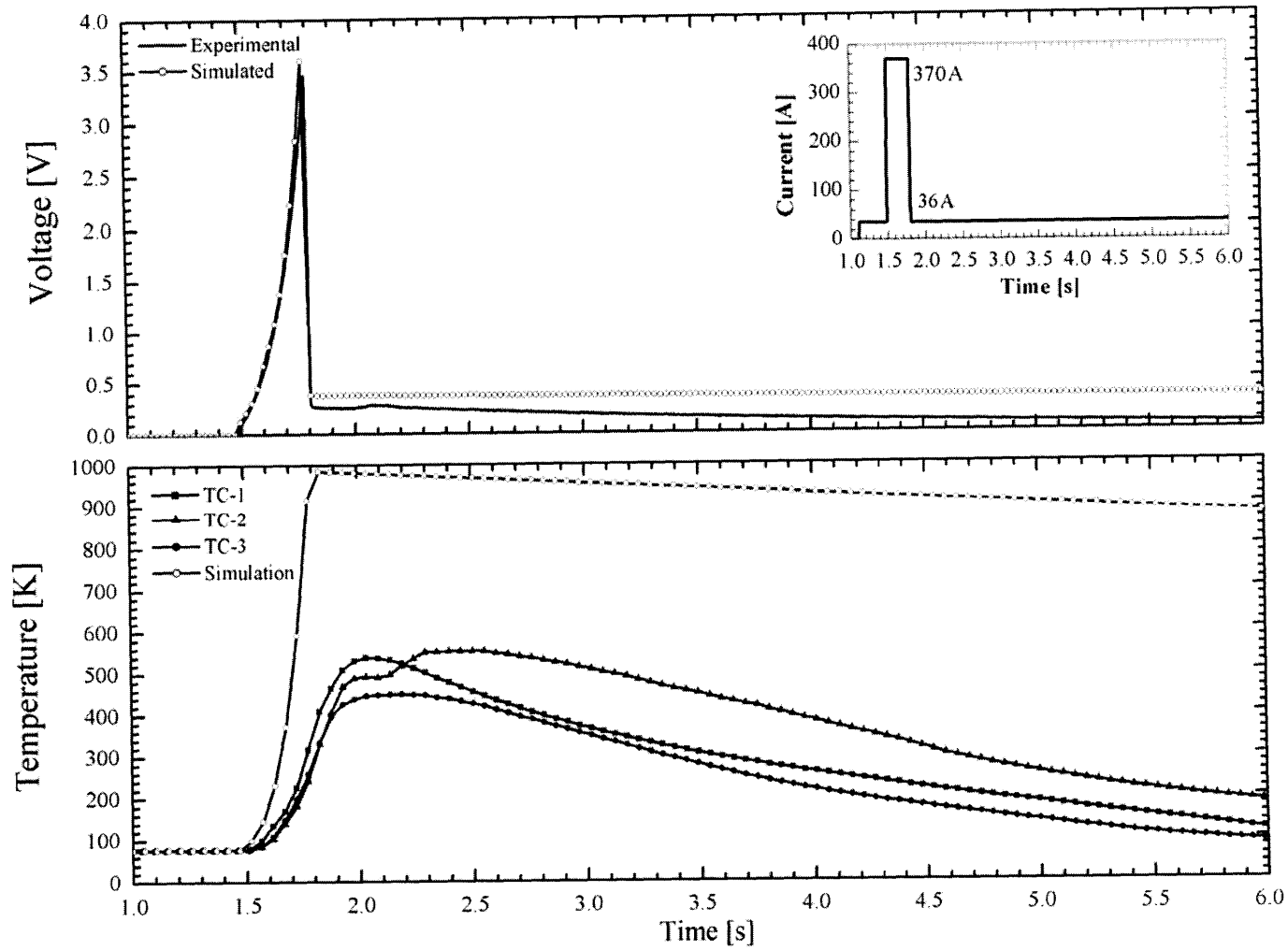


Figure 4-35. Sample SPCC-Cu-G: Run 12, $\tau = 300\text{ms}$, $t_{\text{hold}} = 7.0\text{s}$, $I_{\text{op}} = 36\text{A}$, $I_p = 370\text{A}$, $I_p/I_c = 9.48$.

4.6 Summary of Results and Comparison of Data

Figure 4-36 summarizes I_p/I_c ratios used for all of the YBCO samples measured in this work. In this figure, the black lines represent the experimental data. If the black line is missing, it indicates the absence of experimental data because of instrumentation problems or no measurement because of prior damage to the sample. Note that since the experiment ran for several months, the pulse durations between samples varied significantly, in part because of request from both AMSC and SPI. The pulse duration used for each sample is included in Figure 4-36.

The simulated model was used to generate a quench condition for each sample using a 100-ms pulse. These results are shown in Figure 4-37.

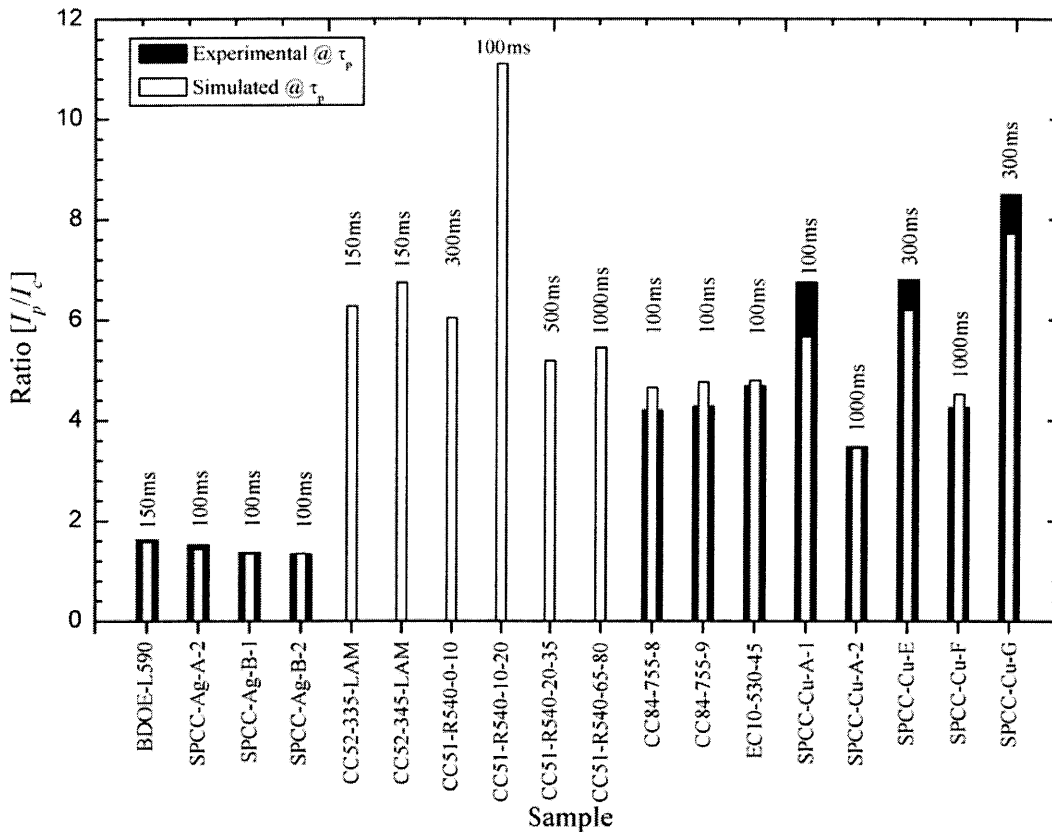


Figure 4-36. Experimental and simulated I_p/I_c ratios for each sample.

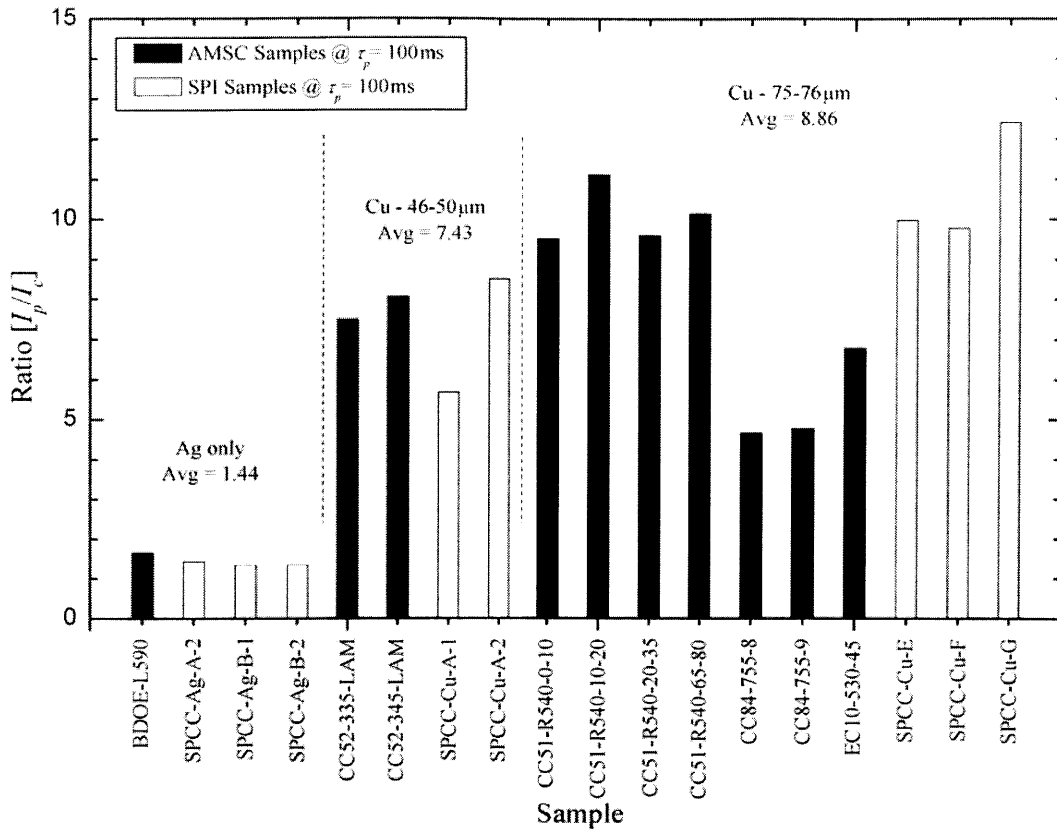


Figure 4-37. Simulated results for each sample using a 100-ms pulse and 400K burnout criterion.

In Figure 4-37, the samples have been separated into three categories based on their copper lamination thickness. In each section, the samples were grouped according to manufacturer to illustrate the differences in stability between manufacturing processes.

In Figure 4-37, the I_p/I_c ratios for samples CC84-755-5, CC84-755-9, and EC10-530-45 are lower than the other AMSC and SPI samples of similar copper thickness. These low ratios are consistent with experimental data because all three samples were subject to a 100-ms pulse. For these three 4-mm wide AMSC samples, the n -values are similar to those of the 4-mm wide SPI and 10-mm wide AMSC samples, and the low pulse ratio may be attributed to the effects of the slitting process used for these tapes. However, there were not enough AMSC 4-mm samples available to verify this conclusion.

Chapter 5

Conclusions and Recommendations

5.1 Conclusions

Both experiment and simulation demonstrated the importance of copper lamination for stability of YBCO superconductor. Both the experimental data and analytical model demonstrate that the over-current pulse capacity for non-copper stabilized conductor is significantly lower than that of the copper stabilized conductor. The 46- μm thick copper stabilized samples could withstand a pulse amplitude up to five times that of the silver-only samples, while the 76- μm thick copper stabilized samples could withstand a pulse amplitude eight times higher than the silver-only samples.

In general, the silver laminated samples failed through a runaway quench when the pulse amplitude was $1.5I_c$. Provided the sample remained partially superconducting during the pulse, the sample recovered. This extreme sensitivity to small changes in current was not present in the copper stabilized samples.

In contrast to the silver-only samples, the failure mode for the copper laminated samples was primarily due to overheating-induced degradation of I_c . Stability improves with increasing copper lamination thickness. For the copper stabilized samples, the superconductor was degraded when the pulse resulted in a uniform conductor temperature around 400K. Accordingly, since this temperature limit is controlled by the total power input to the tape, a longer pulse duration would require a smaller pulse current to ensure recovery. This observation can be seen in Figure 4-36, where the I_p/I_c ratio was significantly lower for longer pulse durations.

We may conclude that a copper lamination of sufficient thickness is required for YBCO superconductor for use in power devices. Although the overall conductor J_c decreases with the addition of copper lamina, the benefits should outweigh this reduction in engineering current density.

Furthermore, it was determined through the simulation that the quench behavior is also dependent on the n -value of the superconductor. With low n -value HTS superconductors, the current sharing above liquid nitrogen temperatures dramatically affects the ability of the tape to recover.

The location of failure where burnout occurred was random, which may be attributed to non-uniformity of the critical current along the conductor's length.

5.2 Recommendations

For further research into the stability of YBCO superconductors, several modifications should be made to the present experimental apparatus. First, longer copper current leads would reduce the effects of contact resistance heating at greater holding currents. Second, longer samples should be used with multiple test sections as this may uncover the effects of non-uniformity in critical current along the sample length.

References

- [1] M. Cyrot and D. Pavuna. *Introduction to Superconductivity and High- T_c Materials*, World Scientific Publishing Company, River Edge, NJ, pp. 4-9. (1992).
- [2] *Webster's New College Dictionary*. Houghton Mifflin Company, Boston, MA. (1996).
- [3] Y. Iwasa. *Case Studies in Superconducting Magnets*. Plenum Press, New York, NY. (1994).
- [4] J.K. Hulm and B.T. Matthias, "Overview of superconducting materials development," in *Superconductor Materials Science – Metallurgy, Fabrication, and Applications*, Eds., S. Foner and B.B. Swartz. Plenum Press, New York, NY. (1981).
- [5] J. Minirvini. Personal communication and class lecture notes. Massachusetts Institute of Technology. (2003).
- [6] S. Torii, S. Akaita, Y. Iijima, K. Takeda, and T. Saitoh. "Transport current properties of Y-Ba-Cu-O tape above critical current region," *IEEE Transactions on Applied Superconductivity*, Vol. 2, No. 1, pp. 1844- 1847. (2001).
- [7] Y. Cengel and M. Boles. *Thermodynamics, an Engineering Approach*. McGraw-Hill, Boston, MA. (1998).
- [8] A. F. Mills. *Heat Transfer*. Prentice Hall, Upper Saddle River, NJ. (1999).
- [9] S. Flechler. Personal communications through E-mail. American Superconductor Corporation. (2003).
- [10] H. Merte and J. Clark. *Advances in cryogenic engineering*, Vol. 7. Plenum Press, New York. (1962).
- [11] P. Titus. Personal communication in a memo to Bob Weggles. Francis Bitter Magnet Laboratory, Massachusetts Institute of Technology. (2002).
- [12] C.A. Thompson, W.M. Manganaro, and F.R. Fickett. *Cryogenic Properties of Copper*. National Institute of Standards and Technology, Boulder, CO. (1990).
- [13] *CRC Handbook of Chemistry and Physics, 84th Edition*. Ed., D. Lide. CRC Press, Boca Raton. (2003).
- [14] V. Johnson. *A Compendium of the Properties of Materials at Low Temperature (Phase II)*. National Bureau of Standards Cryogenic Engineering Laboratory. (1960).

- [15] National Institute of Standards and Technology. Material Properties: Nickel. Cryogenic technologies group. http://cryogenics.nist.gov/NewFiles/Nickel_steel.html. (2004).
- [16] M Aravind and P C W Fung. "Thermal parameter measurements of bulk YBCPO superconductor using PVDF transducer." *Measurement Science Technology*, 10, pp. 979-985. (1999).
- [17] M. Roulin, A. Junod, and E. Walker. "Scaling behavior of the derivatives of the specific heat of $\text{YBa}_2\text{Cu}_3\text{O}_{6.93}$ at the superconducting transition up to 16 tesla." *Physica C*, Vol. 260, Iss. 3, pp. 257-272. (1996).
- [18] N.I. Matskevich and Yu. G. Stenin, Phase Transition in $\text{Yba}_2\text{Cu}_3\text{O}_x$ at 300-900K, *Journal of Structural Chemistry*, 44, No. 2, pp. 222-226, (2003).
- [19] G. K. White, S. J. Collocott, R. Driver, et al., *J. Physics. C: Solid State Physics*, 21, L631-L637. (1988).
- [20] R. Harnois and D. Verebelyi. American Superconductor Technicians who helped prepare and mount samples. (2003).
- [21] F. Trillaud, H. Palanki, U.P. Trociewitz, S.H. Thompson, H. W. Weijers, and J. Swartz. "Normal zone propagation experiments on HTS composite conductors." *Cryogenics*, Vol. 43, pp. 217-229. (2003).
- [22] N. Ickes. Personal communication. Graduate Student in the Department of Electrical Engineering, Massachusetts Institute of Technology. (2004).

Appendix A – Program Code

Appendix A1: Main.m

```
%%%%%%%%%%%%%%%%%%%%%%%%%%%%%%%%%%%%%%%%%%%%%%%%%%%%%%%%%%%%%%%%%%%%%%%%%% Begin Main.m %%%%%%%%%%%%%%%%%%%%%%%%%%%%%%%%%%%%%%%%%%%%%%%%%%%%%%%%%%%%%%%%%%%%%%%%%%%
clc
clear all
close all
%%%%%%%%%%%%%%%%%%%%%%%%%%%%%%%%%%%%%%%%%%%%%%%%%%%%%%%%%%%%%%%%%%%%%%%%%% Set Current and Time of Experiment %%%%%%%%%%%%%%%%%%%%%%%%%%%%%%%%%%%%%%%%%%%%%%%%%%%%%%%%%%%%%%%%%%%%%%%%%%%
    Supplied_Current          % Calls Supplied_Current.m %%%%%%%%%%%%%%%%%%%%%%%%%%%%%%%%%%%%%%%%%%%%%%%%%%%%%%%%%%%%%%%%%%%%%%%%%%%
%%%%%%%%%%%%%%%%%%%%%%%%%%%%%%%%%%%%%%%%%%%%%%%%%%%%%%%%%%%%%%%%%%%%%%%%%% End Set Current and Time of Experiment %%%%%%%%%%%%%%%%%%%%%%%%%%%%%%%%%%%%%%%%%%%%%%%%%%%%%%%%%%%%%%%%%%%%%%%%%%%
%%%%%%%%%%%%%%%%%%%%%%%%%%%%%%%%%%%%%%%%%%%%%%%%%%%%%%%%%%%%%%%%%%%%%%%%%% Set Material Properties %%%%%%%%%%%%%%%%%%%%%%%%%%%%%%%%%%%%%%%%%%%%%%%%%%%%%%%%%%%%%%%%%%%%%%%%%%%
%%%%%%%%%%%%%%%%%%%%%%%%%%%%%%%%%%%%%%%%%%%%%%%%%%%%%%%%%%%%%%%%%%%%%%%%%% Tape %%%%%%%%%%%%%%%%%%%%%%%%%%%%%%%%%%%%%%%%%%%%%%%%%%%%%%%%%%%%%%%%%%%%%%%%%%%
    Length=0.05;              % (m) - Between Voltage Tabs %%%%%%%%%%%%%%%%%%%%%%%%%%%%%%%%%%%%%%%%%%%%%%%%%%%%%%%%%%%%%%%%%%%%%%%%%%%
    Width=0.004;              % (m) %%%%%%%%%%%%%%%%%%%%%%%%%%%%%%%%%%%%%%%%%%%%%%%%%%%%%%%%%%%%%%%%%%%%%%%%%%%
%%%%%%%%%%%%%%%%%%%%%%%%%%%%%%%%%%%%%%%%%%%%%%%%%%%%%%%%%%%%%%%%%%%%%%%%%% YBCO %%%%%%%%%%%%%%%%%%%%%%%%%%%%%%%%%%%%%%%%%%%%%%%%%%%%%%%%%%%%%%%%%%%%%%%%%%%
    VCritical=1e-4;           % (V/m) %%%%%%%%%%%%%%%%%%%%%%%%%%%%%%%%%%%%%%%%%%%%%%%%%%%%%%%%%%%%%%%%%%%%%%%%%%%
    Vc=VCritical*Length;      % (V) %%%%%%%%%%%%%%%%%%%%%%%%%%%%%%%%%%%%%%%%%%%%%%%%%%%%%%%%%%%%%%%%%%%%%%%%%%%
    Critical_Current_at_77=39; % (A) %%%%%%%%%%%%%%%%%%%%%%%%%%%%%%%%%%%%%%%%%%%%%%%%%%%%%%%%%%%%%%%%%%%%%%%%%%%
    Thickness_HTS=1e-6;       % (m) %%%%%%%%%%%%%%%%%%%%%%%%%%%%%%%%%%%%%%%%%%%%%%%%%%%%%%%%%%%%%%%%%%%%%%%%%%%
    Cross_Sectional_Area_HTS=Thickness_HTS*Width; %%%%%%%%%%%%%%%%%%%%%%%%%%%%%%%%%%%%%%%%%%%%%%%%%%%%%%%%%%%%%%%%%%%%%%%%%%%
    N_Value                    % Calls N_Value.m %%%%%%%%%%%%%%%%%%%%%%%%%%%%%%%%%%%%%%%%%%%%%%%%%%%%%%%%%%%%%%%%%%%%%%%%%%%
%%%%%%%%%%%%%%%%%%%%%%%%%%%%%%%%%%%%%%%%%%%%%%%%%%%%%%%%%%%%%%%%%%%%%%%%%% Substrate %%%%%%%%%%%%%%%%%%%%%%%%%%%%%%%%%%%%%%%%%%%%%%%%%%%%%%%%%%%%%%%%%%%%%%%%%%%
    Thickness_Sub=100e-6;      %%%%%%%%%%%%%%%%%%%%%%%%%%%%%%%%%%%%%%%%%%%%%%%%%%%%%%%%%%%%%%%%%%%%%%%%%%%
    Cross_Sectional_Area_Sub=Thickness_Sub*Width; %%%%%%%%%%%%%%%%%%%%%%%%%%%%%%%%%%%%%%%%%%%%%%%%%%%%%%%%%%%%%%%%%%%%%%%%%%%
%%%%%%%%%%%%%%%%%%%%%%%%%%%%%%%%%%%%%%%%%%%%%%%%%%%%%%%%%%%%%%%%%%%%%%%%%% Copper %%%%%%%%%%%%%%%%%%%%%%%%%%%%%%%%%%%%%%%%%%%%%%%%%%%%%%%%%%%%%%%%%%%%%%%%%%%
    Thickness_Cu=76e-6;        %%%%%%%%%%%%%%%%%%%%%%%%%%%%%%%%%%%%%%%%%%%%%%%%%%%%%%%%%%%%%%%%%%%%%%%%%%%
    Cross_Sectional_Area_Cu=Thickness_Cu*Width; %%%%%%%%%%%%%%%%%%%%%%%%%%%%%%%%%%%%%%%%%%%%%%%%%%%%%%%%%%%%%%%%%%%%%%%%%%%
%%%%%%%%%%%%%%%%%%%%%%%%%%%%%%%%%%%%%%%%%%%%%%%%%%%%%%%%%%%%%%%%%%%%%%%%%% Silver %%%%%%%%%%%%%%%%%%%%%%%%%%%%%%%%%%%%%%%%%%%%%%%%%%%%%%%%%%%%%%%%%%%%%%%%%%%
    Thickness_Ag=3e-6;         %%%%%%%%%%%%%%%%%%%%%%%%%%%%%%%%%%%%%%%%%%%%%%%%%%%%%%%%%%%%%%%%%%%%%%%%%%%
    Cross_Sectional_Area_Ag=Thickness_Ag*Width; %%%%%%%%%%%%%%%%%%%%%%%%%%%%%%%%%%%%%%%%%%%%%%%%%%%%%%%%%%%%%%%%%%%%%%%%%%%
%%%%%%%%%%%%%%%%%%%%%%%%%%%%%%%%%%%%%%%%%%%%%%%%%%%%%%%%%%%%%%%%%%%%%%%%%% LN2 %%%%%%%%%%%%%%%%%%%%%%%%%%%%%%%%%%%%%%%%%%%%%%%%%%%%%%%%%%%%%%%%%%%%%%%%%%%
    Surface_Area=Width*Length; %%%%%%%%%%%%%%%%%%%%%%%%%%%%%%%%%%%%%%%%%%%%%%%%%%%%%%%%%%%%%%%%%%%%%%%%%%%
    T_LN2=77.3;               %%%%%%%%%%%%%%%%%%%%%%%%%%%%%%%%%%%%%%%%%%%%%%%%%%%%%%%%%%%%%%%%%%%%%%%%%%%
%%%%%%%%%%%%%%%%%%%%%%%%%%%%%%%%%%%%%%%%%%%%%%%%%%%%%%%%%%%%%%%%%%%%%%%%%% End Set Material Properties %%%%%%%%%%%%%%%%%%%%%%%%%%%%%%%%%%%%%%%%%%%%%%%%%%%%%%%%%%%%%%%%%%%%%%%%%%%
%%%%%%%%%%%%%%%%%%%%%%%%%%%%%%%%%%%%%%%%%%%%%%%%%%%%%%%%%%%%%%%%%%%%%%%%%% Definition of Variables %%%%%%%%%%%%%%%%%%%%%%%%%%%%%%%%%%%%%%%%%%%%%%%%%%%%%%%%%%%%%%%%%%%%%%%%%%%
Nucleate_Peak=88.8+(Ratio-3); %%%%%%%%%%%%%%%%%%%%%%%%%%%%%%%%%%%%%%%%%%%%%%%%%%%%%%%%%%%%%%%%%%%%%%%%%%%
DelTransTemp=100000000;      %%%%%%%%%%%%%%%%%%%%%%%%%%%%%%%%%%%%%%%%%%%%%%%%%%%%%%%%%%%%%%%%%%%%%%%%%%%
counter=0;                    %%%%%%%%%%%%%%%%%%%%%%%%%%%%%%%%%%%%%%%%%%%%%%%%%%%%%%%%%%%%%%%%%%%%%%%%%%%
Inew=0;                       %%%%%%%%%%%%%%%%%%%%%%%%%%%%%%%%%%%%%%%%%%%%%%%%%%%%%%%%%%%%%%%%%%%%%%%%%%%
error=1;                      %%%%%%%%%%%%%%%%%%%%%%%%%%%%%%%%%%%%%%%%%%%%%%%%%%%%%%%%%%%%%%%%%%%%%%%%%%%
k=1;                          %%%%%%%%%%%%%%%%%%%%%%%%%%%%%%%%%%%%%%%%%%%%%%%%%%%%%%%%%%%%%%%%%%%%%%%%%%%
Temperature_Counter(k)=0;     %%%%%%%%%%%%%%%%%%%%%%%%%%%%%%%%%%%%%%%%%%%%%%%%%%%%%%%%%%%%%%%%%%%%%%%%%%%
Place(k)=0;                   %%%%%%%%%%%%%%%%%%%%%%%%%%%%%%%%%%%%%%%%%%%%%%%%%%%%%%%%%%%%%%%%%%%%%%%%%%%
Ta=T_LN2;                     %%%%%%%%%%%%%%%%%%%%%%%%%%%%%%%%%%%%%%%%%%%%%%%%%%%%%%%%%%%%%%%%%%%%%%%%%%%
R_Cu(k)=0;                    %%%%%%%%%%%%%%%%%%%%%%%%%%%%%%%%%%%%%%%%%%%%%%%%%%%%%%%%%%%%%%%%%%%%%%%%%%%
Rs(k)=0;                      %%%%%%%%%%%%%%%%%%%%%%%%%%%%%%%%%%%%%%%%%%%%%%%%%%%%%%%%%%%%%%%%%%%%%%%%%%%
Rm(k)=0;                      %%%%%%%%%%%%%%%%%%%%%%%%%%%%%%%%%%%%%%%%%%%%%%%%%%%%%%%%%%%%%%%%%%%%%%%%%%%
Is(k)=0;                      %%%%%%%%%%%%%%%%%%%%%%%%%%%%%%%%%%%%%%%%%%%%%%%%%%%%%%%%%%%%%%%%%%%%%%%%%%%
Im(k)=0;                      %%%%%%%%%%%%%%%%%%%%%%%%%%%%%%%%%%%%%%%%%%%%%%%%%%%%%%%%%%%%%%%%%%%%%%%%%%%
Temperature(k)=T_LN2;         %%%%%%%%%%%%%%%%%%%%%%%%%%%%%%%%%%%%%%%%%%%%%%%%%%%%%%%%%%%%%%%%%%%%%%%%%%%
QsM(k)=0;                     %%%%%%%%%%%%%%%%%%%%%%%%%%%%%%%%%%%%%%%%%%%%%%%%%%%%%%%%%%%%%%%%%%%%%%%%%%%
QsHTS(k)=0;                   %%%%%%%%%%%%%%%%%%%%%%%%%%%%%%%%%%%%%%%%%%%%%%%%%%%%%%%%%%%%%%%%%%%%%%%%%%%
QsAll(k)=QsM(k)+QsHTS(k);     %%%%%%%%%%%%%%%%%%%%%%%%%%%%%%%%%%%%%%%%%%%%%%%%%%%%%%%%%%%%%%%%%%%%%%%%%%%
DeltaT(k)=0;                  %%%%%%%%%%%%%%%%%%%%%%%%%%%%%%%%%%%%%%%%%%%%%%%%%%%%%%%%%%%%%%%%%%%%%%%%%%%
```

```

Del_T(k)=0; %%%%%%%%%
Qout(k)=0; %%%%%%%%%
QRemain(k)=QsAll(k)-Qout(k); %%%%%%%%%
Vm=0; %%%%%%%%%
Vs=0; %%%%%%%%%
Temp_Counter=0; %%%%%%%%%
k=k+1; %%%%%%%%%
%%%%%%%%% End Definition of Variables %%%%%%%%%%
%%%%%%%%% Soution to Energy Equation %%%%%%%%%%
while k<=size(time,1) %%%%%%%%%
    Ta=Temperature(k-1); %%%%%%%%%
    Del_T(k)=(Ta-T_LN2)*1.8; %%%%%%%%%
    if Ta<93 %%%%%%%%%
        RSub=Sub_Res(Ta)*Length/Cross_Sectional_Area_Sub; %%%%%%%%%
        RAg=Ag_Res(Ta)*Length/Cross_Sectional_Area_Ag; %%%%%%%%%
        RCu=Cu_Res(Ta)*Length/Cross_Sectional_Area_Cu; %%%%%%%%%
        Rm=( (RSub*RAg*RCu) / ( (RSub*RAg) + (RSub*RCu) + (RCu*RAg) ) ); %%%%%%%%%
        Ic(k)=(Critical_Current_at_77/-0.1848)*log(Ta/93); %%%%%%%%%
        while abs(error)>=0.0001 %%%%%%%%%
            A=Vc / (Rm*Ic(k)^n); %%%%%%%%%
            B=Inew^n; %%%%%%%%%
            C=Inew; %%%%%%%%%
            D=(A*B)+C; %%%%%%%%%
            error=Current(k)-D; %%%%%%%%%
            Inew=Inew+(error/10001); %%%%%%%%%
            if Inew>0 %%%%%%%%%
                Vm=(Current(k)-Inew)*Rm; %%%%%%%%%
                if Vm<0 %%%%%%%%%
                    Vm=0; %%%%%%%%%
                end %%%%%%%%%
                Rs=Vm/Inew; %%%%%%%%%
            else %%%%%%%%%
                Inew=0; %%%%%%%%%
                Vm=Current(k)*Rm; %%%%%%%%%
                Rs=100000000; %%%%%%%%%
            end %%%%%%%%%
        end %%%%%%%%%
        Is(k)=Inew; %%%%%%%%%
        Im(k)=Current(k)-Is(k); %%%%%%%%%
        if Im(k)<0 %%%%%%%%%
            Im(k)=0; %%%%%%%%%
            Is(k)=Current(k); %%%%%%%%%
        end %%%%%%%%%
        QsM(k)=Im(k)*Im(k)*Rm*Delta_Time; %%%%%%%%%
        QsHTS(k)=Is(k)*Is(k)*Rs*Delta_Time; %%%%%%%%%
        QsAll(k)=QsM(k)+QsHTS(k); %%%%%%%%%
        %%%%%%%%%% % Calls cooling.m code %%%%%%%%%%
        cooling %%%%%%%%%%
        QRemain(k)=QRemain(k-1)+QsAll(k)-Qout(k); %%%%%%%%%
        if QRemain(k)<0 %%%%%%%%%
            QRemain(k)=0; %%%%%%%%%
        end %%%%%%%%%
        Cp_Sub(k)=Sub_Cp(Ta)*(Length*Width*Thickness_Sub); %%%%%%%%%
        Cp_Cu(k)=Cu_Cp(Ta)*(Length*Width*Thickness_Cu); %%%%%%%%%
        Cp_Ag(k)=Ag_Cp(Ta)*(Length*Width*Thickness_Ag); %%%%%%%%%
        Specific_Heat_HTS(k)=YBCO_Cp(Ta)*(Length*Width*

```

```

        Thickness_HTS)*6380;                                %%%%%%%%%
DeltaT(k)=QRemain(k)/(Cp_Sub(k)+Specific_Heat_HTS(k)+
        Cp_Ag(k)+Cp_Cu(k));                                %%%%%%%%%
Ta=DeltaT(k)+T_LN2;                                       %%%%%%%%%
Is(k)=Inew;                                               %%%%%%%%%
Vs=Is(k)*Rs;                                              %%%%%%%%%
Voltage_HTS(k)=Vs;                                         %%%%%%%%%
error=1;                                                   %%%%%%%%%
Temperature(k)=Ta;                                         %%%%%%%%%
R_M(k)=Rm;                                                 %%%%%%%%%
Voltage_M(k)=Im(k)*R_M(k);                                %%%%%%%%%
R_HTS(k)=Rs;                                              %%%%%%%%%
k=k+1;                                                     %%%%%%%%%
else                                                       %%%%%%%%%
    R_Sub(k)=Sub_Res(Ta)*Length/Cross_Sectional_Area_Sub; %%%%%%%%%
    R_Cu(k)=Cu_Res(Ta)*Length/Cross_Sectional_Area_Cu;    %%%%%%%%%
    R_Ag(k)=Ag_Res(Ta)*Length/Cross_Sectional_Area_Ag;    %%%%%%%%%
    Rm=((R_Sub(k)*R_Ag(k)*R_Cu(k))/(R_Sub(k)*R_Ag(k))+
        (R_Sub(k)*R_Cu(k)+(R_Cu(k)*R_Ag(k))));            %%%%%%%%%
    Ic(k)=0;                                               %%%%%%%%%
    Is(k)=0;                                               %%%%%%%%%
    Im(k)=Current(k)-Is(k);                                %%%%%%%%%
    QsM(k)=Im(k)*Im(k)*Rm*Delta_Time;                      %%%%%%%%%
    QsHTS(k)=Is(k)*Is(k)*Rs*Delta_Time;                   %%%%%%%%%
    QsAll(k)=QsM(k)+QsHTS(k);                              %%%%%%%%%
    %%%%%%%%%%%%%%%
    cooling % Calls cooling.m code %%%%%%%%%%%%%%%
    %%%%%%%%%%%%%%%
    QRemain(k)=QRemain(k-1)+QsAll(k)-Qout(k);              %%%%%%%%%
    if QRemain(k)<0                                         %%%%%%%%%
        QRemain(k)=0;                                       %%%%%%%%%
    end                                                     %%%%%%%%%
    Cp_Sub(k)=Sub_Cp(Ta)*(Length*Width*Thickness_Sub);    %%%%%%%%%
    Cp_Cu(k)=Cu_Cp(Ta)*(Length*Width*Thickness_Cu);       %%%%%%%%%
    Cp_Ag(k)=Ag_Cp(Ta)*(Length*Width*Thickness_Ag);       %%%%%%%%%
    Specific_Heat_HTS(k)=YBCO_Cp(Ta)*(Length*Width*
        Thickness_HTS)*6380;                                %%%%%%%%%
    DeltaT(k)=QRemain(k)/(Cp_Sub(k)+Specific_Heat_HTS(k)+
        Cp_Ag(k)+Cp_Cu(k));                                %%%%%%%%%
    Ta=DeltaT(k)+T_LN2;                                       %%%%%%%%%
    error=1;                                                   %%%%%%%%%
    Temperature(k)=Ta;                                         %%%%%%%%%
    R_M(k)=Rm;                                                 %%%%%%%%%
    Voltage_M(k)=Im(k)*R_M(k);                                %%%%%%%%%
    Voltage_HTS(k)=Voltage_M(k);                            %%%%%%%%%
    R_HTS(k)=1000000000;                                       %%%%%%%%%
    k=k+1;                                                     %%%%%%%%%
end
end
%%%%%%%%%%%%%%%%%%%%%%%%%%%%%%%%%%%%%%%%%%%%%%%%%%%%%%%%%%%%%%%%%%%%%%%% End Soutlion to Energy Equation %%%%%%%%%
%%%%%%%%%%%%%%%%%%%%%%%%%%%%%%%%%%%%%%%%%%%%%%%%%%%%%%%%%%%%%%%%%%%%%%%% Generates Output Text File %%%%%%%%%
X=[time';Temperature;Voltage_HTS;Current'];              %%%%%%%%%
Y=X';                                                       %%%%%%%%%
save Cooled.txt -ascii Y                                    %%%%%%%%%
%%%%%%%%%%%%%%%%%%%%%%%%%%%%%%%%%%%%%%%%%%%%%%%%%%%%%%%%%%%%%%%%%%%%%%%% End Generates Output Text File %%%%%%%%%
%%%%%%%%%%%%%%%%%%%%%%%%%%%%%%%%%%%%%%%%%%%%%%%%%%%%%%%%%%%%%%%%%%%%%%%% End Main.m Program%%%%%%%%%%%%%%%%%%%%%%%%%%%%%%%%%%%%%%%%%%%%%%%%%%%%%%%%%%%%%%%%%%%%%%%%

```

Appendix A2: Supplied_Current.m

```

%%%%%%%%%%%%%%%%%%%%%%%%%%%%%%%%%%%%%%%%%%%%%%%%%%%%%%%%%%%%%%%%%%%%%%%%%% Begin Supplied_Current.m %%%%%%%%%%%%%%%%%%%%%%%%%%%%%%%%%%%%%%%%%%%%%%%%%%%%%%%%%%%%%%%%%%%%%%%%%%%
%%%%%%%%%%%%%%%%%%%%%%%%%%%%%%%%%%%%%%%%%%%%%%%%%%%%%%%%%%%%%%%%%%%%%%%%%% Set time for piecewise current trace %%%%%%%%%%%%%%%%%%%%%%%%%%%%%%%%%%%%%%%%%%%%%%%%%%%%%%%%%%%%%%%%%%%%%%%%%%%
    start_time=0.0;
%%%%%%%%%%%%%%%%%%%%%%%%%%%%%%%%%%%%%%%%%%%%%%%%%%%%%%%%%%%%%%%%%%%%%%%%%% Begin User input for desired ramp time %%%%%%%%%%%%%%%%%%%%%%%%%%%%%%%%%%%%%%%%%%%%%%%%%%%%%%%%%%%%%%%%%%%%%%%%%%%
    supplied_holding_current=input('Please enter holding current:');
    supplied_peak_current=input('Please enter peak current:');
%%%%%%%%%%%%%%%%%%%%%%%%%%%%%%%%%%%%%%%%%%%%%%%%%%%%%%%%%%%%%%%%%%%%%%%%%% End User input for desired ramp time %%%%%%%%%%%%%%%%%%%%%%%%%%%%%%%%%%%%%%%%%%%%%%%%%%%%%%%%%%%%%%%%%%%%%%%%%%%
    Ratio=supplied_peak_current/supplied_holding_current;
    Delta_Time=.001;
    ramp_time=0.01;
    start_of_pulse=0.375;
    pulse_time=0.120-(2*ramp_time);
    total_time=3.0;
    time_ramp_1_starts=(start_time+0.1);
    time_ramp_1_ends=(time_ramp_1_starts+ramp_time);
    time_ramp_2_starts=(time_ramp_1_ends+start_of_pulse);
    time_ramp_2_ends=(time_ramp_2_starts+ramp_time);
    time_pulse_ends=(time_ramp_2_ends+pulse_time);
    time_ramp_3_ends=(time_pulse_ends+ramp_time);
    time_ramp_4_starts=(time_ramp_1_ends+total_time);
    time_ramp_4_ends=(time_ramp_4_starts+ramp_time);
    time_ends=(time_ramp_4_ends+0.5);
%%%%%%%%%%%%%%%%%%%%%%%%%%%%%%%%%%%%%%%%%%%%%%%%%%%%%%%%%%%%%%%%%%%%%%%%%% End Set time for piecewise current trace %%%%%%%%%%%%%%%%%%%%%%%%%%%%%%%%%%%%%%%%%%%%%%%%%%%%%%%%%%%%%%%%%%%%%%%%%%%
%%%%%%%%%%%%%%%%%%%%%%%%%%%%%%%%%%%%%%%%%%%%%%%%%%%%%%%%%%%%%%%%%%%%%%%%%% Create Time Matrix %%%%%%%%%%%%%%%%%%%%%%%%%%%%%%%%%%%%%%%%%%%%%%%%%%%%%%%%%%%%%%%%%%%%%%%%%%%
    time_1=linspace(start_time,time_ramp_1_starts,
        ((time_ramp_1_starts-start_time)/Delta_Time));
    time_1(1)=[];
    time_2=linspace(time_ramp_1_starts,time_ramp_1_ends,
        ((time_ramp_1_ends-time_ramp_1_starts)/Delta_Time));
    time_2(1)=[];
    time_3=linspace(time_ramp_1_ends,time_ramp_2_starts,
        ((time_ramp_2_starts-time_ramp_1_ends)/Delta_Time));
    time_3(1)=[];
    time_4=linspace(time_ramp_2_starts,time_ramp_2_ends,
        ((time_ramp_2_ends-time_ramp_2_starts)/Delta_Time));
    time_4(1)=[];
    time_5=linspace(time_ramp_2_ends,time_pulse_ends,
        ((time_pulse_ends-time_ramp_2_ends)/Delta_Time));
    time_5(1)=[];
    time_6=linspace(time_pulse_ends,time_ramp_3_ends,
        ((time_ramp_3_ends-time_pulse_ends)/Delta_Time));
    time_6(1)=[];
    time_7=linspace(time_ramp_3_ends,time_ramp_4_starts,
        ((time_ramp_4_starts-time_ramp_3_ends)/Delta_Time));
    time_7(1)=[];
    time_8=linspace(time_ramp_4_starts,time_ramp_4_ends,
        ((time_ramp_4_ends-time_ramp_4_starts)/Delta_Time));
    time_8(1)=[];
    time_9=linspace(time_ramp_4_ends,time_ends,
        ((time_ends-time_ramp_4_ends)/Delta_Time));
    time_9(1)=[];
time=[time_1;time_2;time_3;time_4;time_5;time_6;time_7;time_8;time_9];
%%%%%%%%%%%%%%%%%%%%%%%%%%%%%%%%%%%%%%%%%%%%%%%%%%%%%%%%%%%%%%%%%%%%%%%%%% End Create Time Matrix %%%%%%%%%%%%%%%%%%%%%%%%%%%%%%%%%%%%%%%%%%%%%%%%%%%%%%%%%%%%%%%%%%%%%%%%%%%

```

```

%%%%%%%%%%%%%%%%%%%%%%%%%%%%%%%%%%%%%%%%%%%%%%%%%%%%%%%%%%%%%%%%%%%%%%%% Create Current Matrix %%%%%%%%%%%%%%%%%%%%%%%%%%%%%%%%%%%%%%%%%%%%%%%%%%%%%%%%%%%%%%%%%%%%%%%%%
current_1=linspace(0,0,
    ((time_ramp_1_starts-start_time)/Delta_Time))';          %%%%%
current_1(1)=[];                                           %%%%%
current_2=linspace(0,supplied_holding_current,
    ((time_ramp_1_ends-time_ramp_1_starts)/Delta_Time))';    %%%%%
current_2(1)=[];                                           %%%%%
current_3=linspace(supplied_holding_current,
    supplied_holding_current,((time_ramp_2_starts-
    time_ramp_1_ends)/Delta_Time))';                          %%%%%
current_3(1)=[];                                           %%%%%
current_4=linspace(supplied_holding_current,
    supplied_peak_current,((time_ramp_2_ends-
    time_ramp_2_starts)/Delta_Time))';                          %%%%%
current_4(1)=[];                                           %%%%%
current_5=linspace(supplied_peak_current,
    supplied_peak_current,((time_pulse_ends-
    time_ramp_2_ends)/Delta_Time))';                          %%%%%
current_5(1)=[];                                           %%%%%
current_6=linspace(supplied_peak_current,
    supplied_holding_current,((time_ramp_3_ends-
    time_pulse_ends)/Delta_Time))';                          %%%%%
current_6(1)=[];                                           %%%%%
current_7=linspace(supplied_holding_current,
    supplied_holding_current,((time_ramp_4_starts-
    time_ramp_3_ends)/Delta_Time))';                          %%%%%
current_7(1)=[];                                           %%%%%
current_8=linspace(supplied_holding_current,0,
    ((time_ramp_4_ends-time_ramp_4_starts)/Delta_Time))';    %%%%%
current_8(1)=[];                                           %%%%%
current_9=linspace(0,0,((time_ends-time_ramp_4_ends)/
    Delta_Time))';                                          %%%%%
current_9(1)=[];                                           %%%%%
Current=[current_1;current_2;current_3;current_4;current_5;
    current_6;current_7;current_8;current_9];                %%%%%
%%%%%%%%%%%%%%%%%%%%%%%%%%%%%%%%%%%%%%%%%%%%%%%%%%%%%%%%%%%%%%%%%%%%%%%% End Create Current Matrix %%%%%%%%%%%%%%%%%%%%%%%%%%%%%%%%%%%%%%%%%%%%%%%%%%%%%%%%%%%%%%%%%%%%%%%%%
%%%%%%%%%%%%%%%%%%%%%%%%%%%%%%%%%%%%%%%%%%%%%%%%%%%%%%%%%%%%%%%%%%%%%%%% End Supplied_Current.m %%%%%%%%%%%%%%%%%%%%%%%%%%%%%%%%%%%%%%%%%%%%%%%%%%%%%%%%%%%%%%%%%%%%%%%%%

```

Appendix A3: Cooling.m

```

%%%%%%%%%%%%%%%%%%%%%%%%%%%%%%%%%%%%%%%%%%%%%%%%%%%%%%%%%%%%%%%%%%%%%%%%%% Begin Cooling.m %%%%%%%%%%%%%%%%%%%%%%%%%%%%%%%%%%%%%%%%%%%%%%%%%%%%%%%%%%%%%%%%%%%%%%%%%%%
if Temperature_Counter(k-1)==0
    if Del_T(k)>=Del_T(k-1)
        if Del_T(k)<3.5
            q=(Del_T(k))*(10^3/3.5);
            Place(k)=1;
        elseif Del_T(k)>((Nucleate_Peak-77.3)*1.8)
            q=65.9*((Nucleate_Peak-77.3)*1.8)^2.1709;
            Place(k)=3;
            C1=q;
        else
            q=65.9*(Del_T(k))^2.1709;
            Place(k)=2;
        end
        PeakT=Del_T(k);
    else
        if Del_T(k)<3.5
            q=(Del_T(k))*(10^3/3.5);
            Place(k)=6;
        else
            q=65.9*(Del_T(k))^2.1709;
            Place(k)=5;
        end
    end
elseif Temperature_Counter(k-1)==1
    if Del_T(k)>=Del_T(k-1)
        if Del_T(k)<3.5
            q=(Del_T(k))*(10^3/3.5);
            Place(k)=1;
        elseif Del_T(k)>((Nucleate_Peak-77.3)*1.8)
            q=65.9*((Nucleate_Peak-77.3)*1.8)^2.1709;
            Place(k)=3;
            C1=q;
        else
            q=65.9*(Del_T(k))^2.1709;
            Place(k)=2;
        end
        PeakT=Del_T(k);
    else
        if counter==0
            B1=C1/(PeakT^0.7686);
            counter=1;
        end
        if counter==1
            DelTransTemp=((8*10^23)/B1)^(1/12.7266);
            counter=2;
        end
        if counter==2
            C2=B1*(DelTransTemp)^0.7686;
            DelTransTemp2=(C2/65.9)^(1/2.1709);
            counter=3;
        end
        if Del_T(k)>((Nucleate_Peak-77.3)*1.8)
            q=65.9*((Nucleate_Peak-77.3)*1.8)^2.1709;

```

```

        Place(k)=4;
else
    if Del_T(k)<3.5
        q=(Del_T(k))*(10^3/3.5);
        Place(k)=6;
    else
        q=65.9*(Del_T(k))^2.1709;
        Place(k)=5;
    end
end
end
else % If Temperature_Counter==2
    if counter==0
        B1=C1/(PeakT^0.7686);
        counter=1;
    end
    if counter==1
        DelTransTemp=((8*10^23)/B1)^(1/12.7266);
        counter=2;
    end
    if counter==2
        C2=B1*(DelTransTemp)^0.7686;
        DelTransTemp2=(C2/65.9)^(1/2.1709);
        counter=3;
    end
    if Del_T(k)>DelTransTemp
        q=B1*(Del_T(k)^0.7686);
        Place(k)=4;
    elseif Del_T(k)<(DelTransTemp2)
        if Del_T(k)<3.5
            q=(Del_T(k))*(10^3/3.5);
            Place(k)=7;
        else
            q=65.9*(Del_T(k))^2.1709;
            Place(k)=6;
        end
    else
        q=B1*(DelTransTemp)^0.7686;
        Place(k)=5;
    end
end
if Del_T(k)<=((Nucleate_Peak-77.3)*1.8)
    Temperature_Counter(k)=0;
end
if Del_T(k)>((Nucleate_Peak-77.3)*1.8)
    Temperature_Counter(k)=1;
end
if Del_T(k)>(DelTransTemp)
    Temperature_Counter(k)=2;
end
if Temperature_Counter(k)<Temperature_Counter(k-1)
    Temperature_Counter(k)=Temperature_Counter(k-1);
end
%%%%%%%%%%%%%%%%%%%%%%%%%%%%%%%%%%%%%%%%%%%%%%%%%%%%%%%%%%%%%%%%%%%%%%%%%% Output to Main.m %%%%%%%%%%%%%%%%%%%%%%%%%%%%%%%%%%%%%%%%%%%%%%%%%%%%%%%%%%%%%%%%%%%%%%%%%%%
Qout(k)=q*(Length*Width)*Delta_Time*3.1546;
%%%%%%%%%%%%%%%%%%%%%%%%%%%%%%%%%%%%%%%%%%%%%%%%%%%%%%%%%%%%%%%%%%%%%%%%%% End Cooling.m %%%%%%%%%%%%%%%%%%%%%%%%%%%%%%%%%%%%%%%%%%%%%%%%%%%%%%%%%%%%%%%%%%%%%%%%%%%

```

Appendix A4: Embeded Functions

Appendix A4.1 - N_Value.m

```
%%%%%%%%%%%%%%%%%%%%%%%%%%%%%%%%%%%%%%%%%%%%%%%%%%%%%%%%%%%%%%%%%%%%%%%%%%%%%% Begin N_Value.m %%%%%%%%%%%%%%%%%%%%%%%%%%%%%%%%%%%%%%%%%%%%%%%%%%%%%%%%%%%%%%%%%%%%%%%%%%%%%%%
%%%%%%%%%%%%%%%%%%%%%%%%%%%%%%%%%%%%%%%%%%%%%%%%%%%%%%%%%%%%%%%%%%%%%%%%%%%%%% Begin User input %%%%%%%%%%%%%%%%%%%%%%%%%%%%%%%%%%%%%%%%%%%%%%%%%%%%%%%%%%%%%%%%%%%%%%%%%%%%%%%
    E_One=0.5; %%%%%%%%%%%%%%%%%%%%%%%%%%%%%%%%%%%%%%%%%%%%%%%%%%%%%%%%%%%%%%%%%%%%%%%%%%%%%%%
    E_Two=5.0; %%%%%%%%%%%%%%%%%%%%%%%%%%%%%%%%%%%%%%%%%%%%%%%%%%%%%%%%%%%%%%%%%%%%%%%%%%%%%%%
    I_One=35; % input('Please enter current for 0.5-microV:'); %%%%%%%%%%%%%%%%%%%%%%%%%%%%%%%%%%%%%%%%%%%%%%%%%%%%%%%%%%%%%%%%%%%%%%%%%%%%%%%
    I_Two=39; % input('Please enter current for 5.0-microV:'); %%%%%%%%%%%%%%%%%%%%%%%%%%%%%%%%%%%%%%%%%%%%%%%%%%%%%%%%%%%%%%%%%%%%%%%%%%%%%%%
%%%%%%%%%%%%%%%%%%%%%%%%%%%%%%%%%%%%%%%%%%%%%%%%%%%%%%%%%%%%%%%%%%%%%%%%%%%%%% End User input %%%%%%%%%%%%%%%%%%%%%%%%%%%%%%%%%%%%%%%%%%%%%%%%%%%%%%%%%%%%%%%%%%%%%%%%%%%%%%%
    gggg=log(E_Two/E_One); %%%%%%%%%%%%%%%%%%%%%%%%%%%%%%%%%%%%%%%%%%%%%%%%%%%%%%%%%%%%%%%%%%%%%%%%%%%%%%%
    hhhh=log(I_Two/I_One); %%%%%%%%%%%%%%%%%%%%%%%%%%%%%%%%%%%%%%%%%%%%%%%%%%%%%%%%%%%%%%%%%%%%%%%%%%%%%%%
%%%%%%%%%%%%%%%%%%%%%%%%%%%%%%%%%%%%%%%%%%%%%%%%%%%%%%%%%%%%%%%%%%%%%%%%%%%%%% Function Output %%%%%%%%%%%%%%%%%%%%%%%%%%%%%%%%%%%%%%%%%%%%%%%%%%%%%%%%%%%%%%%%%%%%%%%%%%%%%%%
    n=gggg/hhhh;
%%%%%%%%%%%%%%%%%%%%%%%%%%%%%%%%%%%%%%%%%%%%%%%%%%%%%%%%%%%%%%%%%%%%%%%%%%%%%% End N_Value.m %%%%%%%%%%%%%%%%%%%%%%%%%%%%%%%%%%%%%%%%%%%%%%%%%%%%%%%%%%%%%%%%%%%%%%%%%%%%%%%
```

Appendix A4.2 - Cu_Cp.m

```
%%%%%%%%%%%%%%%%%%%%%%%%%%%%%%%%%%%%%%%%%%%%%%%%%%%%%%%%%%%%%%%%%%%%%%%%%%%%%% Begin Cu_Cp.m %%%%%%%%%%%%%%%%%%%%%%%%%%%%%%%%%%%%%%%%%%%%%%%%%%%%%%%%%%%%%%%%%%%%%%%%%%%%%%%
function [ Cu_Cp_Out ] = Cu_Cp( T ) %%%%%%%%%%%%%%%%%%%%%%%%%%%%%%%%%%%%%%%%%%%%%%%%%%%%%%%%%%%%%%%%%%%%%%%%%%%%%%%
    Rho_Cu=9020.665-0.30358*T; %%%%%%%%%%%%%%%%%%%%%%%%%%%%%%%%%%%%%%%%%%%%%%%%%%%%%%%%%%%%%%%%%%%%%%%%%%%%%%%
    if T<=200 %%%%%%%%%%%%%%%%%%%%%%%%%%%%%%%%%%%%%%%%%%%%%%%%%%%%%%%%%%%%%%%%%%%%%%%%%%%%%%%
        a=(368.53324*(1-exp(-0.02322*T))^3.65205)*Rho_Cu; %%%%%%%%%%%%%%%%%%%%%%%%%%%%%%%%%%%%%%%%%%%%%%%%%%%%%%%%%%%%%%%%%%%%%%%%%%%%%%%
    else %%%%%%%%%%%%%%%%%%%%%%%%%%%%%%%%%%%%%%%%%%%%%%%%%%%%%%%%%%%%%%%%%%%%%%%%%%%%%%%
        a=((2.3181*10^-07*T^3)-(0.00052*T^2) %%%%%%%%%%%%%%%%%%%%%%%%%%%%%%%%%%%%%%%%%%%%%%%%%%%%%%%%%%%%%%%%%%%%%%%%%%%%%%%
            +(0.44648*T)+287.47602)*Rho_Cu; %%%%%%%%%%%%%%%%%%%%%%%%%%%%%%%%%%%%%%%%%%%%%%%%%%%%%%%%%%%%%%%%%%%%%%%%%%%%%%%
    end %%%%%%%%%%%%%%%%%%%%%%%%%%%%%%%%%%%%%%%%%%%%%%%%%%%%%%%%%%%%%%%%%%%%%%%%%%%%%%%
%%%%%%%%%%%%%%%%%%%%%%%%%%%%%%%%%%%%%%%%%%%%%%%%%%%%%%%%%%%%%%%%%%%%%%%%%%%%%% Function Output %%%%%%%%%%%%%%%%%%%%%%%%%%%%%%%%%%%%%%%%%%%%%%%%%%%%%%%%%%%%%%%%%%%%%%%%%%%%%%%
Cu_Cp_Out=a; %%%%%%%%%%%%%%%%%%%%%%%%%%%%%%%%%%%%%%%%%%%%%%%%%%%%%%%%%%%%%%%%%%%%%%%%%%%%%%%
%%%%%%%%%%%%%%%%%%%%%%%%%%%%%%%%%%%%%%%%%%%%%%%%%%%%%%%%%%%%%%%%%%%%%%%%%%%%%% End Cu_Cp.m %%%%%%%%%%%%%%%%%%%%%%%%%%%%%%%%%%%%%%%%%%%%%%%%%%%%%%%%%%%%%%%%%%%%%%%%%%%%%%%
```

Appendix A4.3 - Cu_Res.m

```
%%%%%%%%%%%%%%%%%%%%%%%%%%%%%%%%%%%%%%%%%%%%%%%%%%%%%%%%%%%%%%%%%%%%%%%%%%%%%% Begin Cu_Res.m %%%%%%%%%%%%%%%%%%%%%%%%%%%%%%%%%%%%%%%%%%%%%%%%%%%%%%%%%%%%%%%%%%%%%%%%%%%%%%%
function [ Cu_Res_Out ] = Cu_Res( T ) %%%%%%%%%%%%%%%%%%%%%%%%%%%%%%%%%%%%%%%%%%%%%%%%%%%%%%%%%%%%%%%%%%%%%%%%%%%%%%%
    if T<=190 %%%%%%%%%%%%%%%%%%%%%%%%%%%%%%%%%%%%%%%%%%%%%%%%%%%%%%%%%%%%%%%%%%%%%%%%%%%%%%%
        a=((-1.1787e-06*T^3)+(0.00067*T^2)-0.02399*T+0.3855) %%%%%%%%%%%%%%%%%%%%%%%%%%%%%%%%%%%%%%%%%%%%%%%%%%%%%%%%%%%%%%%%%%%%%%%%%%%%%%%
            *1e-9; %%%%%%%%%%%%%%%%%%%%%%%%%%%%%%%%%%%%%%%%%%%%%%%%%%%%%%%%%%%%%%%%%%%%%%%%%%%%%%%
    else %%%%%%%%%%%%%%%%%%%%%%%%%%%%%%%%%%%%%%%%%%%%%%%%%%%%%%%%%%%%%%%%%%%%%%%%%%%%%%%
        a=((-118.11359+(34.4038*(exp((T+2715.04572) / %%%%%%%%%%%%%%%%%%%%%%%%%%%%%%%%%%%%%%%%%%%%%%%%%%%%%%%%%%%%%%%%%%%%%%%%%%%%%%%
            2191.4633))))+.52)*1e-9; %%%%%%%%%%%%%%%%%%%%%%%%%%%%%%%%%%%%%%%%%%%%%%%%%%%%%%%%%%%%%%%%%%%%%%%%%%%%%%%
    end %%%%%%%%%%%%%%%%%%%%%%%%%%%%%%%%%%%%%%%%%%%%%%%%%%%%%%%%%%%%%%%%%%%%%%%%%%%%%%%
%%%%%%%%%%%%%%%%%%%%%%%%%%%%%%%%%%%%%%%%%%%%%%%%%%%%%%%%%%%%%%%%%%%%%%%%%%%%%% Function Output %%%%%%%%%%%%%%%%%%%%%%%%%%%%%%%%%%%%%%%%%%%%%%%%%%%%%%%%%%%%%%%%%%%%%%%%%%%%%%%
Cu_Res_Out=a; %%%%%%%%%%%%%%%%%%%%%%%%%%%%%%%%%%%%%%%%%%%%%%%%%%%%%%%%%%%%%%%%%%%%%%%%%%%%%%%
%%%%%%%%%%%%%%%%%%%%%%%%%%%%%%%%%%%%%%%%%%%%%%%%%%%%%%%%%%%%%%%%%%%%%%%%%%%%%% End Cu_Res.m %%%%%%%%%%%%%%%%%%%%%%%%%%%%%%%%%%%%%%%%%%%%%%%%%%%%%%%%%%%%%%%%%%%%%%%%%%%%%%%
```

Appendix A4.4 - Ag_Cp.m

```
%%%%%%%%%%%%%%%%%%%%%%%%%%%%%%%%%%%%%%%%%%%%%%%%%%%%%%%%%%%%%%%%%%%%%%%%%%%%%% Begin Ag_Cp.m %%%%%%%%%%%%%%%%%%%%%%%%%%%%%%%%%%%%%%%%%%%%%%%%%%%%%%%%%%%%%%%%%%%%%%%%%%%%%%%
function [ Ag_Cp_Out ] = Ag_Cp( T ) %%%%%%%%%%
    Rho_Ag=10500; %%%%%%%%%%
%%%%%%%%%%%%%%%%%%%%%%%%%%%%%%%%%%%%%%%%%%%%%%%%%%%%%%%%%%%%%%%%%%%%%%%%%%%%%% Function Output %%%%%%%%%%%%%%%%%%%%%%%%%%%%%%%%%%%%%%%%%%%%%%%%%%%%%%%%%%%%%%%%%%%%%%%%%%%%%%%
Ag_Cp_Out=(571302.22046*(T^(0.00011))-571442.51725)*Rho_Ag; %%%%%%%%%%
%%%%%%%%%%%%%%%%%%%%%%%%%%%%%%%%%%%%%%%%%%%%%%%%%%%%%%%%%%%%%%%%%%%%%%%%%%%%%% End Ag_Cp.m %%%%%%%%%%%%%%%%%%%%%%%%%%%%%%%%%%%%%%%%%%%%%%%%%%%%%%%%%%%%%%%%%%%%%%%%%%%%%%%
```

Appendix A4.5 - Ag_Res.m

```
%%%%%%%%%%%%%%%%%%%%%%%%%%%%%%%%%%%%%%%%%%%%%%%%%%%%%%%%%%%%%%%%%%%%%%%%%%%%%% Begin Ag_Res.m %%%%%%%%%%%%%%%%%%%%%%%%%%%%%%%%%%%%%%%%%%%%%%%%%%%%%%%%%%%%%%%%%%%%%%%%%%%%%%%
function [ Ag_Res_Out ] = Ag_Res( T ) %%%%%%%%%%
    if T>=293 %%%%%%%%%%
        a=((0.0685*T)-3.77476)*1e-9; %%%%%%%%%%
    else %%%%%%%%%%
        a=(-1.0796e-06*T^3)+(0.00046*T^2)+0.01555* %%%%%%%%%%
            T-0.38874)*1e-9; %%%%%%%%%%
    end %%%%%%%%%%
%%%%%%%%%%%%%%%%%%%%%%%%%%%%%%%%%%%%%%%%%%%%%%%%%%%%%%%%%%%%%%%%%%%%%%%%%%%%%% Function Output %%%%%%%%%%%%%%%%%%%%%%%%%%%%%%%%%%%%%%%%%%%%%%%%%%%%%%%%%%%%%%%%%%%%%%%%%%%%%%%
Ag_Res_Out=a; %%%%%%%%%%
%%%%%%%%%%%%%%%%%%%%%%%%%%%%%%%%%%%%%%%%%%%%%%%%%%%%%%%%%%%%%%%%%%%%%%%%%%%%%% End Ag_Res.m %%%%%%%%%%%%%%%%%%%%%%%%%%%%%%%%%%%%%%%%%%%%%%%%%%%%%%%%%%%%%%%%%%%%%%%%%%%%%%%
```

Appendix A4.6 - Sub_Cp.m

```
%%%%%%%%%%%%%%%%%%%%%%%%%%%%%%%%%%%%%%%%%%%%%%%%%%%%%%%%%%%%%%%%%%%%%%%%%%%%%% Begin Sub_Cp.m %%%%%%%%%%%%%%%%%%%%%%%%%%%%%%%%%%%%%%%%%%%%%%%%%%%%%%%%%%%%%%%%%%%%%%%%%%%%%%%
function [ Sub_Cp_Out ] = Sub_Cp( T ) %%%%%%%%%%
    Rho_Sub=8890; %%%%%%%%%%
    if T<=300 %%%%%%%%%%
        b=15503.108-(37280.377*log10(T))+(26788.417* %%%%%%%%%%
            log10(T)^2)+(7010.0877*log10(T)^3)- %%%%%%%%%%
            (22731.651*log10(T)^4)+(15386.526*log10(T)^5)- %%%%%%%%%%
            (5175.7968*log10(T)^6)+(896.97274*log10(T)^7)- %%%%%%%%%%
            (64.055866*log10(T)^8); %%%%%%%%%%
        a=(10^b)*Rho_Sub; %%%%%%%%%%
    else %%%%%%%%%%
        a=((0.1581*T)+410.24)*Rho_Sub; %%%%%%%%%%
    end %%%%%%%%%%
%%%%%%%%%%%%%%%%%%%%%%%%%%%%%%%%%%%%%%%%%%%%%%%%%%%%%%%%%%%%%%%%%%%%%%%%%%%%%% Function Output %%%%%%%%%%%%%%%%%%%%%%%%%%%%%%%%%%%%%%%%%%%%%%%%%%%%%%%%%%%%%%%%%%%%%%%%%%%%%%%
Sub_Cp_Out=a; %%%%%%%%%%
%%%%%%%%%%%%%%%%%%%%%%%%%%%%%%%%%%%%%%%%%%%%%%%%%%%%%%%%%%%%%%%%%%%%%%%%%%%%%% End Sub_Cp.m %%%%%%%%%%%%%%%%%%%%%%%%%%%%%%%%%%%%%%%%%%%%%%%%%%%%%%%%%%%%%%%%%%%%%%%%%%%%%%%
```

Appendix A4.7 - Sub_Res.m

```
%%%%%%%%%%%%%%%%%%%%%%%%%%%%%%%%%%%%%%%%%%%%%%%%%%%%%%%%%%%%%%%%%%%%%%%%%%%%%% Begin Sub_Res.m %%%%%%%%%%%%%%%%%%%%%%%%%%%%%%%%%%%%%%%%%%%%%%%%%%%%%%%%%%%%%%%%%%%%%%%%%%%%%%%
function [ Sub_Res_Out ] = Sub_Res( T ) %%%%%%%%%%
    a=1.30*1e-6; %%%%%%%%%%
%%%%%%%%%%%%%%%%%%%%%%%%%%%%%%%%%%%%%%%%%%%%%%%%%%%%%%%%%%%%%%%%%%%%%%%%%%%%%% Function Output %%%%%%%%%%%%%%%%%%%%%%%%%%%%%%%%%%%%%%%%%%%%%%%%%%%%%%%%%%%%%%%%%%%%%%%%%%%%%%%
Sub_Res_Out=a; %%%%%%%%%%
%%%%%%%%%%%%%%%%%%%%%%%%%%%%%%%%%%%%%%%%%%%%%%%%%%%%%%%%%%%%%%%%%%%%%%%%%%%%%% End Sub_Res.m %%%%%%%%%%%%%%%%%%%%%%%%%%%%%%%%%%%%%%%%%%%%%%%%%%%%%%%%%%%%%%%%%%%%%%%%%%%%%%%
```

Appendix A4.8 - YBCO_Cp.m

```

%%%%%%%%%%%%%%%%%%%%%%%%%%%%%%%%%%%%%%%%%%%%%%%%%%%%%%%%%%%%%%%%%%%%%%%%%% Begin YBCO_Cp.m %%%%%%%%%%%%%%%%%%%%%%%%%%%%%%%%%%%%%%%%%%%%%%%%%%%%%%%%%%%%%%%%%%%%%%%%%%%
function [ YBCO_Cp_Output ] = YBCO_Cp( T ) %%%%%%%%%%
    if T<=80.5 %%%%%%%%%%
        Cybco=1.2173*T+91.659; %%%%%%%%%%
    else %%%%%%%%%%
        if T<=84 %%%%%%%%%%
            Cybco=-19.423*T+1752.4; %%%%%%%%%%
        else %%%%%%%%%%
            if T<=90 %%%%%%%%%%
                Cybco=5.0661*T-304.24; %%%%%%%%%%
            else %%%%%%%%%%
                if T<=92 %%%%%%%%%%
                    Cybco=-3.9285*T+504.7; %%%%%%%%%%
                else %%%%%%%%%%
                    if T<=200 %%%%%%%%%%
                        Cybco=(-456.60151*exp(-T/65.99887))+ %%%%%%%%%%
                            260.40759; %%%%%%%%%%
                    else %%%%%%%%%%
                        if T<=300 %%%%%%%%%%
                            Cybco=(-0.0183*T^2)+(11.254*T)-1281.1; %%%%%%%%%%
                        else %%%%%%%%%%
                            if T<=500 %%%%%%%%%%
                                Cybco=(334.68-(0.28854*T)+ %%%%%%%%%%
                                    (5.7220*10^(-4))*T^2))* %%%%%%%%%%
                                    (1/0.668); %%%%%%%%%%
                            else %%%%%%%%%%
                                if T<=900 %%%%%%%%%%
                                    Cybco=(316.92-(0.10258*T)+ %%%%%%%%%%
                                        (1.9478*10^(-4))* %%%%%%%%%%
                                        T^2))*(1/0.665); %%%%%%%%%%
                                else %%%%%%%%%%
                                    Cybco=(316.92-(0.10258*T)+ %%%%%%%%%%
                                        (1.9478*10^(-4))* %%%%%%%%%%
                                        T^2))*(1/0.665); %%%%%%%%%%
                                end %%%%%%%%%%
                            end %%%%%%%%%%
                        end %%%%%%%%%%
                    end %%%%%%%%%%
                end %%%%%%%%%%
            end %%%%%%%%%%
        end %%%%%%%%%%
    end %%%%%%%%%%
end %%%%%%%%%%
%%%%%%%%%%%%%%%%%%%%%%%%%%%%%%%%%%%%%%%%%%%%%%%%%%%%%%%%%%%%%%%%%%%%%%%%%% Function Output %%%%%%%%%%%%%%%%%%%%%%%%%%%%%%%%%%%%%%%%%%%%%%%%%%%%%%%%%%%%%%%%%%%%%%%%%%%
YBCO_Cp_Output=Cybco;
%%%%%%%%%%%%%%%%%%%%%%%%%%%%%%%%%%%%%%%%%%%%%%%%%%%%%%%%%%%%%%%%%%%%%%%%%% End YBCO_Cp.m %%%%%%%%%%%%%%%%%%%%%%%%%%%%%%%%%%%%%%%%%%%%%%%%%%%%%%%%%%%%%%%%%%%%%%%%%%%

```

Appendix A4.9 - YBCO_Ic.m

```
%%%%%%%%%%%%%%%%%%%%%%%%%%%%%%%%%%%%%%%%%%%%%%%%%%%%%%%%%%%%%%%%%%%%%%%%%% Begin YBCO_Ic.m %%%%%%%%%%%%%%%%%%%%%%%%%%%%%%%%%%%%%%%%%%%%%%%%%%%%%%%%%%%%%%%%%%%%%%%%%%%
function [ YBCO_Ic_Out ] = YBCO_Ic( T,Critical_Current_at_77,
    T_LN2 ) %%%%%%%%%%
    a=Critical_Current_at_77*(93-T)/(93-T_LN2); %%%%%%%%%%
    if a<0 %%%%%%%%%%
        a=0; %%%%%%%%%%
    end %%%%%%%%%%
%%%%%%%%%%%%%%%%%%%%%%%%%%%%%%%%%%%%%%%%%%%%%%%%%%%%%%%%%%%%%%%%%%%%%%%%%% Function Output %%%%%%%%%%%%%%%%%%%%%%%%%%%%%%%%%%%%%%%%%%%%%%%%%%%%%%%%%%%%%%%%%%%%%%%%%%%
YBCO_Ic_Out=a;
%%%%%%%%%%%%%%%%%%%%%%%%%%%%%%%%%%%%%%%%%%%%%%%%%%%%%%%%%%%%%%%%%%%%%%%%%% End YBCO_Ic.m %%%%%%%%%%%%%%%%%%%%%%%%%%%%%%%%%%%%%%%%%%%%%%%%%%%%%%%%%%%%%%%%%%%%%%%%%%%
```

Appendix B – Material Properties

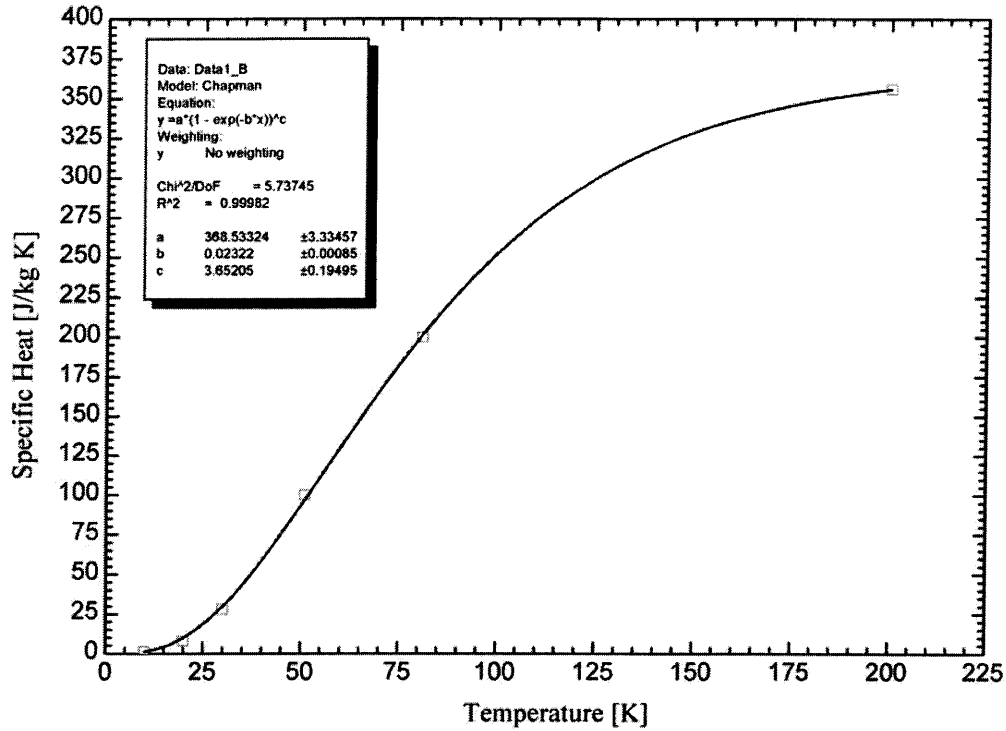


Figure B-1. Specific Heat of Copper 100 for 10K < T < 200K [12].

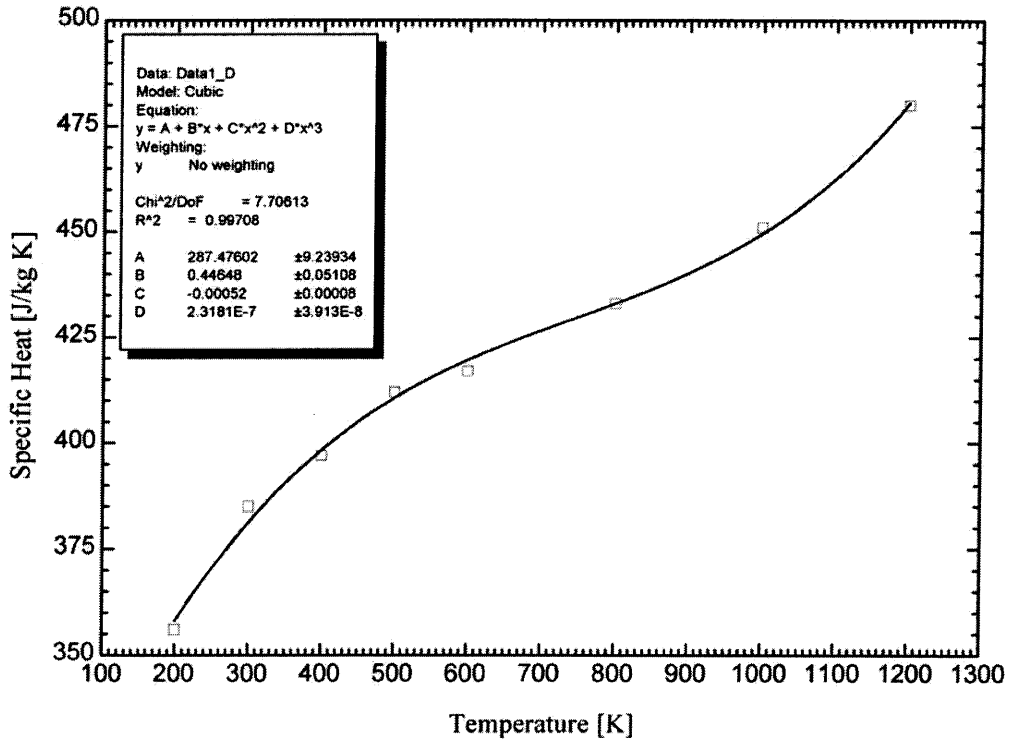


Figure B-2. Specific Heat of Copper 100 for 200K < T < 1200K [8].

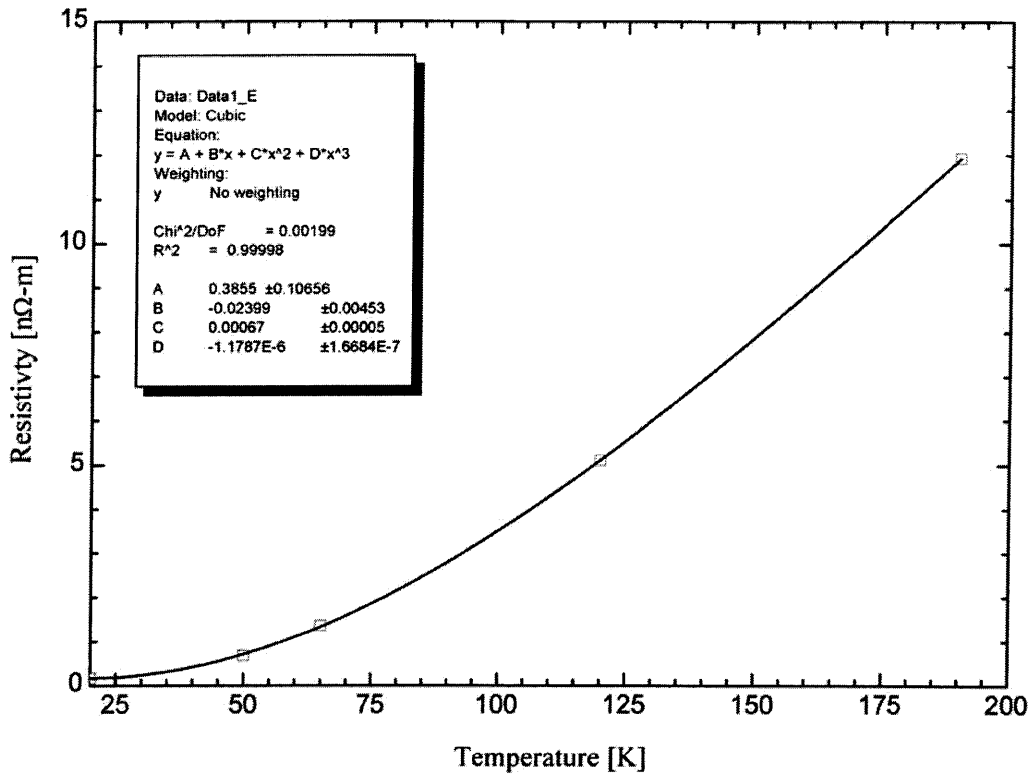


Figure B-3. Resistivity of Copper 100 for $20\text{K} < T < 190\text{K}$ [3].

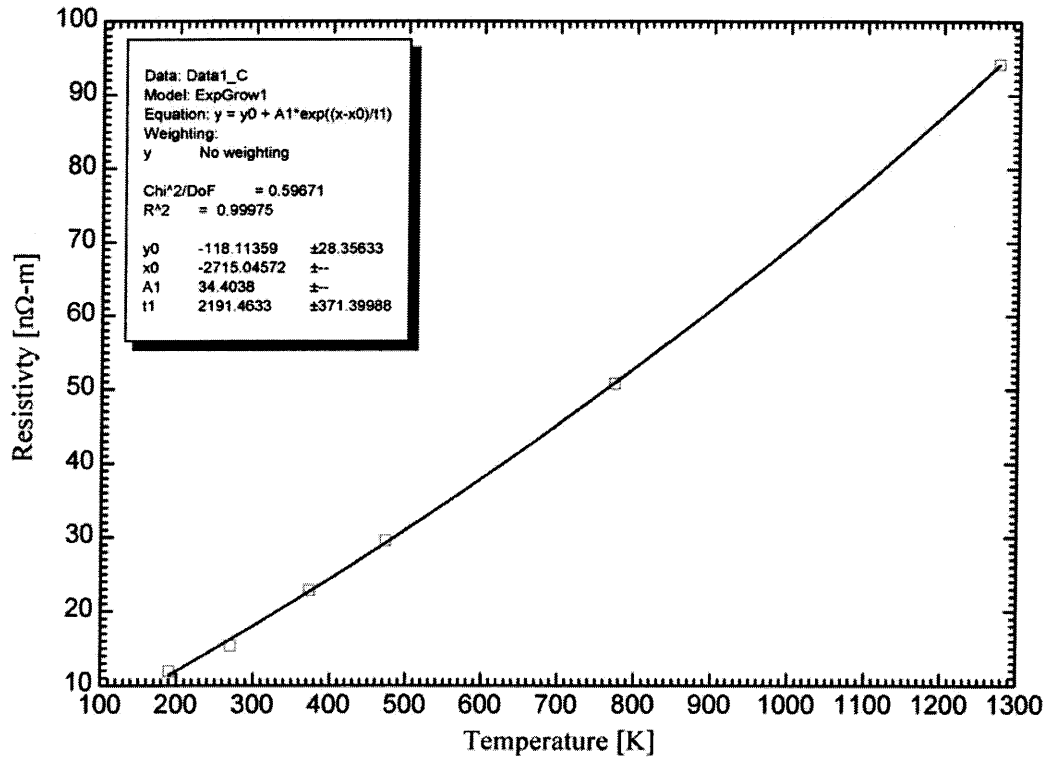


Figure B-4. Resistivity of Copper 100 for $190\text{K} < T < 1300\text{K}$ [13].

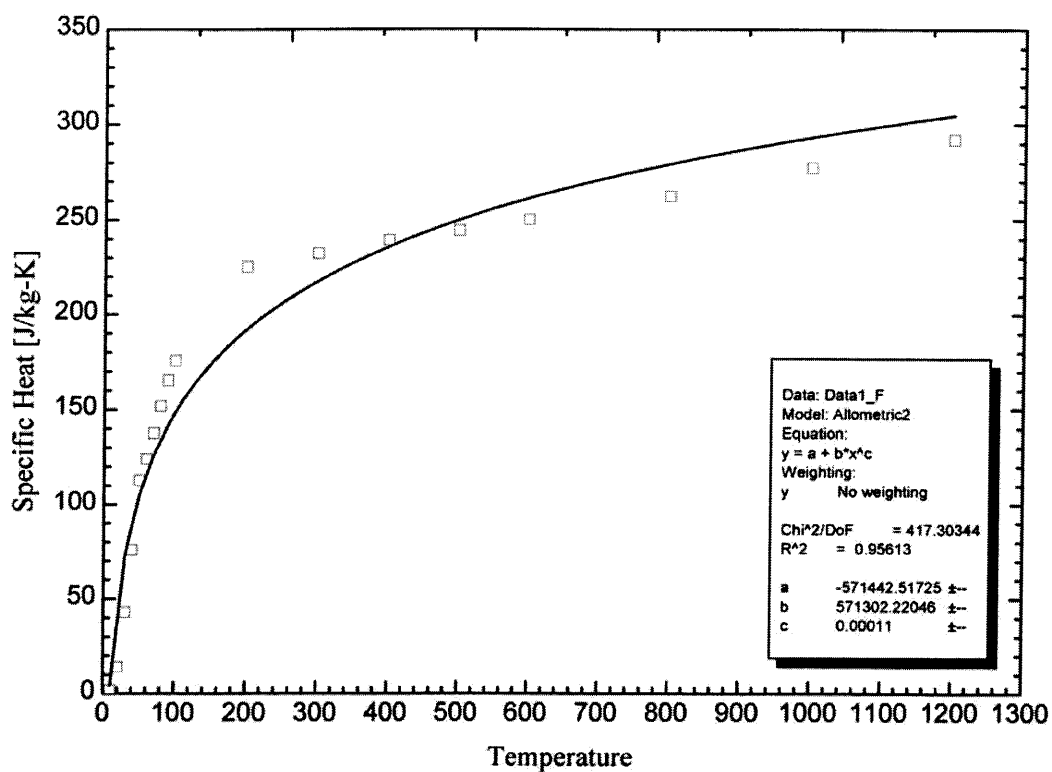


Figure B-5. Specific Heat of Silver for $10\text{K} < T < 1200\text{K}$ [8 & 14].

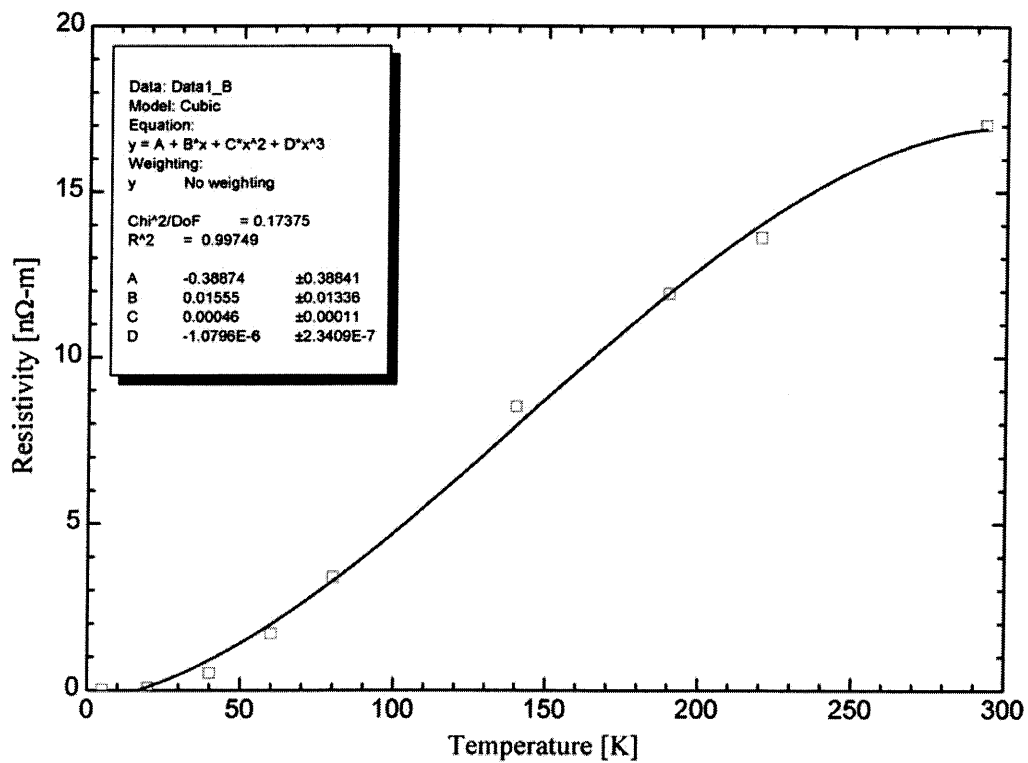


Figure B-6. Resistivity of Silver for $0\text{K} < T < 293\text{K}$ [3].

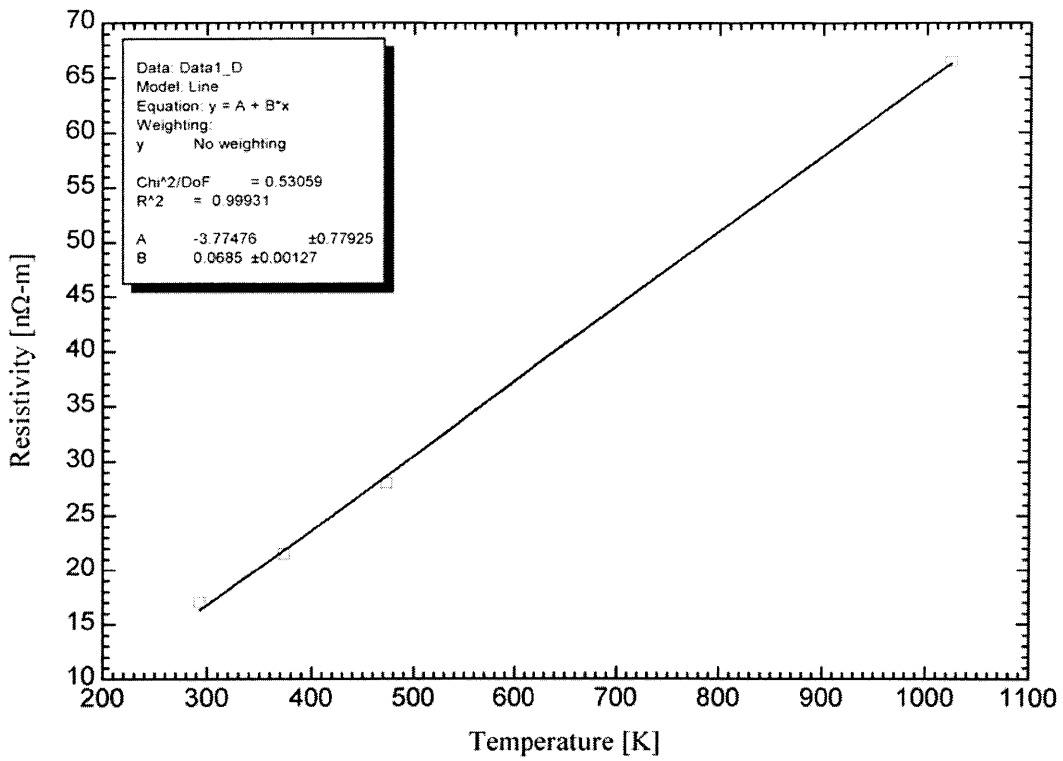


Figure B-7. Resistivity of Silver for $293\text{K} < T < 1000\text{K}$ [13].

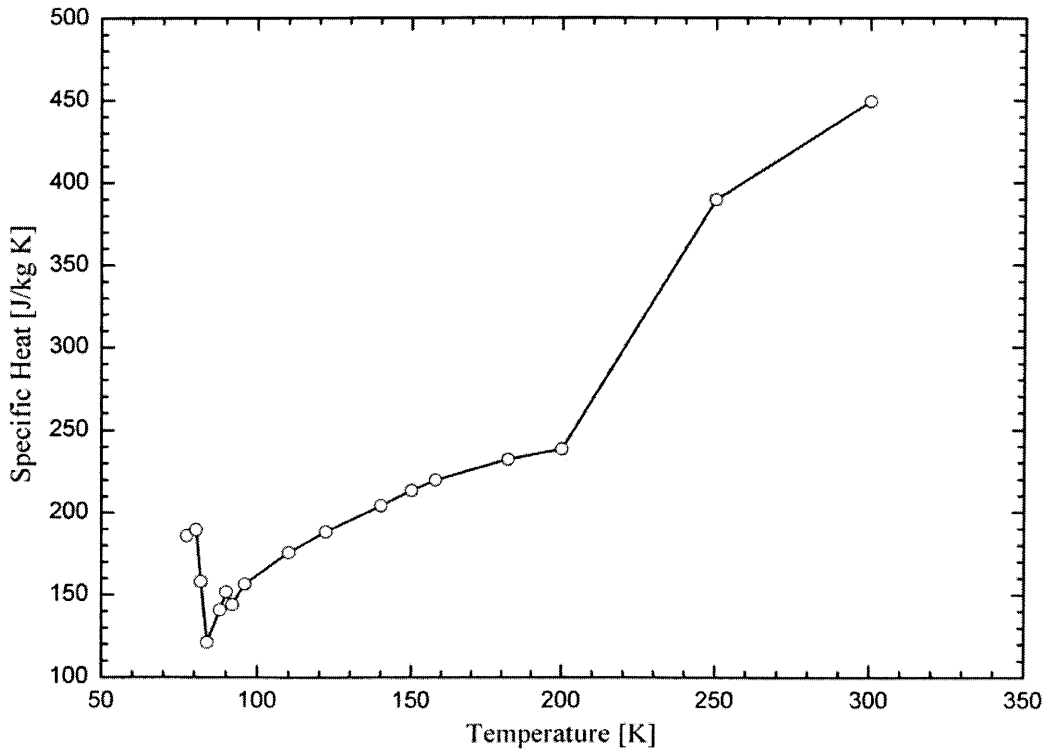


Figure B-8. Specific Heat of YBCO for $77.3\text{K} < T < 300\text{K}$ [16 & 17].

Appendix C - LabView Code

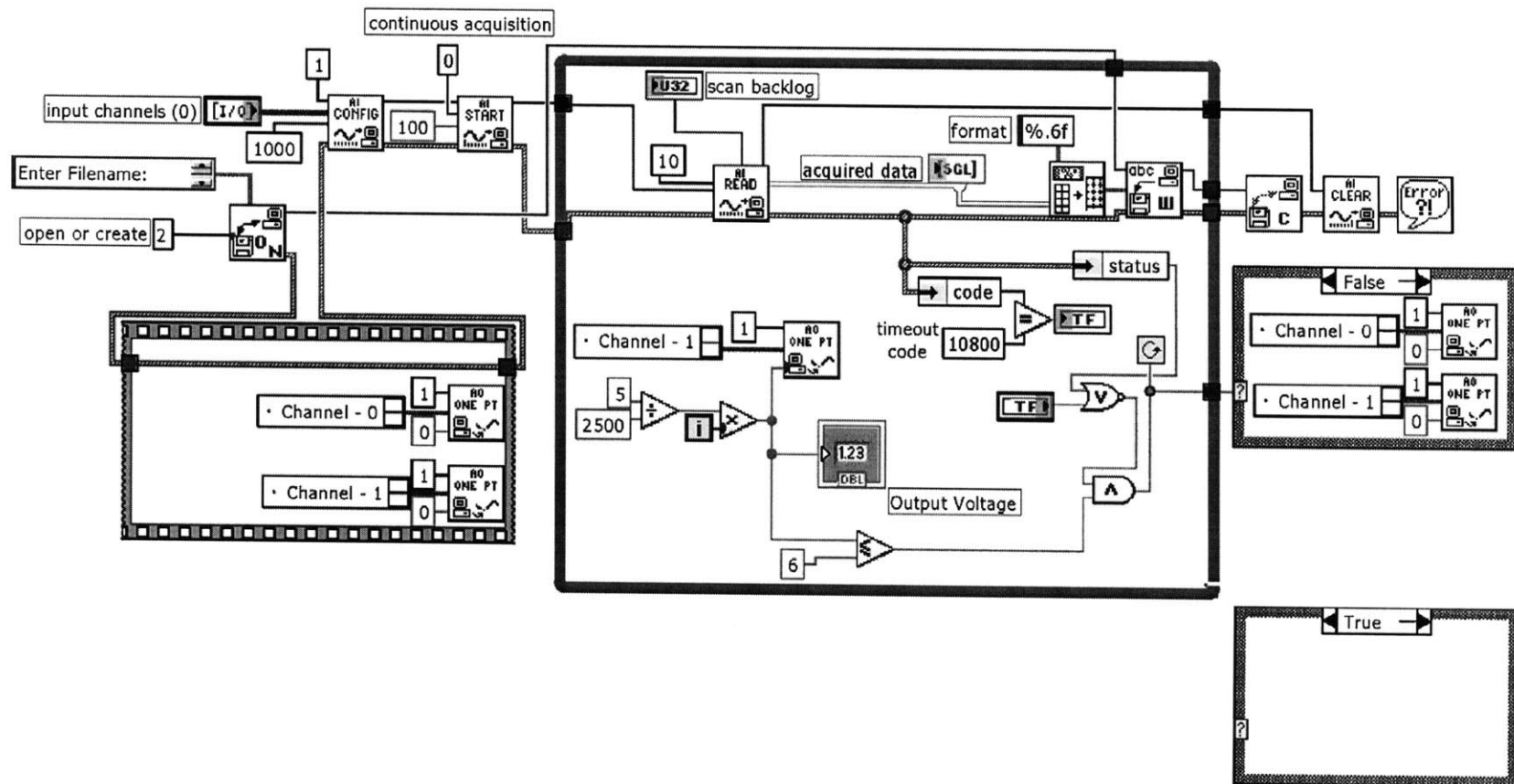


Figure C-1. LabView code used to generate the pulse control for the power supplies. This was used with a voltage divider inline to the power supply signal.

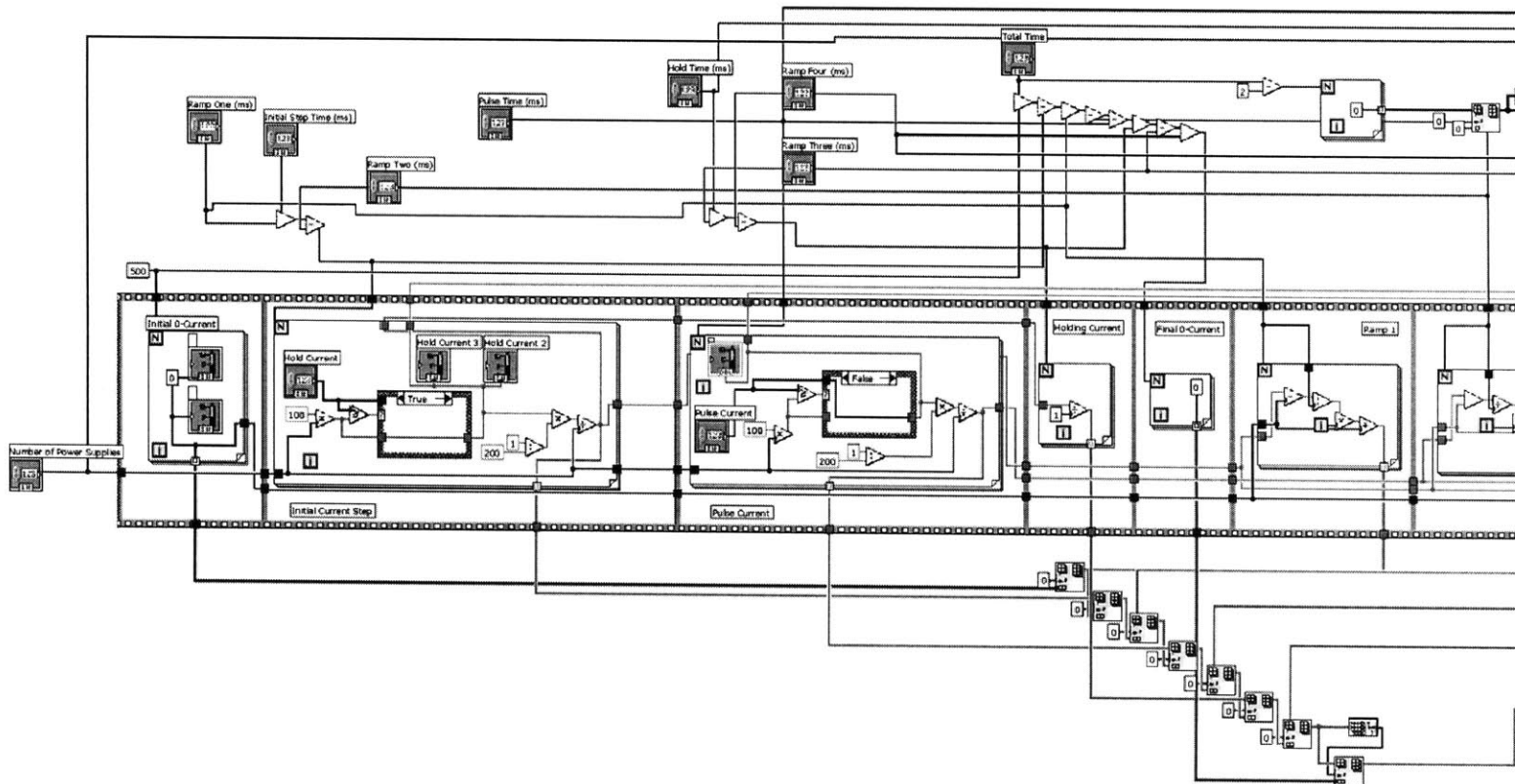


Figure C-2. LabView code used to generate the pulse current signal. This figure is the left portion, continued in Figure C-3.

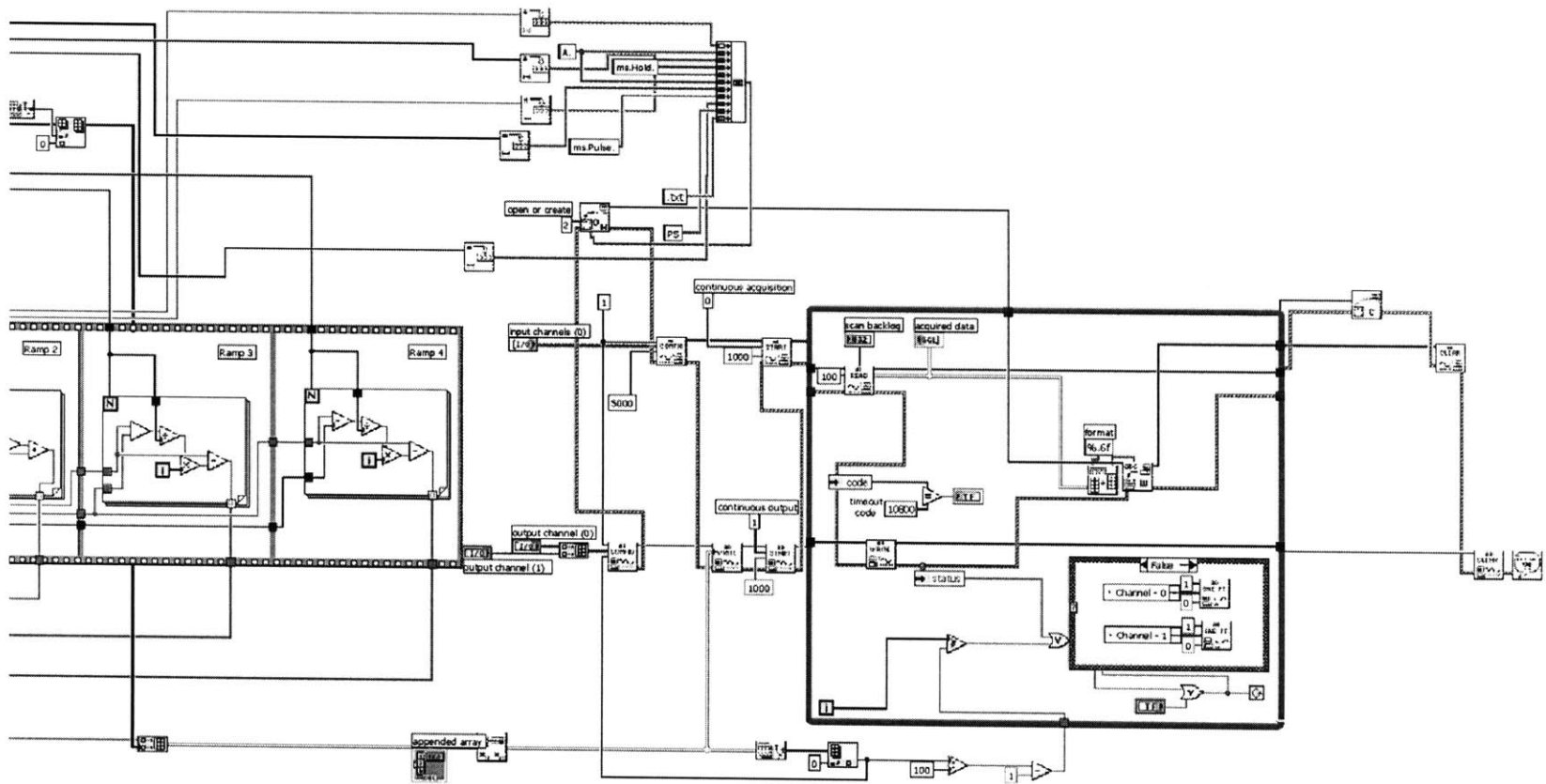


Figure C-3. LabView code used to generate the pulse current signal. This figure is the right portion, continued from Figure C-2.

Appendix D - Sample to DAQ Connection

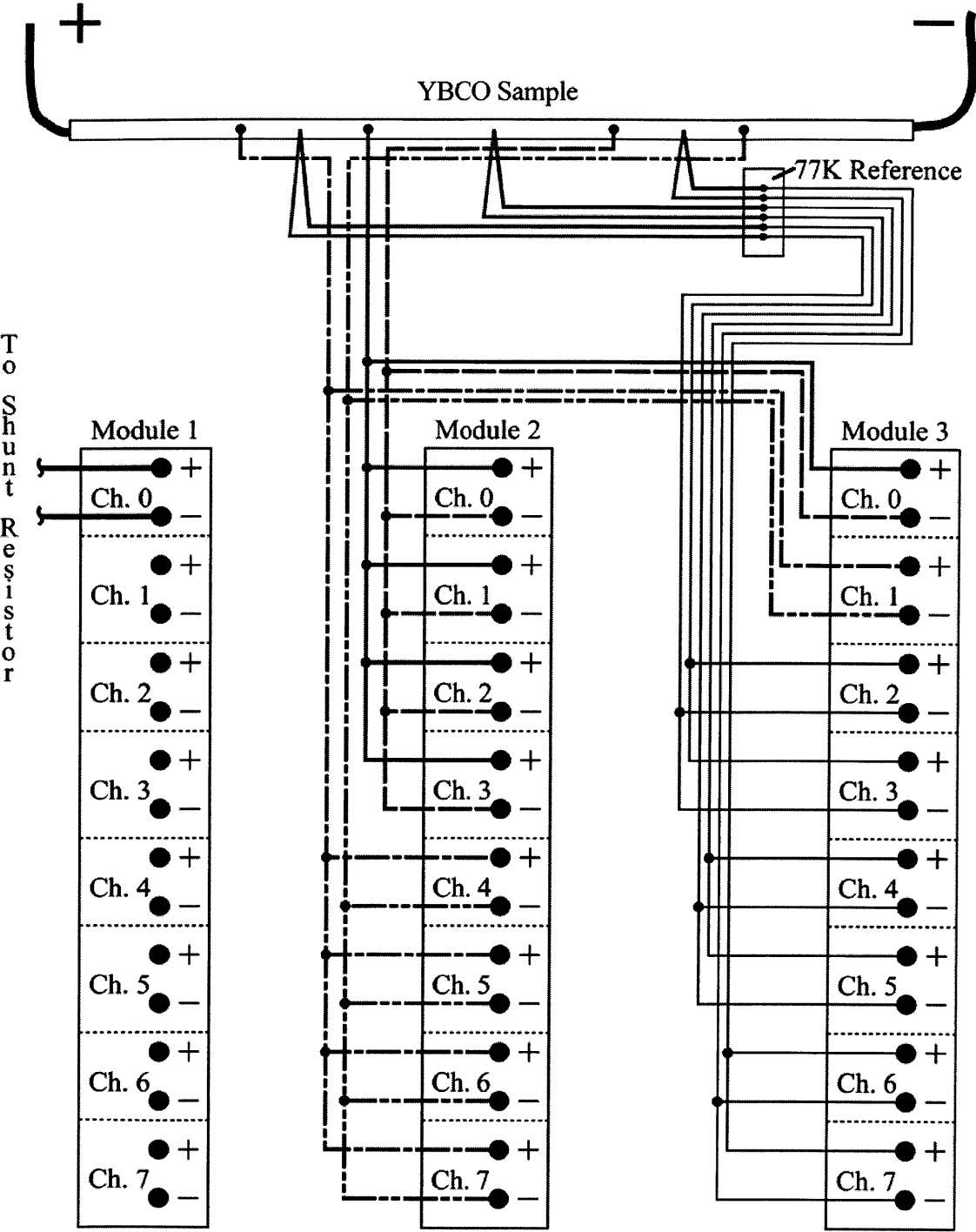


Figure D-1. Electrical Diagram for Sample to DAQ Connections.